

# Postsynthetic fluorescent labeling of COMBO- and 1,2,4-Triazine-modified DNA as bioorthogonal tools for live cell imaging

Zur Erlangung des akademischen Grades eines  
DOKTORS DER NATURWISSENSCHAFTEN  
(Dr. rer. nat.)

der KIT-Fakultät für Chemie und Biowissenschaften  
des Karlsruher Instituts für Technologie (KIT)



genehmigte

**DISSERTATION**

von

**M.Sc. Organic Chemistry. Krisana Peewasan**

aus

Khon Kaen, Thailand

**Karlsruhe, 2017**

KIT-Dekan:	Prof. Dr. Willem Klopper
Referent:	Prof. Dr. Hans-Achim Wagenknecht
Korreferent:	Prof. Dr. Michael A.R. Meier
Tag der mündlichen Prüfung:	28. April 2017







My family and my dear love Marcel Merkel



*“If they want to write about me in a good way,  
they should write how I do things that are useful”*

**King Bhumibol Adulyadej**

## Acknowledgements

This thesis was carried out from February 2014 to April 2017 at the institute for Organic Chemistry at the Karlsruhe institute of technology (KIT) under supervisor of Prof. Dr. Hans-Achim Wagenknecht.

First of all I would like to thank Prof. Dr. Hans-Achim Wagenknecht for giving me an opportunity to do my PhD study in the best cozy and very welcoming atmosphere in AKW group. Moreover, I would like to thank for a very kindness, excellent support and interesting topic.

In addition, I would like to thank deeply from my heart to all:

- ❖ Claudia Sommer: for your kindness and a cozy atmosphere every times when the door room no. 212 is opened

- ❖ Annette Hochgesand: for measuring all the masses, for ordering all chemicals and a nice conversation.

- ❖ Dr. Andreas Rapp: Tanja Ohmer, Anne-Lena Emmerich, Lennart Oberle and Pia Lang for numerous NMR measurements.

- ❖ Ingrid Roßnagel and Angelika Möhle: for measuring all the molecular masses.

- ❖ Ciske Faber and Lennart Oberle: for helping with refill the solvents' canister.

- ❖ My bachelor students: Fabian Schweigardt and Lev Korzhenevich for helping me with the COMBO synthesis.

- ❖ Andreas Dittmer: for being gentle man and best neighbor (fume) hood in Labor 204.

- ❖ Damian, Sergej and David: for NMR measurement.

- ❖ Damian, Steffie, Shuaib Umaira and Marcel: for correcting my thesis, for the best idea and nice suggestions.

❖ My colleagues; Dr. Claudia Stubinitzky, Dr. Stefanie Arndt, Dr Nadine Gass, Dr. Marcus Merkel, Dr. Sebastian Barrois, Dr. Philipp Enßlen, Dr. Heidi Walter, Barbara Reiß, Yannic Fritz, Dr. Sabrina Sezi, Dr. Christian Wellner, Dr. Effi Bätzner, Jeannine Steinmeyer, Benjamin Lehmann, Andreas Dittmer, David Rombach, Dr. Alexander Penner, Linda Antusch, Samantha Wörner, Tamina Schneider, Larissa Doll, Robert Hofsäß, Dr. Peggy Bohländer, Christian Schwechheimer, Ulrike Reisacher, Damian Ploschik, Dr. Martin Weiser, Sergej Hermann, Christoph Bickmann, Leonora Nurcaj, Nathalie Wagener: for helping with the reactions, nice conversation and cozy atmosphere.

❖ My colleagues in labor 204: for a great time and a cozy atmosphere.

❖ Dr. Claudia Stubinitzky: for inviting me to visit Karlsruhe and introduced me to the best working group ever.

❖ Dr. Marcus Merkel: Ich danke dir für alles, du bist mein Lehrer; triphosphate synthesis, gel electrophoresis and so on.

❖ Dr. Stefanie Arndt: for being nice lab mate, enjoy eating my foods (not spicy one) and always give me good suggestions for my experiments.

❖ Dr. Nadine Gass: for being the best lab mate ever, helping me to go through the PhD enrollment processes, taught an appropriate Deutsch and corrected me when I made a mistake, enjoy eating whatever I had cooked (I love to see you eat so much).

❖ Dr. Sebastian Barrois: for nice bicycle and nice suggestion for my thesis.

❖ Dr. Philipp Enßlen: for nice conversation and being a nice friend.

❖ Dr. Heidi Walter: for a good conversation and helping solve the HPLC problem.

❖ Barbara Reiß: for a good conversation.

❖ Yannic Fritz: for organizing all drinks; juice, water and of course beer!!!.

❖ Jeannine Steinmeyer: for being around and helping me with Deutsch home work.

❖ Benjamin Lehmann: for helping with technology problems and being always nice lab mate.

❖ David Rombach: for nice conversation and helping with the experiments.

❖ Linda Antusch: for being nice lab mate and bring in a lot of laugh.

❖ Samantha Wörner: for being nice lab mate and good conversation.

❖ Tamina Schneider: for being nice lab mate and bring in a lot of laugh and fun.

❖ Robert Hofsäß: for such a nice talk, good suggestion and being a good student (Thai cooking class).

❖ Christian Schwechheimer: for a nice conversation and good party.

❖ Damian Ploschik: for being nice and helping with thesis and good conversation.

❖ Ulrike Reisacher: for a nice conversation.

❖ Sergej Hermann: for being nice colleague and inviting me for watching volley ball.

❖ Christoph Bickmann: for nice greeting in every morning and good conversation.

❖ All instruments which helping me to collect all data for my thesis: Rudi, Fritz, Chantal, Schorsch, Stella, Cary, Flouri, Grape and Schmidt.

❖ My lovely family: for supporting me and cheer me up when I had a bad time, always there for me whenever I asked for. My dear love Marcel Merkel: for everything you have done; delicious breakfast and perfect coffee for every morning, massage, beautiful flowers every month and thank you very much for being beside me.

## Table of Contents

<b>1</b>	<b>Motivation and Objective</b> .....	<b>1</b>
<b>2</b>	<b>Theoretical background</b> .....	<b>5</b>
2.1	Bioorthogonal Chemistry.....	5
2.2.1	Copper-Catalyzed Azide-Alkyne cycloaddition (CuAAC).....	6
2.2.2	Diels-Alder reaction (DA) and inverse electron demand Diels-Alder reaction (IEDDA).....	12
2.2.3	Strain-Promoted Azide-Alkyne cycloaddition (SPAAC).....	18
<b>3</b>	<b>Results and Discussion</b> .....	<b>27</b>
3.1	Preparation of COMBO-modified oligonucleoside building blocks.....	27
3.2	Fluorescent labeling of COMBO-modified DNA.....	30
3.2.1	Spectroscopic experiments.....	31
3.3	Fluorescent labeling in living cells.....	38
3.3.1	Presynthetic fluorescent labeling in cells.....	40
3.3.2	Postsynthetic fluorescent labeling in cells.....	41
3.4	Enzymatic DNA synthesis.....	45
3.4.1	Preparation of COMBO-modified triphosphate ( <b>24</b> ).....	48
3.4.2	Primer extension experiment (PEX).....	50
3.4.3	Postsynthetic labeling of COMBO-modified DNA.....	53
3.5	Preparation of the 1,2,4-triazine-modified triphosphate ( <b>35</b> ).....	58
3.5.1	Primer extension and fluorescent labeling of triazine-modified DNA.....	60
<b>4</b>	<b>Conclusions</b> .....	<b>72</b>
<b>5</b>	<b>Experimental section</b> .....	<b>76</b>
5.1	Materials and Methods.....	76
5.2	Synthesis.....	83
5.2.1	Synthesis of COMBO-modified nucleoside ( <b>14</b> ).....	83
5.2.2	Synthesis of COMBO-modified nucleoside ( <b>19</b> ).....	89
5.2.3	Synthesis of COMBO-modified nucleotide triphosphate ( <b>24</b> ).....	99
5.2.4	Synthesis of triazine-modified nucleoside ( <b>34</b> ).....	102
5.2.5	Synthesis of triazine-modified nucleotide triphosphate ( <b>35</b> ).....	108
5.3	Solid-phase DNA synthesis.....	109

5.3.1	Synthesis.....	109
5.3.2	Purification, characterization and concentration Determination.....	112
5.3.3	Strain-Promoted Azide-Alkyne Cycloaddition.....	114
5.4	Enzymatic DNA synthesis.....	115
5.4.1	Primer extension experiments (PEX).....	115
5.4.2	Polyacrylamide gel electrophoresis (PAGE).....	118
5.5	Click reaction of COMBO-modified DNA with fluorescent dyes.....	119
5.6	Cell experiments.....	119
5.6.1	Pre- and postsynthetic fluorescent labeling in cells.....	119
<b>6</b>	<b>Literatures</b> .....	<b>121</b>
<b>7</b>	<b>Appendix</b> .....	<b>129</b>
7.1	Publications.....	129
7.2	Conferences.....	129
<b>8</b>	<b>Declaration of honor</b> .....	<b>131</b>

## List of abbreviations

°C	Degree centigrade
Å	Angstrom
abs.	Absolute
ACN	Acetonitrile
APS	Ammoniumperoxodisulfat
Ar	Aryl
a.u.	Arbitrary units
BARAC	Biarylazacyclooctynone
BCN	Bicyclo[6.1.0]nonyne
cm	Centimeter
CH <sub>2</sub> Cl <sub>2</sub>	Dichloromethane
Conc.	Concentration
COMBO	Carboxymethylmonobenzocyclooctyne
CPG	Controlled Pore Glass
CuAAC	Copper (I) Catalyzed Azide-Alkyne Cycloaddition
Da	Dalton
DA	Diels-Alder reaction
DAD	Diode array detector
dATP	Deoxyadenosine triphosphate
dCTP	Deoxycytidine triphosphate
DFT	Density Functional theory

DIBAC	Dibenzoazacyclooctyne
DIBO	Dibenzocyclooctyne
DIPEA	Diisopropylethylamine
DIFBO	Difluorinatedbenzocyclooctyne
DIFO	3,3-Difluorocyclooctyne
dGTP	Deoxyguanosine triphosphate
DMF	Dimethylformamide
DMSO	Dimethylsulfoxide
DMTr	Dimethoxytrityl
DNA	Deoxyribonucleic acid
dNTPs	Deoxynucleoside triphosphate
dTTP	Deoxythymidine triphosphate
DV	Deep Vent (-exo)
$\epsilon_{xxxnm}$	Extinction coefficient at xxx nm
EtOAc	Ethylacetate
EDTA	Ethylendiaminetetraacetate
EI	Electron ionization
eq	Equivalent
ESI	Electrospray ionization
EtOH	Ethanol
exc	Excitation
FAB	Fast Atom Bombardment
FC	Flash-Chromatography

Flu	Fluorescein
FP	Full length elongated product
g	Gram
GFP	Green Fluorescent Protein
h	Hour
HeLa	Henrietta Lacks
HBTU	2-(1H-Benzotriazol-1-yl)-1,1,3,3-tetramethyluronium hexafluorophosphate
HOBt	1-Hydroxybenzotriazole
HOMO	Highest Occupied Molecular Orbital
HPLC	High Performance Liquid Chromatography
HR	High Resolution
I	Intensity
IdU	5-Iodo-2'-deoxyuridine
iEDDA	Inverse Electron Demand Diels-Alder Cycloaddition
k	Second order rate constant
kcal	Kilo calories
KOD	Thermococcus kodakarensis
LED	Light-Emitting Diode
LUMO	Lowest Unoccupied Molecular Orbital
M	Molar
mA	Milliampere
MALDI	Matrix-assisted laser desorption/ionization
MeCN	Acetonitrile

MeOH	Methanol
mg	Milligram
MHz	Megahertz
min	Minute
ml	Milliliter
$\mu$ l	Microliter
$\mu$ M	Micromolar
NaPi	Sodium Phosphate Buffer
NEt <sub>3</sub>	Triethylamine
nm	Nanometer
NMR	Nuclear Magnetic Resonance
NT	Nucleotides
OCT	Cyclooctyne
p.a.	Pro analysis
PAGE	Polyacrylamide Gel Electrophoresis
PBS	Phosphate Buffer Saline
PEX	Primer Extension
Pfu	Pyrococcus furiosus
POCl <sub>3</sub>	Phosphorus oxychloride
ppm	Parts per million
quant.	Quantitative
Proton Sponge	<i>N,N,N',N'</i> -Tetramethyl-1,8-naphthalenediamine
Rho	Rhodamine dye

RNA	Ribonucleic acid
RP	Reverse Phase
rpm	Rotations per minute
rt	Room temperature
s	Second
SPAAC	Strain-Promoted Azide-Alkyne Cycloaddition
TBE	Tris-Borat-EDTA
TBTA	Tris[(benzoyl-triazolyl)methyl]amin
TCO	Trans-cyclooctene
TEAB	Triethylammoniumbicarbonate
TEMED	Tetramethylethyldiamine
TFA	Trifluoroacetic acid
THPTA	Tris[(hydroxypropyl-triazolyl)methyl]amin
THAP	2,4,6-Trihydroxyacetophenone
THF	Tetrahydrofuran
TMTH	Thiacycloheptyne
TRIS	Tris(hydroxymethyl-)aminomethane
on	Overnight
UV	Ultraviolet
V	Volt
V	Vent (-exo)
vis	Visible wavelength
W	Watt

The nomenclature used in this thesis is based on the Chemical Abstracts<sup>a</sup> and on the guidelines recommended by the IUPAC-IUB Commission<sup>b</sup>. Technical terms are written in italics.

<sup>a</sup> *Chemical Abstracts*, Index Guide, 77.

<sup>b</sup> IUPAC Commission on Nomenclature of Organic Chemistry (CNO) und IUPAC-IUB Commission on Biochemical Nomenclature (CBN), Tentative Rules for Carbohydrate Nomenclature, *Biochemistry* **1971**, 10, 3983-4004; *Eur. J. Biochem.* **1971**, 21, 455-477.





# 1 Motivation and Objective

Invention of the phase contrast microscope in 1930 resulting in the award of the Nobel Prize in Physics to *Frits Zernike*<sup>[1]</sup>, forefronted the development of a plethora of sophisticated microscope techniques that have now revolutionized the way in which the invisible becomes visible. Ever since the very first cellular structure was pictured, scientists have been fascinated by the investigation of the dynamic processes in living organism. The living cell is not a regular subject; in fact they contain the most complicated functions and complex systems. In order to develop a better understanding of the biological processes using microscopic techniques, some requirements should be considered; (I) the sensitivity of the detection, (II) the speed of acquisition and (III) the viability of the specimen. In addition, it is crucial to consider the cell's health during the imaging process which means not only staying alive but also to remain in a metabolic state with no nonspecific changes. Hence, the development of the visualized techniques has increased in number over the last decade. The fluorescence-based imaging technique has shown to be greatly beneficial over other techniques<sup>[2]</sup>. Live cell fluorescent imaging employs the naturally fluorophore (fluorescent proteins) or synthetically attaches to biomolecules (organic fluorescent dyes) with respect not to interfere with biological systems. The discovery of the naturally occurring green fluorescent protein (GFP) in the early 20<sup>th</sup> century, by the following who were awarded the Noble Prize in Chemistry in 2008; *Osamu Shimomura, Martin Chalfie, and Roger Tsien*<sup>[3]</sup>, revolutionized live cell imaging. Since then, the numerous applications have been reported. The fluorescent proteins (FPs) are considered as nontoxic compounds to cells. However, due to their large size, applications are limited. Recent studies found that the organic fluorophores have provided to be of great benefit to investigate biological processes where the small size of fluorescent probes are required<sup>[4]</sup>. Regarding the labeling process occurring inside cells, it is crucial that the small size of fluorophores do not alter the natural behavior of the molecule, are nontoxic and react selectively with the introduced target molecule under physiological conditions. The conjugation of the fluorescent marker with the reactive partner inside cells has been intensively investigated to date, since the first discovery of bioorthogonal chemistry strategies were reported in 2008 by the group of *Bertozzi*<sup>[5]</sup>. Bioorthogonal reactions are most

promising for evaluating live cell imaging with the advantage of the fluorescence properties of the fluorophore which can be manipulated by the simple chemical reaction and while reaction rate can be tuned by the selection of reactive partners towards the requirement. The ligation between azides and strained alkynes, so called Strain-Promoted Azide-Alkyne Cycloaddition (SPAAC), is the most promising method for probing live organisms. The advantages of this strategy are its reaction with exceptional reaction rate ( $k \approx 2.4\text{-}4000 \times 10^{-3} \text{ M}^{-1}\text{s}^{-1}$ ) without employing any metal catalyst [6] and proceeding smoothly under physiological conditions (37 °C, aqueous media or cells lysate) (Figure 1).

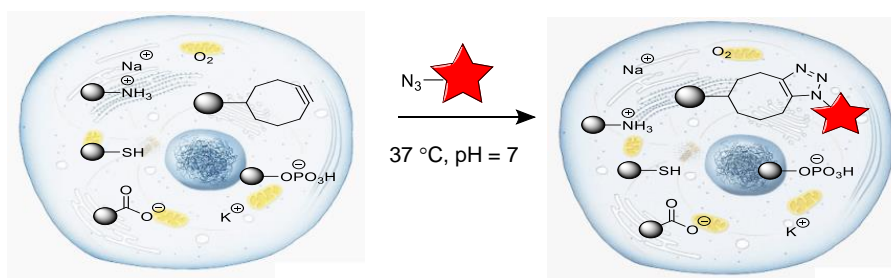


**Figure 1** Bioorthogonal conjugation of reactive functionalized biomolecules in the presence of an abundance biocompatible functional groups.

In this thesis Strain-Promoted Azide-Alkyne cycloaddition reaction (SPAAC) of reactive cyclooctyne- and triazine-modified oligonucleotides with fluorescent dyes will be investigated by both pre- and postsynthetic labeling manners. The SPAAC is a powerful tool for evaluating complex biological processes [7]. This is because of the smooth conjugation when performing under physiological conditions (37 °C, aqueous media or cells lysate), without employing metal catalysts (“copper-free click” reaction) or using high temperatures and a high selectivity towards their reaction partners in the presence of an abundance of nucleophilic groups (in living cells). In addition, the reaction rate constant can be tuned by simple chemical reactions to offer a reaction rate ( $k \approx 2.4\text{-}4000 \times 10^{-3} \text{ M}^{-1}\text{s}^{-1}$ ) which is compatible with biological processes [6]. In order to investigate the capability of structurally simple reactive compounds as biological markers, the carboxymonobenzocyclooctyne (COMBO) **7** and the 3-carboxy-1,2,4-triazine moieties **32** will be attached to position 5 of

2'-deoxyuridine. The corresponding building blocks can be incorporated into DNA via chemical DNA synthesis (by the advances of phosphoramidite method) (Figure 2) or enzymatic DNA synthesis by the use of polymerases (primer extension of unprotected base-modified 2'-deoxyuridine triphosphates) (Figure 3). The corresponding base-modified DNA will further be conjugated with the corresponding reaction partners in both *in vitro* and *in vivo* experiments.

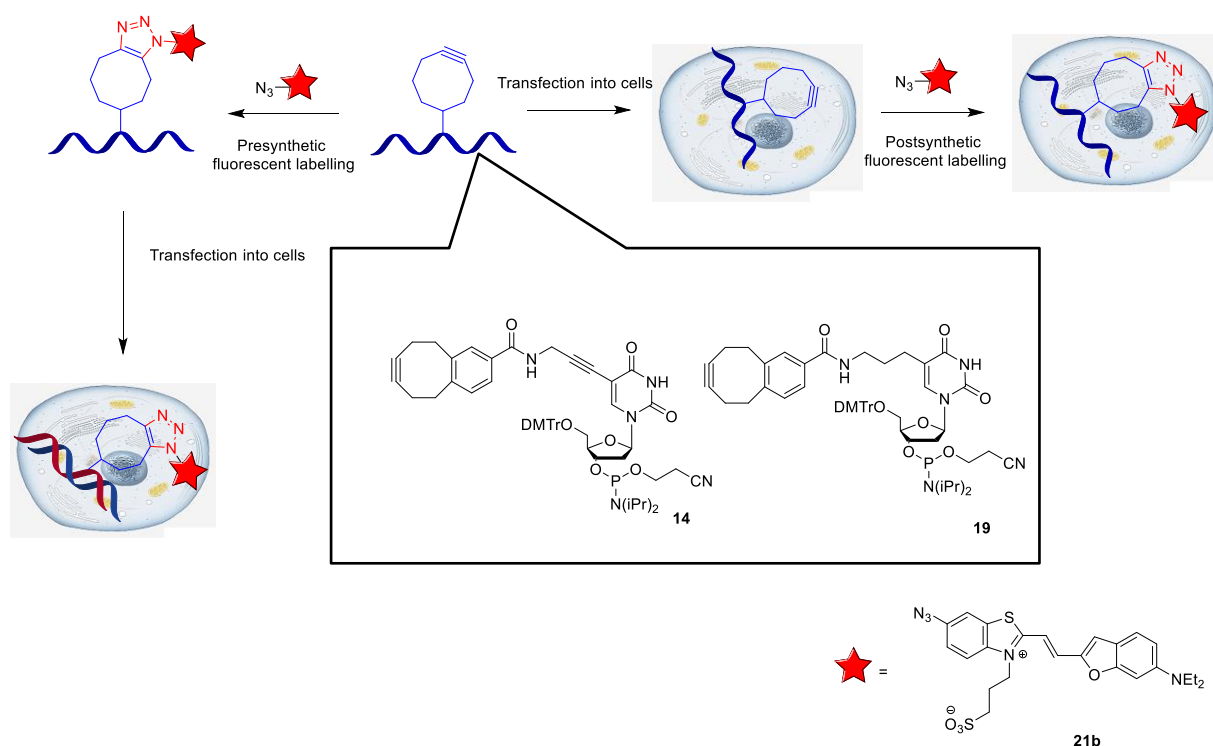


**Figure 2** Strain-promoted reaction of cyclooctyne-modified DNA with azide-modified fluorescent dye **21b** *in vitro* and *in vivo* experiments.

The incorporation of base-modified nucleoside triphosphates using a polymerase has more advantages over solid-phase DNA synthesis, as the defined incorporation of different building blocks into one strand is possible by replacing the natural triphosphate monomers. Also many of different strands can be synthesized via selection of the template strand, and long-stranded DNA/RNA can be synthesized (10 kb - 70 kb) [8] without a significant decrease in its efficiency. Moreover, it is applicable for sensitive moieties which are not able to withstand the harsh conditions

of solid-phase synthesis. In this approach, the base-modified 2'-deoxyuridine triphosphate building blocks **24** and **35** will be singly and multiply incorporated into DNA and subsequently conjugated with their reactive partner.

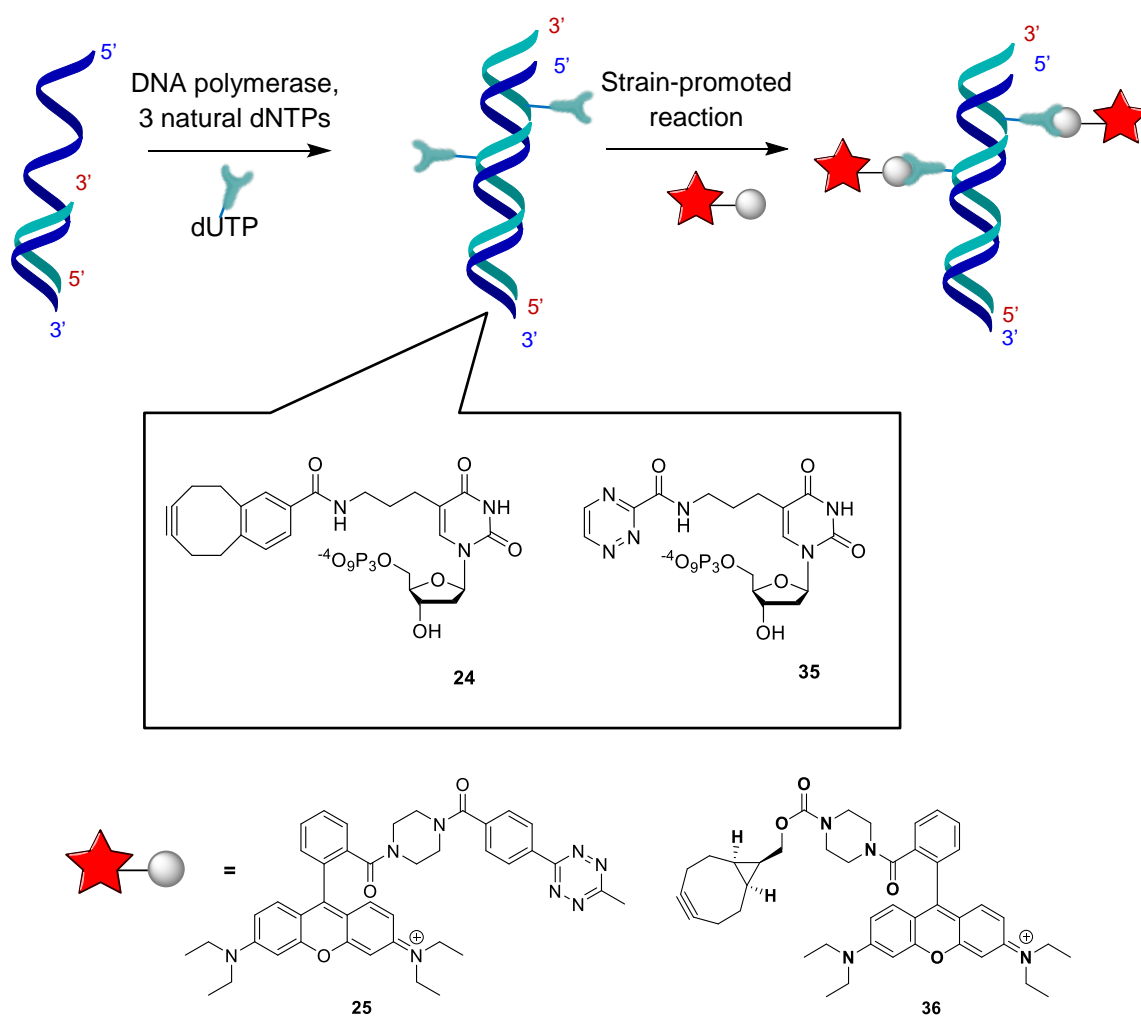


**Figure 3** Enzymatic DNA synthesis (primer extension experiment) of base-modified nucleoside triphosphates. The extension product will further be ligated with fluorescent dyes under physiological conditions.

## 2 Theoretical background

### 2.1 Bioorthogonal Chemistry

Bioconjugation is the process of linking two or more reactive compounds, at least one of them being a biomolecule, under physiological conditions. The term bioorthogonal chemistry was originally coined by *Bertozzi* [5]. It denoted that “*it neither interacts with nor interferes with a biological system*”. Additionally, the participating functional groups must conjugate with high chemo-selectivity towards biocompatible conditions, minimally perturbing the biological system into which it has been introduced and being nontoxic to the living cell (Figure 4).

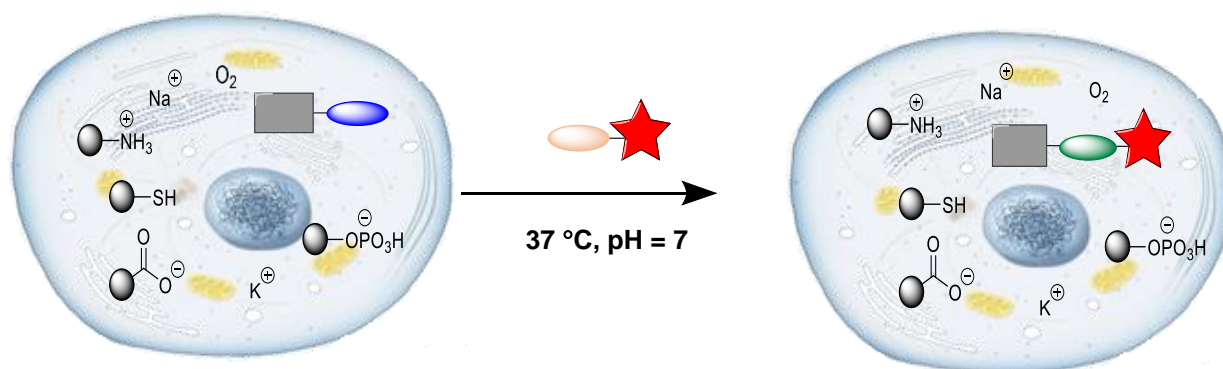


**Figure 4** A general bioorthogonal conjugation of reactive functionalized biomolecules in the presence of an abundance biocompatible functional groups.

The very first example of a bioorthogonal reaction was demonstrated by *Rideout* and co-workers. The condensation of hydrazine and an aldehyde could be selectively harnessed to assemble toxins from inactive prodrugs within living cells [9]. In the late 1990s, *Tsien* and co-workers reported the first example of live cell protein labeling by using bisarsenical dyes [10]. Since then various bioorthogonal reactions have been intensively investigated and demonstrated as an instrument for biological discovery and biotechnology, allowing for selective and controlled introduction of labels [11]. The various bioorthogonal ligation strategies are not only applicable for protein labeling but also on cell surface, in living cells and even in live animal. Including ketones and

aldehydes <sup>[12]</sup>, azides (Staudinger ligation <sup>[13]</sup>, Copper-Catalyzed Azide-Alkyne Cycloaddition <sup>[14]</sup> and Strain-Promoted Azide-Alkyne Cycloaddition <sup>[15]</sup>), nitrones <sup>[16]</sup>, nitrile oxides <sup>[17]</sup>, diazo compounds <sup>[18]</sup>, alkenes <sup>[19]</sup> (Electron demand Diels-Alder reaction), tetrazines <sup>[20]</sup> (Inverse electron demand Diels-Alder reaction) and tetrazoles <sup>[20e, 21]</sup> (“Photoclick” reaction). Although, considerable research on bioconjugation has been demonstrated and can be utilized for studying biological processes, only few examples were reported in the field of nucleic acids <sup>[7c, 22]</sup>.

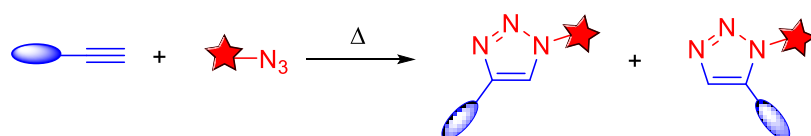
## 2.2 Bioorthogonal reactions

### 2.2.1 Copper-Catalyzed Azide-Alkyne Cycloaddition (CuAAC)

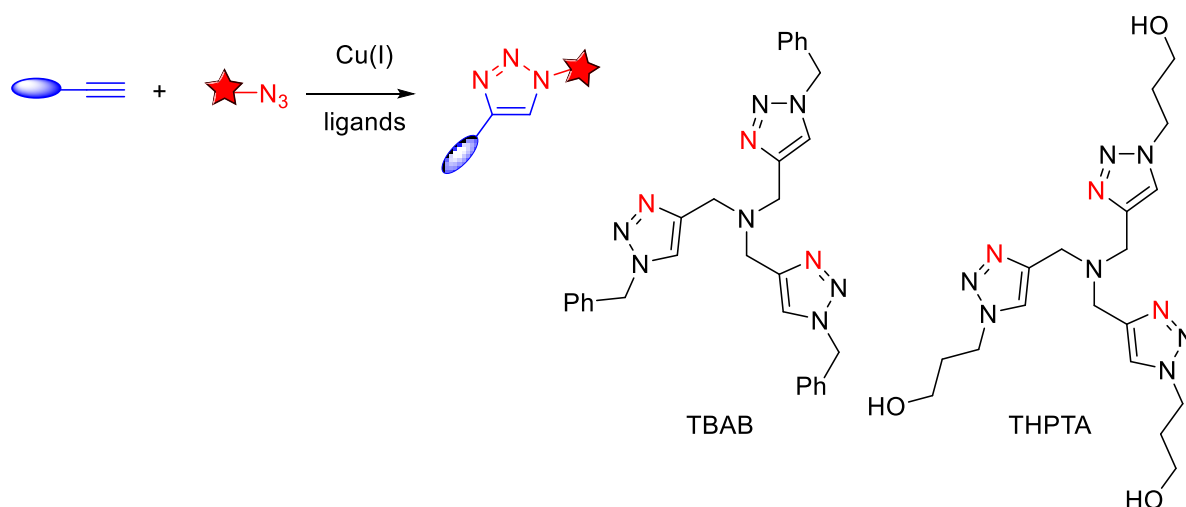
In the middle of 20<sup>th</sup> century *Huisgen* reported the first synthesis of 1,2,3-triazole from 1,3-dipolar cycloaddition reaction of diethyl acetylenedicarboxylate and phenyl azide to provide a mixture of 1,4- and 1,5-disubstitution products <sup>[23]</sup>. Despite the reaction providing a high yield and selective control of the regioselectivity by the introduction of steric hindrance of substituents on substrates and the polarity of solvent, a high temperature is needed (100 °C) <sup>[24]</sup> and is proceeded with a low reaction rate <sup>[25]</sup>. It was *Sharpless* and *Meldal* who independently discovered the use of copper to catalyze the ligation reaction of an alkyne and an azide to increase the reaction rate constant (may increase up to 7 orders of magnitude regarding uncatalyzed version,  $k \approx 10\text{-}200 \text{ M}^{-1}\text{s}^{-1}$ ) as well as the regioselectivity (only 1,4-triazole is formed) <sup>[26]</sup>. Since then the numerous applications of CuAAC have been reported in various fields such as polymer and material science <sup>[27]</sup>, drug discovery <sup>[26a, 28]</sup>, chemical biology <sup>[29]</sup> and bio-imaging <sup>[14c]</sup>. The most attractive benefit of using CuAAC as a bioorthogonal tool are (I) neither azide nor terminal alkyne functional groups can be attached to oligonucleoside building blocks therefore allows the incorporation into DNA via automated solid-phase synthesis with high efficiency, (II) tolerance of a broad range of functional groups which can be applied in *in vivo* when a variety of reactive functional groups are present and (III) significant increase in reaction rate with respect to the uncatalyzed version and smooth proceeding under physiological

conditions to form regioselective 1,4-disubstituted triazole products. However, the major drawback of the use of CuAAC is that copper ions are highly toxic which causes DNA damage, typically yielding strand breaks <sup>[30]</sup>, causing cell death, preventing cell division, and killing small organisms (zebrafish embryos) <sup>[31]</sup>. Thus, introducing of suitable ligands like tris(benzyl)triazolymethyl amine (TBTA) and their water soluble derivatives tris(hydroxypropyl)triazolymethyl amine (THPTA) can overcome this problematic issue <sup>[32]</sup> (Scheme 1).

**A) Huisgen 1,3-dipolar cycloaddition**



**B) Copper-catalysed 1,3-dipolar cycloaddition**



**Scheme 1** The ligation reaction of terminal alkynes and azides: **A)** Huisgen 1,3-dipolar cycloaddition, **B)** Copper-Catalyzes Azide-Alkyne Cycloaddition.

Since then a significant increase in the number of applications using the CuAAC reaction as a novel methodology to label and modify DNA have been reported <sup>[33]</sup>. Oligonucleotides can be labeled with reactive functional groups via two strategies, so

called presynthetic and postsynthetic labeling (Figure 5). Presynthetic labeling signifies that the nucleoside monomer carries the desired label before DNA synthesis. However, the major drawback of this strategy is that phosphoramidites bearing the desired moieties need to be stable enough to survive the harsh conditions employed during automated solid phase synthesis (acidic, alkaline and oxidative condition). An alternative method to label the DNA of interest is the so called postsynthetic labeling, which denotes that the modification process occurs after completion of DNA synthesis<sup>[29a]</sup>. Sensitive or reactive moieties can be coupled with the DNA of interest without any critical conjugation steps needed. Moreover, changing to another label does not require a challenging nucleotide synthesis. According to these advantages, a wide range of biomolecules has been labeled to date, including proteins<sup>[34]</sup>, polysaccharides<sup>[35]</sup>, peptides<sup>[36]</sup> and even living cells<sup>[37]</sup>.

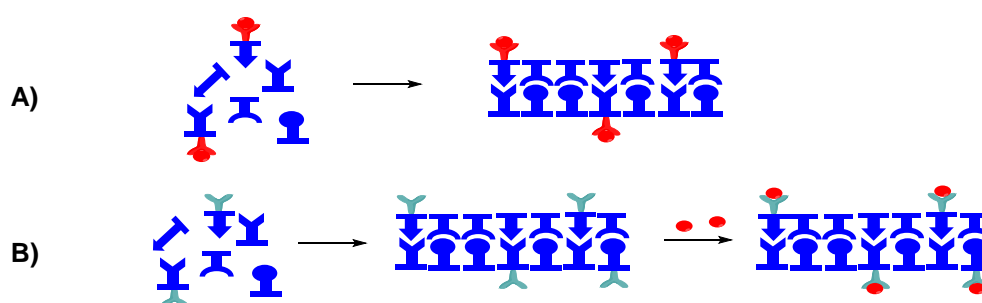
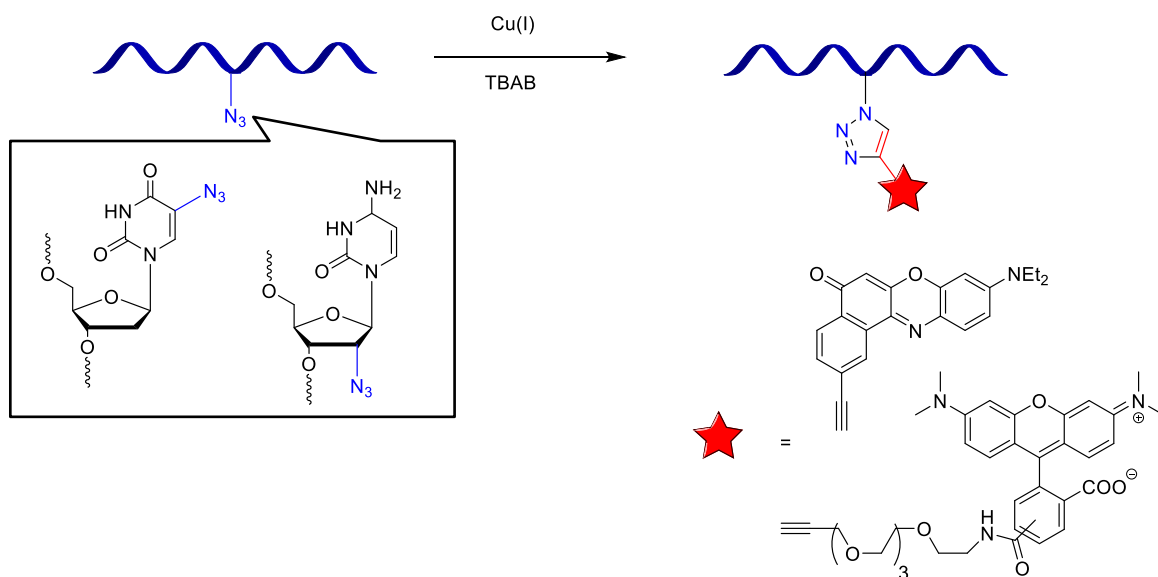


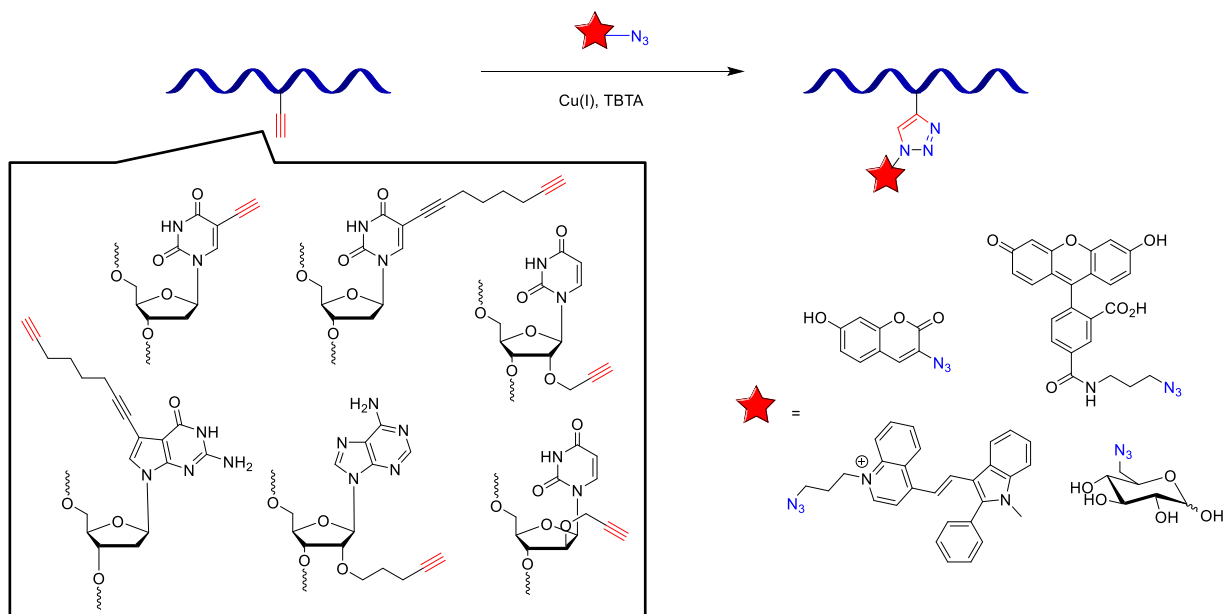
**Figure 5** Schematic representation for presynthesis; **A)** blue: nucleotides, red: markers) and postsynthesis, **B)** blue: nucleotides, green: reactive functional groups, red: marker).

Recently, the modification of nucleoside building blocks as biological markers has gained more interest of scientists in the fields of chemical biology and bioimaging. Azide or alkyne functional groups have been introduced into oligonucleoside monomers either at 5-position for pyrimidines and 7-position for 7-deazapurines or the sugar backbone at 2'-position in the ribofuranoside unit. It is noteworthy that the azide-modified building blocks are intrinsically difficult to incorporate into DNA via solid-phase chemistry, as azides are prone to be reduced by the phosphorus (III) atom of phosphoramidites. These limitations prohibit the accessible incorporation of azide-modified DNA via solid-phase DNA synthesis. The very first example of azido-modified on oligonucleotide was reported by the group of *Wagenknecht* and co-workers [38]. 5-Iodo-2'-deoxyuridine was introduced into oligonucleotides via solid-phase synthesis with further *in situ* nucleophilic substitution by  $\text{NaN}_3$ . The corresponding azide-modified DNA was further conjugated with a compatible fluorescent dye (Scheme 2). Another method was reported by the group of *Micura* [39]. They proposed a novel synthetic method for phosphodiester building blocks of 2'-azido-modified nucleosides which allows efficient site-specific incorporation into RNA by using standard solid-phase RNA synthesis.



**Scheme 2** Copper-Catalyzed Azide-Alkyne Cycloaddition of azide-modified oligonucleotides with fluorescent probes for bioorthogonal labeling.

Regarding the critical step which is needed for the modification of azide moieties on nucleosides, alkyne-modified nucleoside building blocks were chosen as alternative component. *Carell et al.* reported the modification of alkyne-modified DNA at C5 of 2'-deoxyuridine as a reactive partner towards azido-fluorescent probes<sup>[40]</sup>. The high-density labeled DNA was then coupled with azide fluorescent markers, in particular coumarin azides, azido-sugar and fluorescein azides as a strong fluorescent label for use in biophysical applications<sup>[41]</sup> (Scheme 3). The group of *Seela* and co-workers introduced long chain linkers into C5 of pyrimidine and C7 of purine in particular, propynyl and octadiynyl residues which showed a positive influence on the duplex stability by increasing the thermal stability by 2-3 °C per modification, in comparison to unmodified nucleotide strand<sup>[42]</sup> (Scheme 3). An alternative position is at 2'-ribofuranoside, *Wagenknecht et al.*, reported the utilization of CuAAC tool for postsynthetic fluorescent labeling of DNA by incorporation of 2'-propargyluridine into DNA via solid-phase synthesis which is further conjugated with fluorescent coumarin dyes<sup>[43]</sup>. Later studies demonstrated that the configuration of the 2'-propargyl-modified uridine plays an important role in improving the fluorescence and energy transfer properties. The 2'-propargyl-modified arabino-configured uridine was introduced into DNA using phosphoramidite method and conjugated with a set of photostable cyanine-styryl dyes for the FRET pairs in DNA duplex which can be applied for two-color read out in both *in vitro* and *in vivo*<sup>[44]</sup>. Independently, the group of *Floris L. van Delft* proposed acetylene modified adenosines as versatile building blocks for a variety of oligonucleotide hetero- and homoconjugates<sup>[30]</sup>. The alkyne-modified oligonucleotide was linked via [3+2] cycloaddition with azido-fluorescent dyes under mild and efficient reaction conditions. These make the variation of alkyne-modified nucleoside building blocks crucial for the bioconjugation applications.

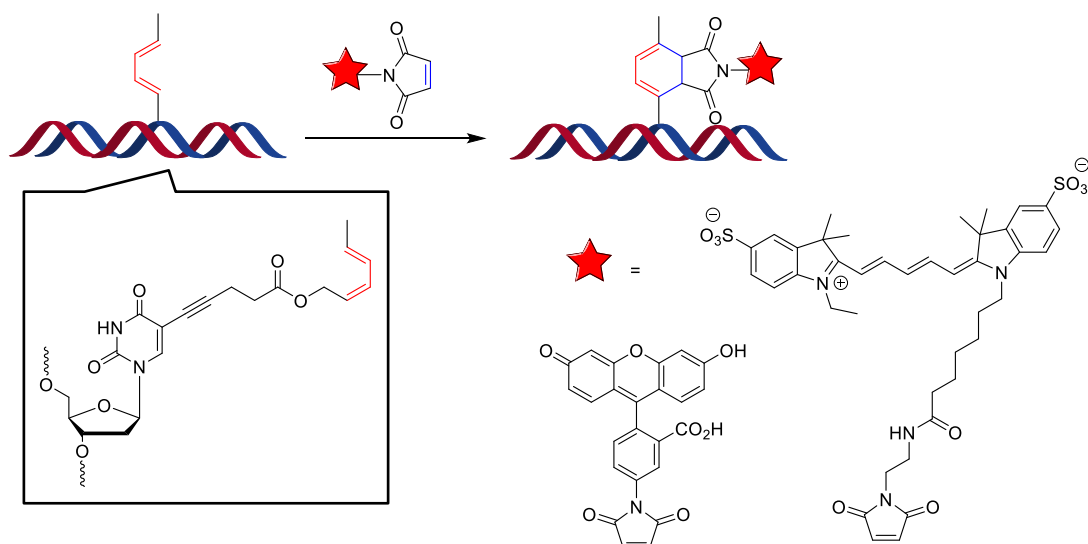


**Scheme 3** Alkyne-modified oligonucleotides for bioorthogonal “click” reaction to azido-fluorescent markers.

In spite of the fact that numerous applications of CuAAC were reported, the use of highly toxic copper catalyst has limited the capability to evaluate biological systems. Regarding the toxicity issue, there are intensively investigated alternative methods, so called metal-free catalyzed cycloaddition reaction including the “Photoclick” reaction, Diels-Alder (DA), Inverse electron demand Diels-Alder reaction (IEDDA) and Strain-Promoted Azide-Alkyne Cycloaddition (SPAAC), in particular.

### 2.2.2 Diel-Alder reaction (DA) and Inverse electron demand Diels-Alder reaction (iEDDA)

The Diels-Alder reaction is defined by a [4+2] cycloaddition between a  $4\pi$  electron system (a diene) with a  $2\pi$  electron system (a dienophile) to form a new stereospecific six-membered ring product <sup>[45]</sup>. The Diels-Alder reaction is controlled by the energy gap between the highest occupied molecular orbital (HOMO) and the lowest unoccupied molecular orbital (LUMO) of the substrates. The reaction rate can be enhanced by lowering the HOMO-LUMO energy gap of the substrates by either introducing electron-withdrawing groups or electron-donating groups on substrates or increase the ring strain of the system. The DA can be classified as normal electron-demand (HOMO-diene) or inverse electron-demand (LUMO-diene) based on the frontier molecular orbitals which take part. The most commonly employed dienophile for the normal electron-demand Diel-Alder reaction (DA) are maleimide derivatives (electron-poor alkenes) <sup>[46]</sup>. These reactive alkenes react smoothly with various conjugated dienes however, due to the high reactivity; it spontaneously reacts with an abundance of nucleophiles occurring in living organisms. The group of *Howorka* reported the use of DA for DNA labeling, where the diene-modified deoxyuridine was incorporated into DNA via primer extension experiment and subsequently conjugated with a maleimide-modified fluorescent dye <sup>[47]</sup> (Scheme 4).



**Scheme 4** The Diels-Alder reaction between diene-modified DNA and a set of maleimide-modified fluorescent dyes.

The latter reaction type is the Inverse electron demand Diels-Alder reaction (IEDDA), classified by the electron-poor diene (LUMO) reacting with the electron-rich dienophile (HOMO). The use of IEDDA for bioorthogonal reactions was first independently reported by *Fox et al.* and *Devaraj* <sup>[20a, 48]</sup>. The ligation of the electron deficient 1,2,4,5-tetrazine conjugated with *trans*-cyclooctene or norbornenes to generate the pyridanzine adducts <sup>[20b]</sup>. The IEDDA type is the most promising for bioorthogonal reactions with the advantages of proceeding within unusually fast reaction rates ( $k \approx 1 \cdot 10^5 \text{ M}^{-1} \text{ s}^{-1}$ ) without employing any metal catalyst <sup>[49]</sup> and performing in various reaction media like water, organic solvents, cell media and cell lysates at ambient temperature. Recently, tetrazine moieties were investigated and applied as bioorthogonal tools for elucidating biological functions in living cells and live organisms <sup>[20a, b, 50]</sup>.

The prior results indicated that the magnitude of the reaction rate constant can be increased by the manipulation of electronic and steric effect on the tetrazine scaffolds. Firstly, the LUMO energy of the diene can be lowered by the introduction of heteroatoms (N or O) or by substitution of the electron-withdrawing group [49, 51]. Another possibility is to raise the HOMO energy of the dienophile by substitution with the electron-donating groups or increasing the ring strain on the system [52] (Figure 6).

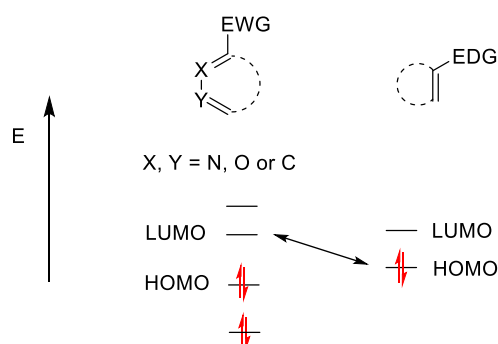
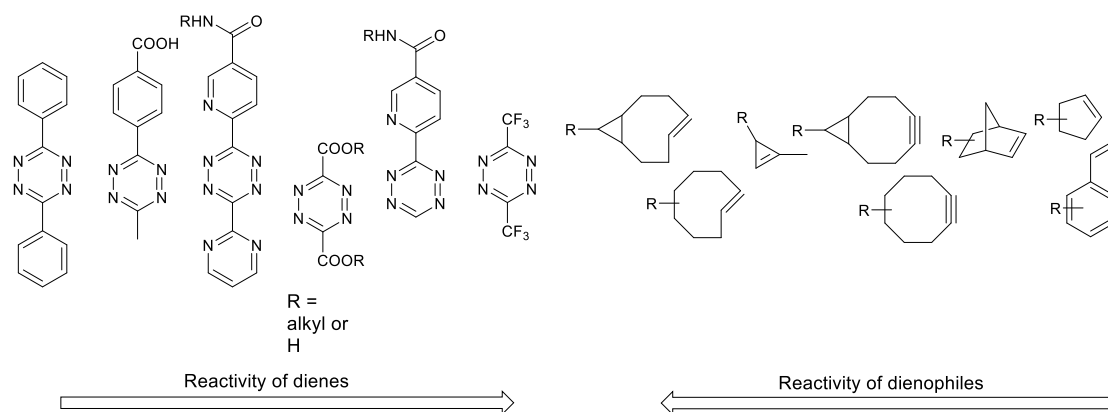


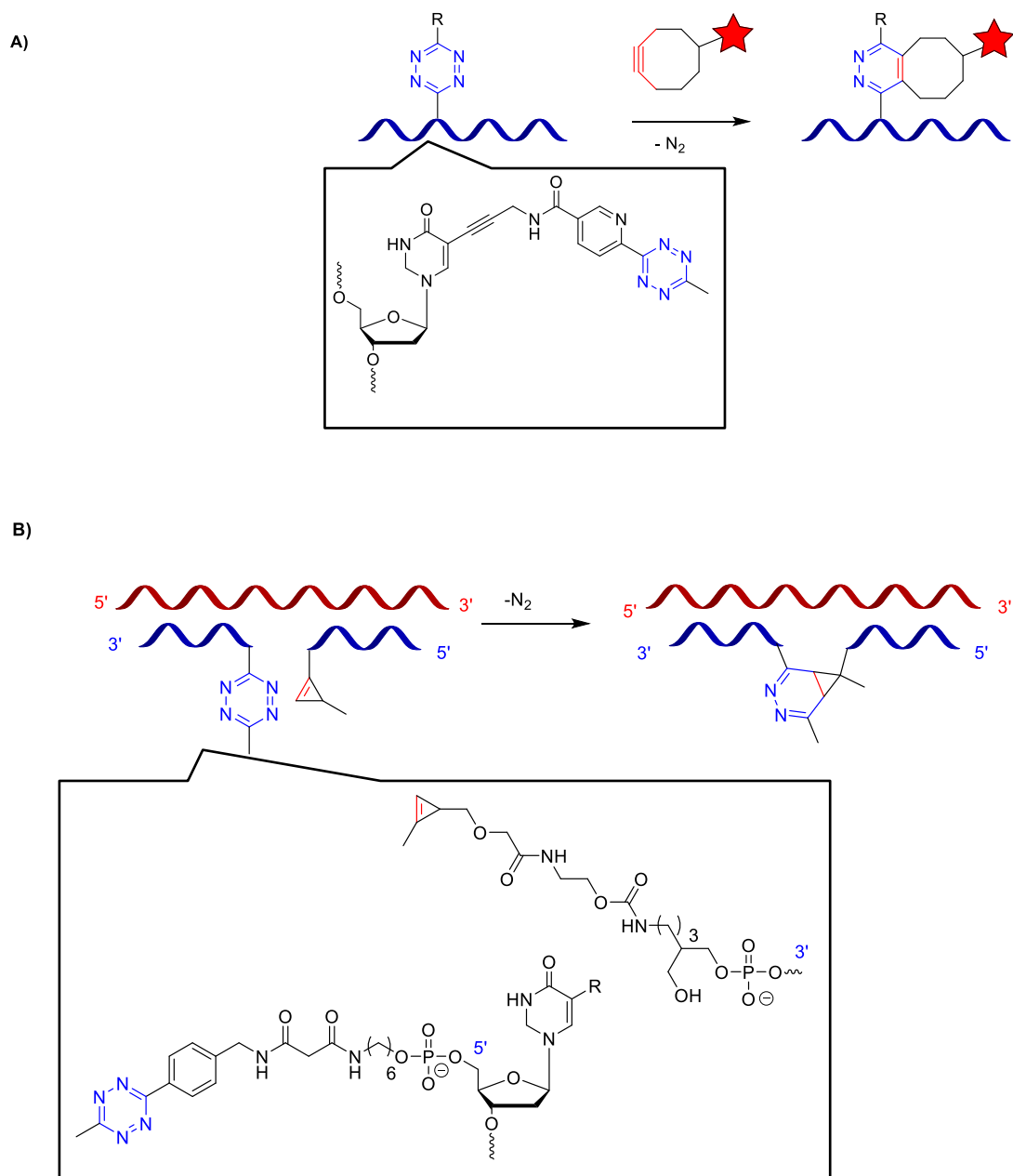
**Figure 6** Frontier orbitals in Inverse electron demand Diels-Alder reactions.

Secondly, the steric demand on the tetrazine derivatives play an important role towards the dienophile partners, *Kele et al.* revealed that the introduction of steric hindrance substituents in close proximity to the reactive center play an important role towards the reactivity of the ligation. The results revealed that the reaction rate constant of the monosubstituted tetrazine compartments ( $k \approx 240 \times 10^{-3} \text{ M}^{-1}\text{s}^{-1}$ ) react approximately 30 times faster than that the disubstituted scaffolds ( $k \approx 8 \times 10^{-3} \text{ M}^{-1}\text{s}^{-1}$ ) [53]. Therefore the reactivity trend of the tetrazine scaffolds and the dienophile derivatives have been investigated by several research groups [52, 54] (Scheme 5).



**Scheme 5** Structure and reactivity trend of the tetrazine scaffolds and the dienophile derivatives.

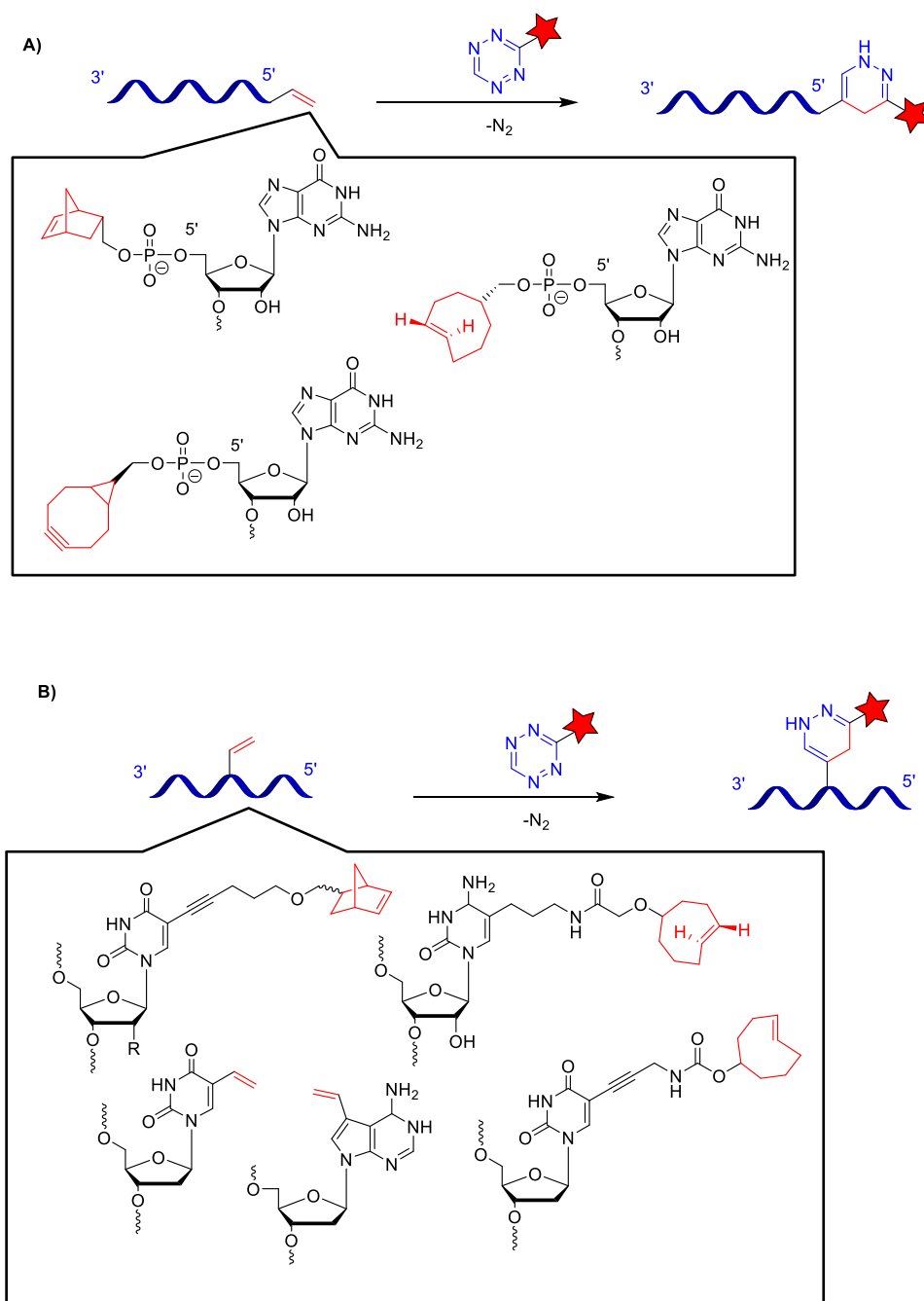
Despite the reaction rate constant of the tetrazine ligation which was found to be extraordinarily fast (in fact, the fastest bioorthogonal reaction rate reported to date,  $k \approx 1 \cdot 10^5 \text{ M}^{-1} \text{ s}^{-1}$ ) [52a, 54]. Conversely, due to the lack of stability toward the harsh conditions of chemical DNA synthesis along with the basic conditions for the cleavage step of the solid-phase, only a few examples of this labeling methodology were published. *Wagenknecht et al.*, was the first to report the tetrazine-modified DNA for fluorescent labeling using phosphoramidite method [53]. The tetrazine-modified 2'-deoxyuridine phosphoramidite was incorporated into DNA via automated solid-phase DNA synthesis and the corresponding DNA was then on-bead labeled with COMBO-modified fluorescein dye (Scheme 6A). Another approach was demonstrated by the group of *Devaraj* and co-workers [55]. The DNA bearing tetrazine moiety at the 5'-end was rapidly ligated with cyclopropene-modified DNA by the advances of DNA/RNA template-dependent ligation (Scheme 6B).



**Scheme 6** A) On-bead postfluorescent labeling of tetrazine-modified DNA with cyclooctyne fluorescent dye, B) Template-dependent ligation of tetrazine-modified DNA with DNA bearing cyclopropane partner.

An alternative strategy involves the introduction of dienophiles as DNA and RNA modifications that can later be postsynthetically labeled with tetrazine-modified dyes or biological compounds. The first example was evaluated by the *Jäschke* group<sup>[56]</sup> and others<sup>[57]</sup>. The dienophile-modified building blocks have been

incorporated into DNA or RNA at 5'-end or in the middle of strands, either via solid-phase synthesis or primer extension using the polymerases. This novel strategy allows the further postsynthetic labeling with biological or fluorogenic compounds (Scheme 7).



**Scheme 7** A) iEDDA of the dienophile-modified RNA at the 5'-terminus with fluorescent tetrazine-modified dyes. B) DNA and RNA bearing dienophile compartment for iEDDA reactions.

### 2.2.3 Strain-Promoted Azide-Alkyne Cycloaddition (SPAAC)

The first discovery of a “copper-free click” reaction was reported in the 19<sup>th</sup> century by *Blomquist* and *Lui* [58]. Together with the results from *Wittig* and *Krebs* [59] which denoted that ring strained cyclooctynes underwent explosive [3+2] cycloaddition with phenylazide without employing a metal catalyst or high temperatures [58] to give a single product; the triazole. Since then, the concept of metal-free catalyzed azide-alkyne cycloaddition has been developed and is well known as Strain-Promoted Azide-Alkyne Cycloaddition (SPAAC). It was the group of *Bertozzi* who first realized the potential of cycloalkynes as dipolarophiles towards azide moieties for bioorthogonal reactions for living cell imaging [15a, 60] (Figure 7).

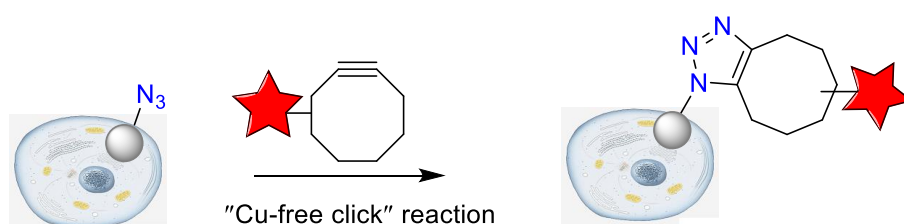


**Figure 7** Strain-Promoted Azide-Alkyne Cycloaddition (SPAAC).

Since the demonstration of the use of cyclooctyne in living cells, a number of applications of SPAAC as a tool to evaluate biological processes such as protein-protein interactions [61], determining DNA modifications [62] and cell visualization in zebrafish [22b] and mice [7c] has been published in the last decade. According to prior reports the improvement of the cyclooctyne reactivity by mean, both the reaction rate constant and lipophilicity had been investigated by many research groups [60, 63]. However, the designs of new cyclooctynes which can react with a high reaction rate and have a high solubility in aqueous media are still difficult.

Many structural perturbations affecting more than one contributor to reactivity must be understood in order to be optimized to achieve the desired outcome. The major characteristics are steric effects (triple bond and azide moiety), the strain angle (distortion bond angle) and the electronic influence on transition state (orbital interaction). The empirical data and a DFT-based distortion/interaction transition state model of a set of 1,3-dipolar cycloadditions were investigated by *Bertozzi* and co-workers<sup>[64]</sup>. The results show that the reactivity can be tunable and predictable by the advances of the relationship between the bond angles of substrates in the transition state and the overlap of their orbitals (Figure 8).

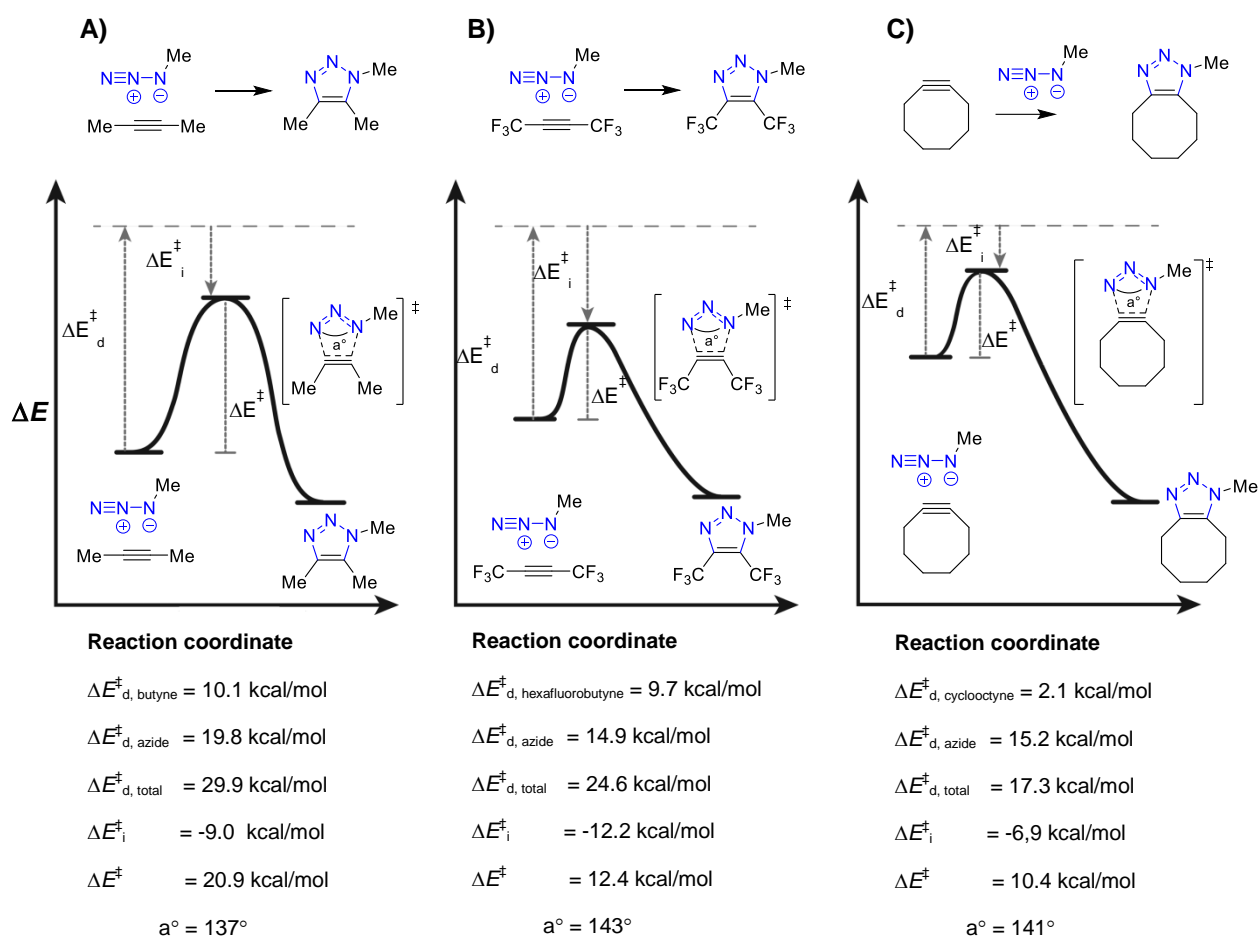


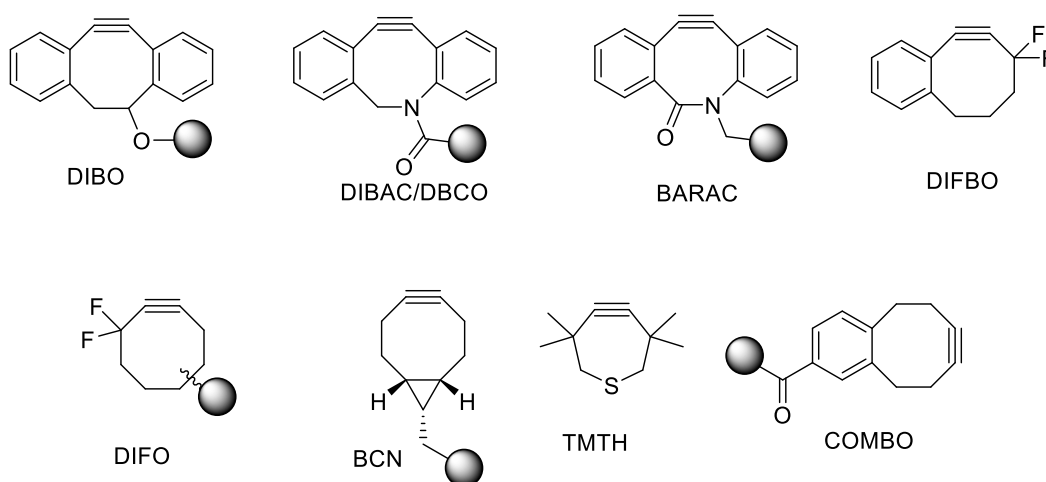
**Figure 8** Distortion/interaction model of 1,3-dipolar cycloaddition: **A)** activation energy ( $\Delta E^\ddagger$ ) for the reaction between methyl azide and 2-butyne, **B)** azide and hexafluorobutyne, **C)** cyclooctyne and azide.

The distortion/interaction energy was calculated by using density functional theory (DFT) model and performed by using B3LYP/6-31G. In this calculation, the activation energy of a reaction was deconstructed into two components which are the distortion energy, that is dependent on ground state strain and the interaction energy which is governed by transition state electronics. In this model, the transition state energy ( $\Delta E^\ddagger$ ) of a reaction is defined as the sum of distortion energies ( $\Delta E_d^\ddagger$ ), the energy required to distort the alkyne and azide into their preferred transition state conformations, and interaction energy ( $\Delta E_i^\ddagger$ ), the energy lowering upon favorable orbital overlap between the azide and alkyne (Equation (1)).

$$\Delta E^\ddagger = \Delta E_d^\ddagger + \Delta E_i^\ddagger \quad (1)$$

Thus, the reactivity of the cycloaddition can be tuned by changing either the distortion energy ( $\Delta E_d^\ddagger$ ) or the interaction energy ( $\Delta E_i^\ddagger$ ). The 1,3-dipolar cycloaddition of 2-butyne, hexafluoro-2-butyne and cyclooctyne with methyl azide were selected as a model. In a case of 2-butyne with methyl azide, the results show that 29.9 kcal/mol energy is required to distort the ground state of substrates into the preferred transition state conformations. Upon distortion, the alkyne and azide interaction are lowering the energy of the overall system by -9.0 kcal/mol through favorable orbital overlapping. Combining the effects of distortion and interaction, the overall transition state activation energy is 20.9 kcal/mol ( $\Delta E^\ddagger = \Delta E_d^\ddagger + \Delta E_i^\ddagger$ ). In order to compare the electronic perturbation, it can affect the interaction and the distortion energies in the transition state. The activation energy for hexafluoro-2-butyne was investigated. The result showed that the overall activation energy ( $\Delta E^\ddagger$ ) is 12.4 kcal/mol which was 8.5 kcal/mol less than that in a case of 2-butyne which reveals that the hyperconjugative donation from the in-plane alkyne  $\pi$ -system to the  $\sigma^*_{C-F}$ -orbital directly leads to transition state stabilization<sup>[65]</sup>. In a case of cyclooctyne moieties, the alkyne bond angles in cyclooctyne are already bent from linearity, and the molecule, therefore is destabilized relatively to a linear isomer.

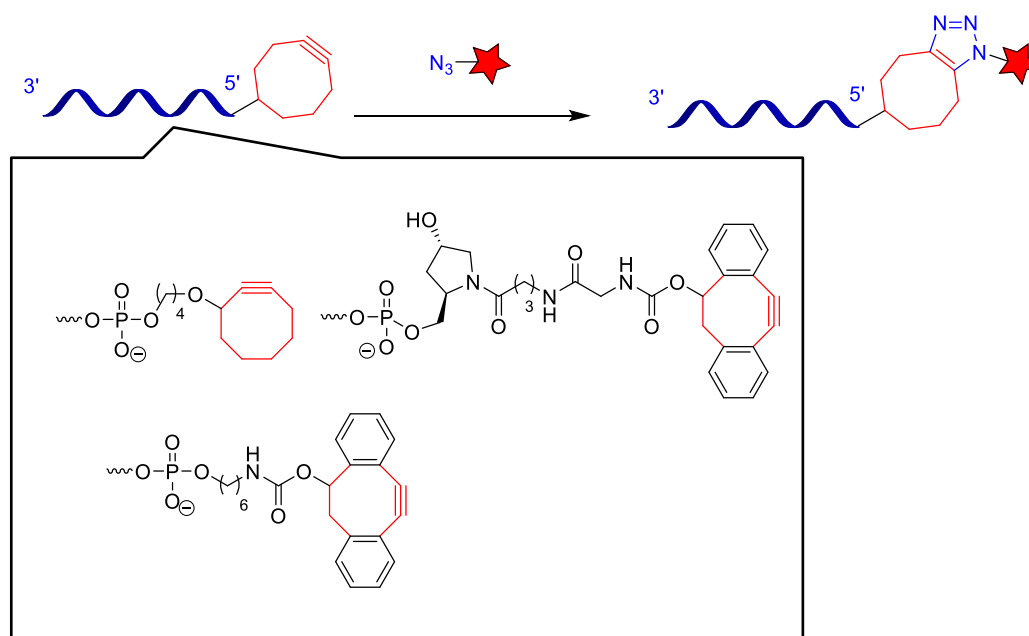
Thus in the transition state, cyclooctyne requires less distortion energy to reach the preferred geometry than those of linear alkynes ( $\Delta E_{d, 2\text{-butyne}}^{\ddagger} = 10.1$  kcal/mol and  $\Delta E_{d, \text{cyclooctyne}}^{\ddagger} = 2.1$  kcal/mol). As a result of the significant reduction in distortion energy, cyclooctyne displays a lower overall activation energy than those of 2-butyne and hexafluoro-2-butyne substrates. According to the DFT-based distortion/interaction transition state model, numerous new ring strain cycloalkyne compounds were reported. In general, two classes of cyclooctyne's can be recognized; aliphatic and (di)benzoannulated cyclooctynes with respect to a high reaction rate together with less lipophilicity (Scheme 8).



**Scheme 8** Structure of ring strained derivatives; dibenzocyclooctyne (DIBO), dibenzoazacyclooctyne (DIBAC), biarylazacyclooctynone (BARAC), difluorobenzocyclooctyne (DIFBO), difluorinated cyclooctyne (DIFO), bicyclo[6.1.0]nonyne (BCN), carboxymethylmonobenzocyclooctyne (COMBO) and tetramethylthiacycloheptyne (TMTH).

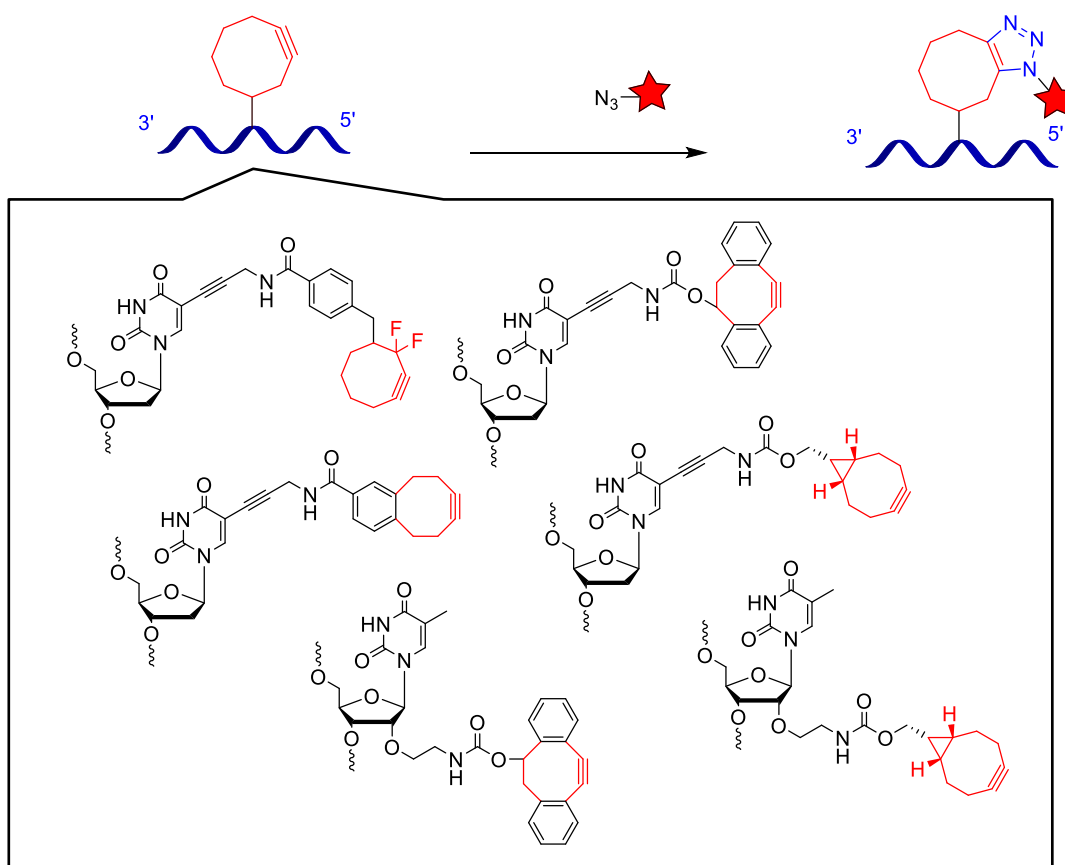
The high reaction rate constant can be achieved by dibenzoannulation on the cyclooctyne parent ring (dibenzocyclooctyne (DIBO) <sup>[7b]</sup>), by addition of sp<sup>2</sup>-hybridization of the ring parent (dibenzoazacyclooctyne (DIBAC) <sup>[66]</sup>, biarylazacyclooctynone (BARAC) <sup>[64]</sup>, (difluorobenzocyclooctyne (DIFBO) <sup>[67]</sup> or an introduction of an electron-withdrawing group (difluorinated cyclooctyne (DIFO) <sup>[68]</sup>), by the presence of fusion cyclopropane (bicyclo[6.1.0]nonyne (BCN) <sup>[7b]</sup>). The new generation of dipolarophiles which is more reactive was achieved by the introduction of sulfur atoms in the seven membered ring is tetramethylthiacycloheptyne (TMTH) <sup>[69]</sup> but it suffers from poor stability which cannot be separated in pure form before rapid decomposition takes place. With respecting to the reactivity and lipophilicity, the major drawback of high reaction rate constants of dibenzoannulated systems is high lipophilicity which is limits the scope of applications particularly in living systems when the reaction is required in aqueous media. Therefore, *Kele et al.*, developed new structurally simple, non-fluorinated and less lipophilic molecules; carboxymethylmonobenzocyclooctyne (COMBO) <sup>[70]</sup>. In comparison with other cyclooctyne compounds COMBO shows an exceptional reaction rate constant ( $k = 0.24 \text{ M}^{-1}\text{s}^{-1}$  in CD<sub>3</sub>CN and interestingly  $k = 0.80 \text{ M}^{-1}\text{s}^{-1}$  in aqueous solution) together with low lipophilicity values which brings interest and more promise to evaluate this structurally simple molecule as a candidate reaction for cell labeling. It has been reported that SPAAC can be applied for postsynthetic modification of nucleic acid in order to overcome the toxicity of copper catalyst (CuAAC). To this end, an increasing number of new reactive building blocks for both DNA and RNA have been reported. *Heaney* and co-workers were the first who demonstrated the use of a resin-supported conjugation method for cyclooctyne-modified DNA at 5'-end which can be postsynthetically conjugated with not only azide components but also nitrile-oxides <sup>[71]</sup>. Later result from *Filippov et al.* revealed that the RNA bearing the reactive dibenzocyclooctyne on 5'-end was conjugated, proceeding quantitatively with the azide dyes and the biological compounds <sup>[63c, 72]</sup>. The same reactive dibenzocyclooctyne building block was also introduced into DNA at 5' terminus for fast templated DNA strand ligations <sup>[73]</sup>. In order to extend the use of SPAAC in cellular delivery the development of a non-nucleosidic dibenzocyclooctyne building block was investigated by *Manoharan* and co-workers <sup>[74]</sup>.

The results show that the monomer can be applied both at 3'-end and at an internal position in the RNA strands which was further reacted with azidoglyco derivatives (Scheme 9).



**Scheme 9** SPAAC of DNA and RNA bearing cyclooctyne derivatives with azido fluorescent dyes or biological compounds.

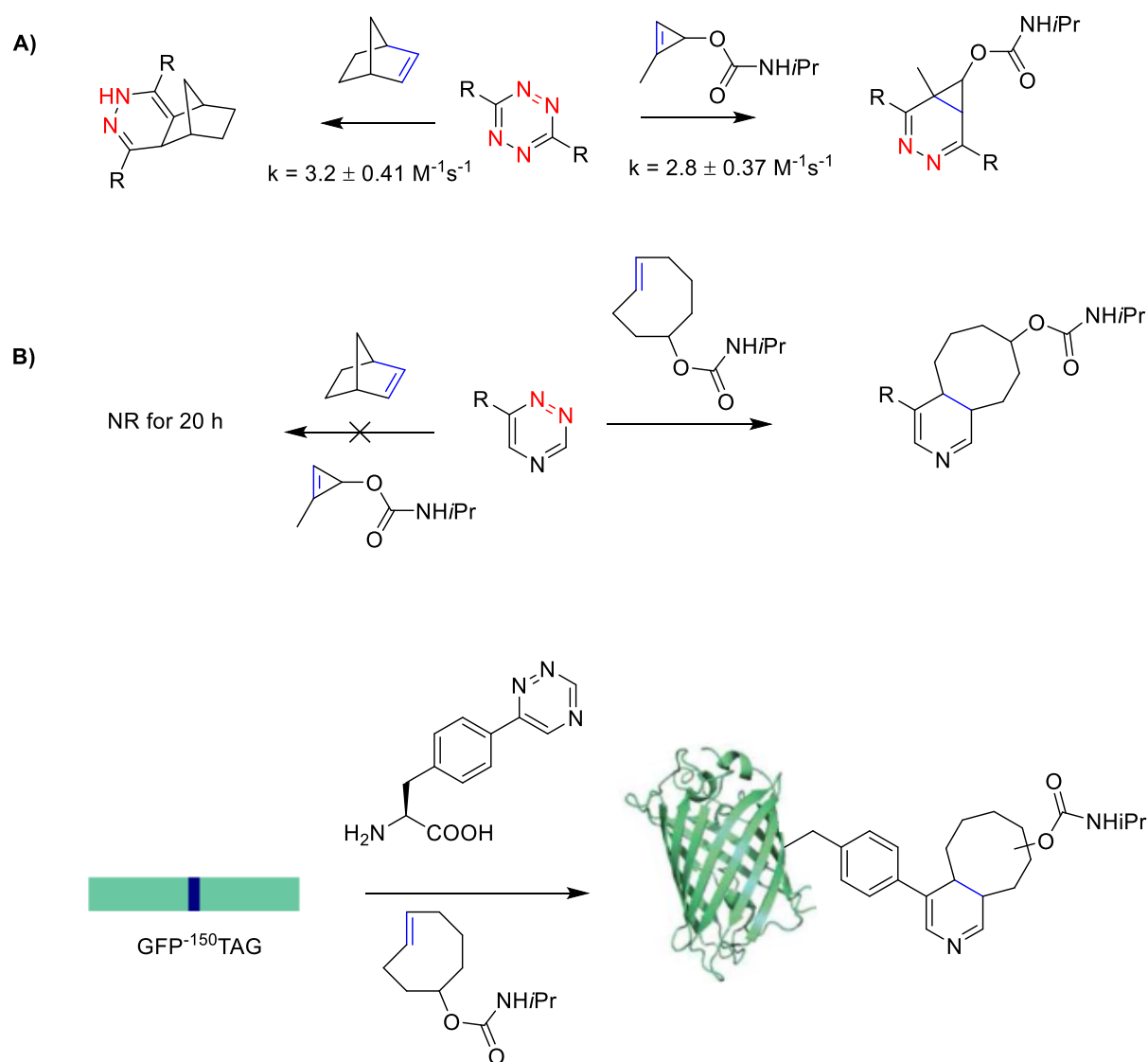
Since then the exploration of SPAAC of nucleotide carrying cyclooctyne as reactive compartment towards azide derivatives have been intensively evaluated in the field of nucleic acid. The cyclooctyne-modified oligonucleosides have been introduced into DNA and RNA either via solid-phase synthesis or enzymatic DNA/RNA synthesis and the corresponding DNA/RNA bearing reactive group was quantitatively conjugated with azido boronic moieties <sup>[75]</sup>, azido fluorescent dyes <sup>[63b, 76]</sup>. Recently, the application of SPAAC for far-red labeling of DNA was demonstrated by the group of *Wagenknecht et al.*, where the monobenzocyclooctyne-modified DNA was smoothly “copper-free click” with the azide dye at room temperature to provide the desired DNA labeled in high yield <sup>[63d]</sup> (Scheme 10).



**Scheme 10** Cyclooctyne-modified oligonucleoside building blocks for the fluorescent labeling in DNA and RNA for bioorthogonal reactions.

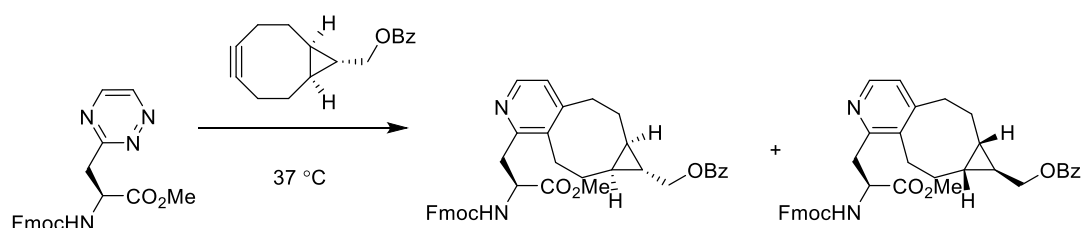
Recent studies have shown that not only azides and strained cyclooctynes can undergo the strain-promoted reactions but also tetrazine scaffolds can rapidly proceed a Strain-Promoted Inverse Electron Demand Diels-Alder Cycloaddition (SPIEDAC) between strained dienophiles (*trans*-cyclooctene (TCO) or strained bicyclo[6.1.0]nonynes (BCN))<sup>[49, 77]</sup>. As mentioned above tetrazines have the fastest reaction rate constant ( $k \approx 1 \cdot 10^5 \text{ M}^{-1} \text{ s}^{-1}$ ) over those bioorthogonal reagents<sup>[52a, 54]</sup>. Unfortunately, the fastest reacting tetrazines are prone to hydrolysis<sup>[54b]</sup> and react with endogenous thiols<sup>[78]</sup>, limiting their application in living cells<sup>[48, 50a, 78]</sup>. An alternative component which drawn the attention of many research groups are triazine scaffolds<sup>[51, 79]</sup>. Advantages over tetrazines are high stability (remained stable for over one week at 37 °C in *d*-PBS and  $\text{CD}_3\text{CN}$ ) and inertness to cytosine over a similar time period, unless, it reacts slower ( $k = 10^{-3} \text{ M}^{-1} \text{ s}^{-1}$ ).

Recently, *Prescher et al.* demonstrated the use of 1,2,4-triazines as a new class of bioorthogonal reagents which reacts efficiently and selectively with TCO but not with norbornene and cyclopropene <sup>[79a]</sup>. Additionally, these triazines can be attached to proteins via an amino acid linker and is sufficiently stable for genetic code expansion prior to subsequent tagging with TCO (Scheme 11).



**Scheme 11** **A)** Strain-Promoted Inverse Electron Demand Diels-Alder Cycloaddition (SPIEDAC) of tetrazine and stained dienophiles. **B)** The bioorthogonality of triazine scaffolds towards dienophiles and its application as bioorthogonal reactions.

Independently, *Webb* and co-workers<sup>[80]</sup> reported the cycloaddition of 1,2,4-triazine-modified amino acids with strained bicyclononyne dienophiles, which are compatible with conventional peptide-synthesis strategies, which allows broad ranges of applications such as protein- and site-specific labeling in *in vitro* and *in vivo*, respectively (Scheme 12).



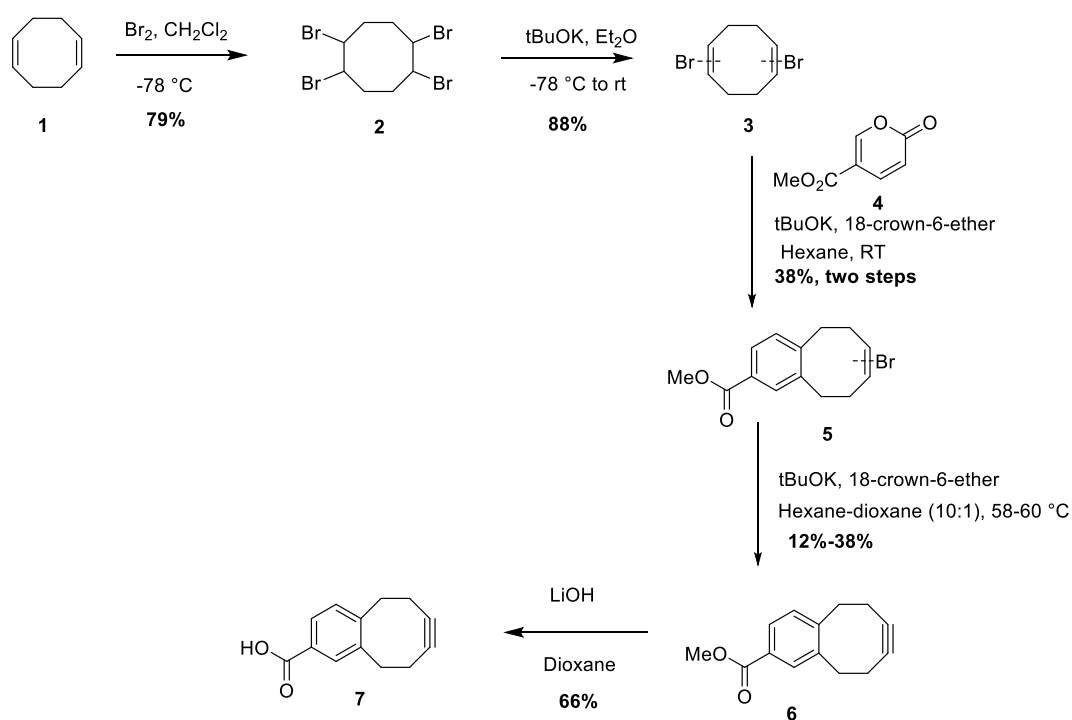
**Scheme 12** 1,2,4-triazine-modified amino acid as new class of bioorthogonal reagent for protein-labeling applications.

To the best of my knowledge, the application of 1,2,4-triazine scaffolds are only demonstrated in amino acid modifications for protein-labeling, not in nucleic acids.

### 3 Results and Discussion

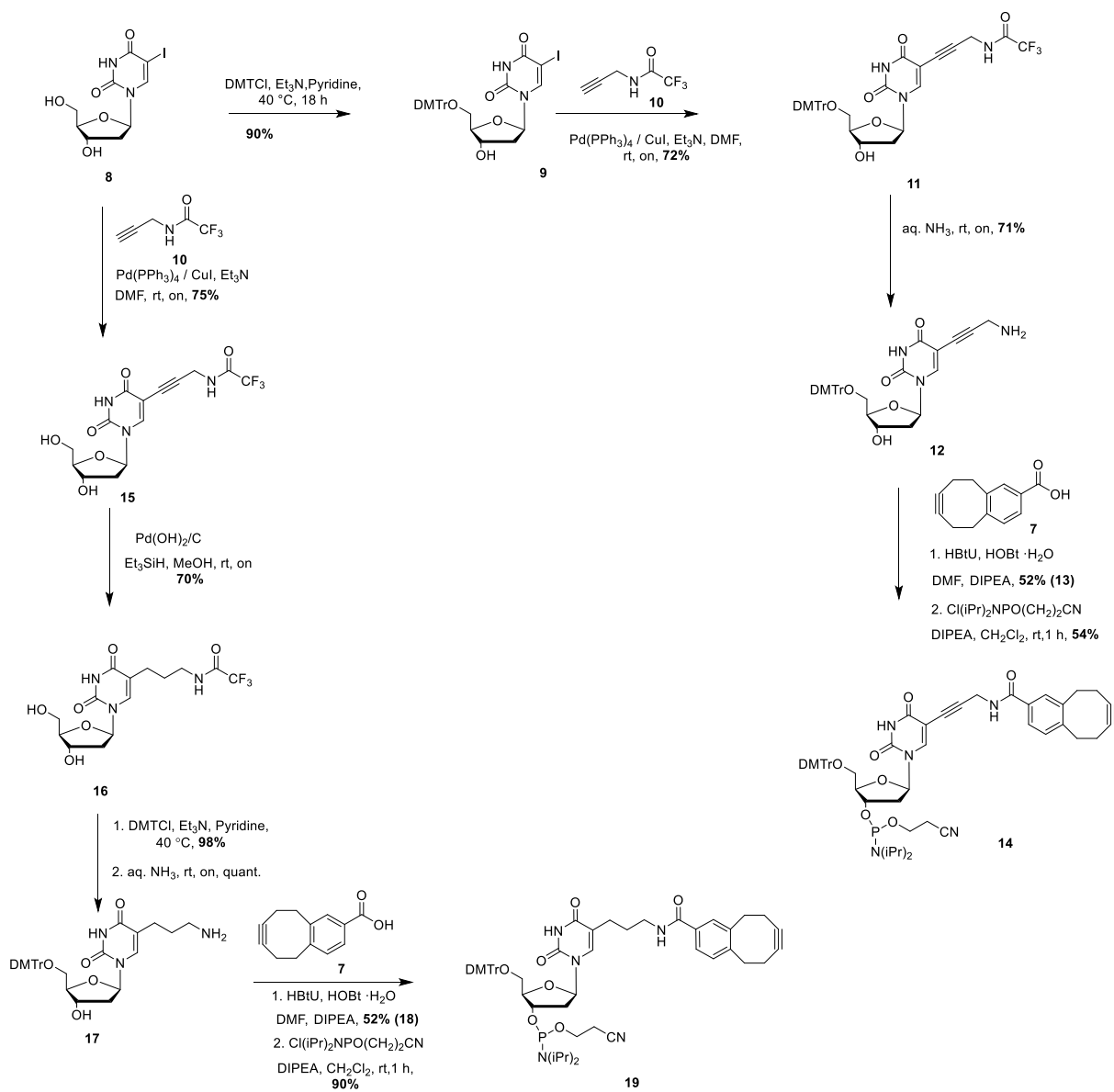
#### 3.1 Preparation of COMBO-modified oligonucleoside building blocks

The COMBO acid **7** was achieved in 6 steps by the bromination of commercially available cyclooctadiene **1** to provide the precursor **2** in 79% yield, which was further partially eliminated HBr using tBuOK to obtain the intermediate **3** in 88% yield. The corresponding intermediate **3** was then coupled with methyl coumalate **4** using 18-crown-6-ether and tBuOK to provide the key intermediate **5** in 38% yield. The corresponding intermediate **5** was treated with the same base in the presence of 18-crown-6-ether at 58-60 °C in the mixture solution of hexane and 1,4-dioxane (10:1) to generate the desired COMBO **6** in 38% yield. After treatment with LiOH followed by an acidic work-up the desired precursor COMBO acid **7** was obtained in 65% yield (Scheme 13).



**Scheme 13** Preparation of COMBO acid.

Having COMBO acid **7** in hand, the COMBO-modified building block **14** was synthesized in 5 steps. The commercially available 5-iodo-2'-deoxyuridine (**8**) was first protected with DMTr at the 5'-position and subsequently coupled with 2,2,2-trifluoro-*N*-prop-2-ynylacetamide (**10**) via a Sonogashira coupling. After deprotection of the TFA by concentration of  $\text{NH}_3$  the corresponding 5-(3''-aminopropynyl)-2'-deoxyuridine (**12**) was further coupled with COMBO acid **7** via standard peptide coupling to provide the desired intermediate **13** in 52% yield. The key intermediate **14** was formed in 54% yield by the treatment of **13** with  $\beta$ -cyanoethyl-*N,N*-diisopropylchlorophosphoramidite in the presence of DIPEA at room temperature. On the other hand, the propyl linker building block **19** was achieved in 5 steps. The Sonogashira coupling of 5-iodo-2'-deoxyuridine **8** with TFA-protected propargylamine **10** was performed under the same conditions to obtain the intermediate **15** in 75% yield. Hence, the key step for achieving the precursor **19** was to reduce the propynyl linker of **15** to the alkyl linker of **16**. This was done by the reduction of the propargylic moiety by using  $\text{Pd}(\text{OH})_2$  on a carbon matrix in the presence of  $\text{Et}_3\text{SiH}$  as the hydrogen source which yielded the crucial building block **16** in 70% yield. After protection of the 5'-OH group with DMTr moiety and cleavage of the TFA protecting group the corresponding compound **17** was further coupled with COMBO acid **7** via a standard peptide coupling method. Subsequently phosphitylation by reacting with  $\beta$ -cyanoethyl-*N,N*-diisopropylchlorophosphoramidite under standard reaction conditions formed the desired product **19** in 90% yield (Scheme 14).



**Scheme 14** Preparation of phosphoramidite COMBO-modified building blocks **14** and **19** as intermediated for automated solid-phase DNA synthesis.

### 3.2 Fluorescent labeling of COMBO-modified DNA

The COMBO-modified DNA strands DNA**1**, **2**, **5** and **6** were synthesized via standard automated solid-phase DNA synthesis (Figure 9). After cleavage from solid phase the corresponding products DNA**1**-DNA**8** were subsequently purified by RP-HPLC, identified by MALDI-TOF mass spectrometry and quantified by UV/vis absorption spectroscopy. The fluorescent labeling of COMBO-modified DNAs with azido-modified dye **21b** were performed in the mixture of H<sub>2</sub>O-DMSO (10:1) at room temperature for 3 h. Surprisingly, the color of the azido-modified fluorescent dye turned from purple to light blue immediately after adding DNA to a mixture solution. It can be explained that the ligation of COMBO-modified DNA with dye **21b** was rapidly occurred to generate the triazole covalently linked between the dye **21b** and COMBO-DNA corresponding to the shift of the maxima absorption of the free azied-modified dye **21b**. After purifying the labeling adducts by RP-HPLC and characterization by MALDI-TOF, the labeled DNA products were obtained in 58% yield (DNA**3**), 63% yield (DNA**4**), 76% yield (DNA**7**) and 87% yield (DNA**8**). The labeled strands DNA**3**-DNA**8** were hybridized with their unmodified complementary strands and their optical properties were evaluated by UV/vis and fluorescence spectroscopy.

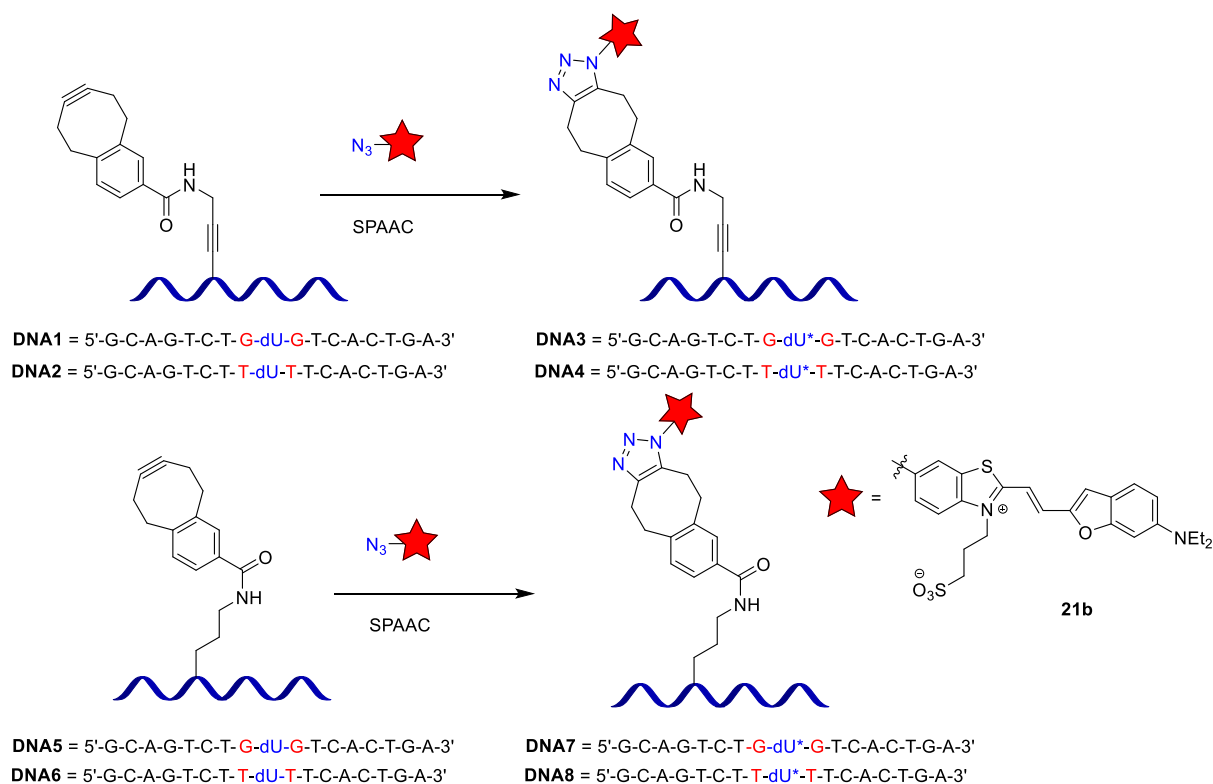


**Figure 9** Strain-Promoted Azide-Alkyne Cycloaddition (SPAAC) of COMBO-modified DNA with azide-modified fluorescent dye **21b**.

### 3.2.1 Spectroscopic experiments

The optical properties of DNA3-DNA8 were evaluated by UV/vis and fluorescence spectroscopy. The results showed that the maxima of absorption of the azide dye **21b** appeared in a bathochromic shift when conjugated with COMBO-modified DNA from 591 nm to 670 nm (DNA3), 612 nm (DNA4), 664 nm (DNA7) and 658 nm (DNA8), respectively. The fluorescence intensity dramatically increased in all cases and was found in a range of 8-14 folds higher than dye **21b** itself. Additionally, the quantum yield values of the azide-modified labeled DNAs were also found higher than that the dye **21b** alone ( $\phi_F = 1.64\%$ , Table1). It could be explained that in the solution without interaction with DNA the two heterocycles have the possibility to rotate around their methane bridge which quenches fluorescence<sup>[81]</sup>. In contrast, the

triazole adduct covalently linked to DNA prohibits the rotation of the fluorescent dye together with the interaction of the surrounding nucleobases resulted in an increase in fluorescence intensity. The maxima of emission of the conjugated products were found slightly bathochromic shifted from 715 nm (**21b**) to 732 nm (DNA**3**), 730 nm (DNA**4**), 732 nm (DNA**7**) and 730 nm (DNA**8**), respectively (Figure 10).

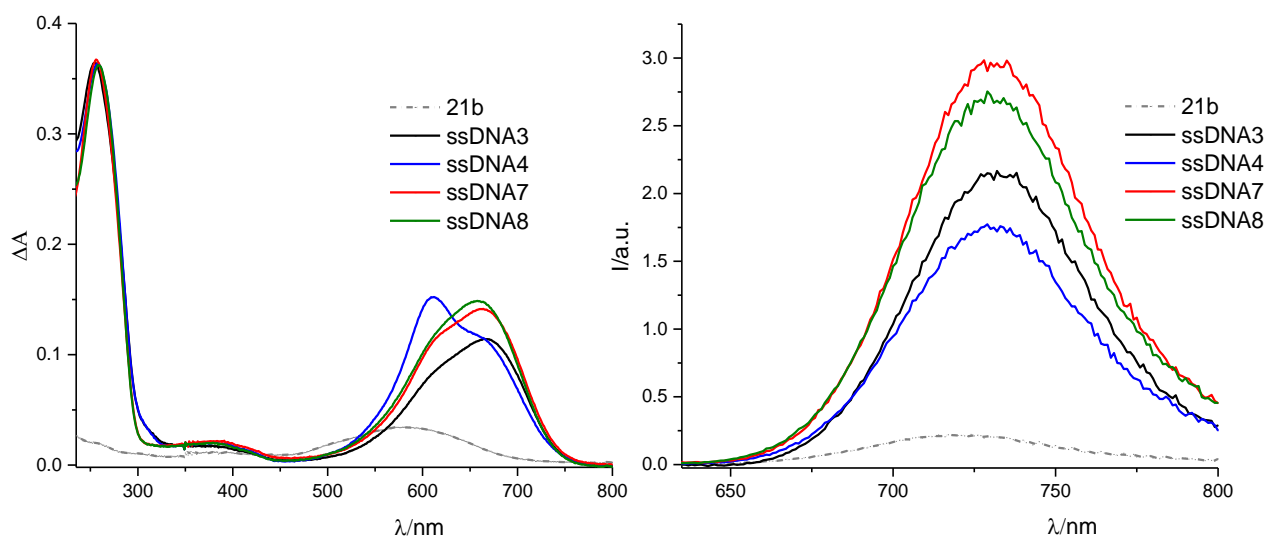


**Figure 10** UV/Vis absorption (left), fluorescence (right) of ssDNA**3** (2.5  $\mu\text{M}$ ), ssDNA**4** (2.5  $\mu\text{M}$ ), ssDNA**7** (2.5  $\mu\text{M}$ ), and ssDNA**8** (2.5  $\mu\text{M}$ ), azide **21b** (2.5  $\mu\text{M}$ ), in comparison; 10 mM NaPi buffer, pH = 7, 250 mM NaCl,  $\lambda_{\text{exc}} = 615$  nm, maxima at  $\lambda_{\text{em}} = 715$  nm (**21b**),  $\lambda_{\text{em}} = 732$  nm (ssDNA**3**),  $\lambda_{\text{em}} = 730$  nm (ssDNA**4**),  $\lambda_{\text{em}} = 732$  nm (ssDNA**7**),  $\lambda_{\text{em}} = 730$  nm (ssDNA**8**).

In order to investigate the effect of the neighboring bases which are located adjacent to the fluorescent dye in DNA3 and DNA4 that contain the triple bond linker (nucleoside **14**), and DNA7 and DNA8 that contain the flexible single bond linker (nucleoside **19**) were hybridized with their unmodified complementary DNA strands. It was noteworthy that the fluorescence intensity was significantly decreased in both cases but still higher than the intensity of the free dye **21b** itself. In the case of DNA3 (in the vicinity of guanosine) and DNA4 (in the vicinity of thymidine) where the dye **21b** is linked via a triple bond, the fluorescence intensity of the double stranded DNA was found to have decreasing by 60% and 23% respectively compared to single strands. It was evident that the interaction of the fluorophore and nucleobase plays an important role to the fluorescence intensity of the dye. An explanation could be that in a double helix, guanosine has stronger H-bonding and  $\pi$ - $\pi$  stacking interactions than thymine bases which influence the fluorophore **21b** to rearrange to the preferable orientation, which means less steric and repulsion resulted in the low fluorescence intensity of DNA3 which is approximately 37% lower than that in DNA4 (Figure 11).

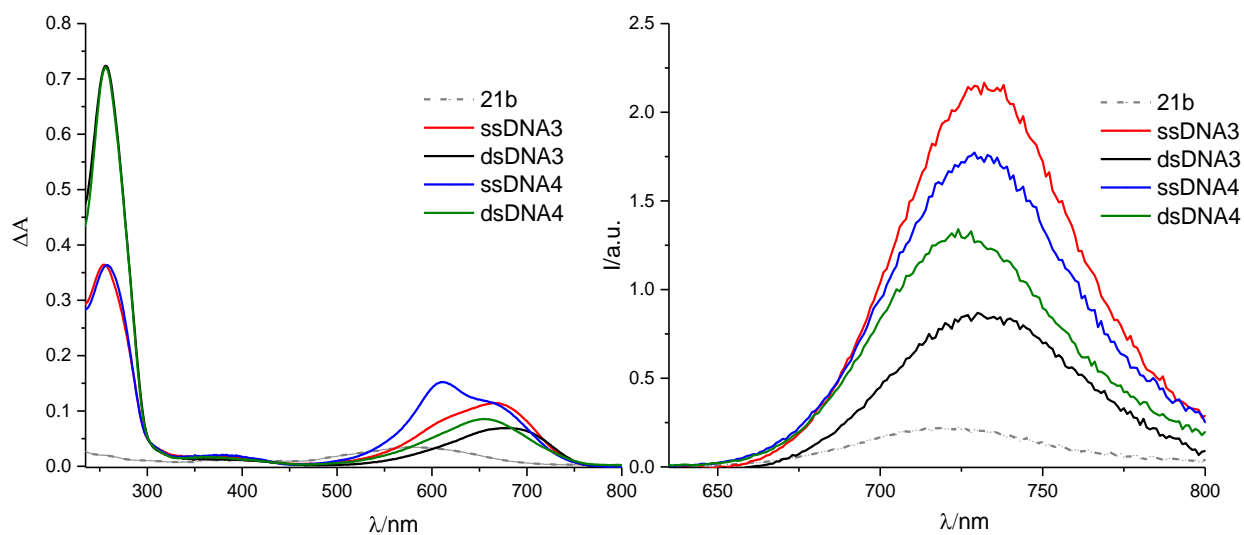


**Figure 11** UV/Vis absorption (left), fluorescence (right) of ssDNA3 (2.5  $\mu\text{M}$ ), ssDNA4 (2.5  $\mu\text{M}$ ), azide **21b** (2.5  $\mu\text{M}$ ), in comparison; 10 mM NaPi buffer, pH = 7, 250 mM NaCl,  $\lambda_{\text{exc}} = 615$  nm, maxima at  $\lambda_{\text{em}} = 715$  nm (**21b**),  $\lambda_{\text{em}} = 732$  nm (ssDNA3),  $\lambda_{\text{em}} = 732$  nm (dsDNA3),  $\lambda_{\text{em}} = 730$  nm (ssDNA4),  $\lambda_{\text{em}} = 724$  nm (dsDNA4).

Likewise, DNA7 and DNA8 that contain the flexible single bond linker (nucleoside **19**) have shown similar characteristics. The decrease in the fluorescence intensity was 60% (dsDNA7) and 20% (dsDNA8) in comparison to their corresponding single strands (Figure 12).

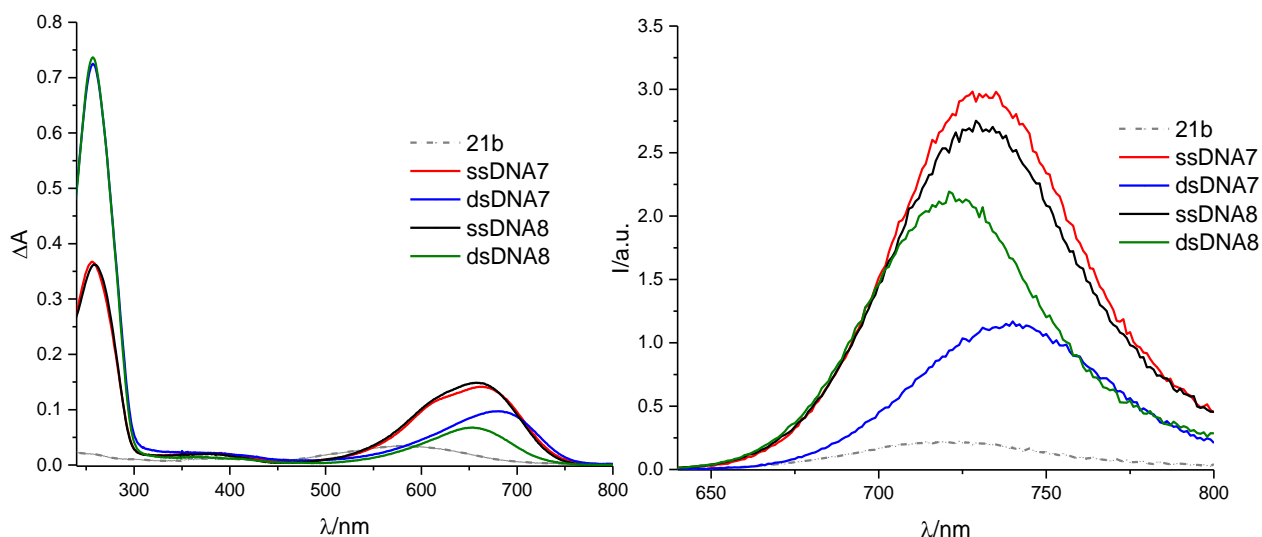


**Figure 12** UV/Vis Absorption (left), fluorescence (right) of ssDNA7 (2.5  $\mu$ M), ssDNA8 (2.5  $\mu$ M), azide 21B (2.5  $\mu$ M), in comparison; 10 mM NaPi buffer, pH = 7, 250 mM NaCl,  $\lambda_{exc}$  = 615 nm, maxima at  $\lambda_{em}$  = 715 nm (**21b**),  $\lambda_{em}$  = 732 nm (ssDNA7),  $\lambda_{em}$  = 742 nm (dsDNA7),  $\lambda_{em}$  = 730 nm (ssDNA8),  $\lambda_{em}$  = 722 nm (dsDNA8).

Accordingly, prior results indicated that the interaction between the fluorophore and nucleobase could increase the fluorescence intensity by prohibiting the possibility of the rotation of the two heterocycles of fluorescent dye through the methane linker. In addition, the comparison of flexible linker and rigid bridge (surrounded by the same bases: guanosine) were also investigated. The comparison of the fluorescence characteristics of DNA3 and DNA7 indicated that the more flexible linker (DNA7) influences the interaction of fluorophore and nucleobases due to the increase in the fluorescence intensity (Figure 13).

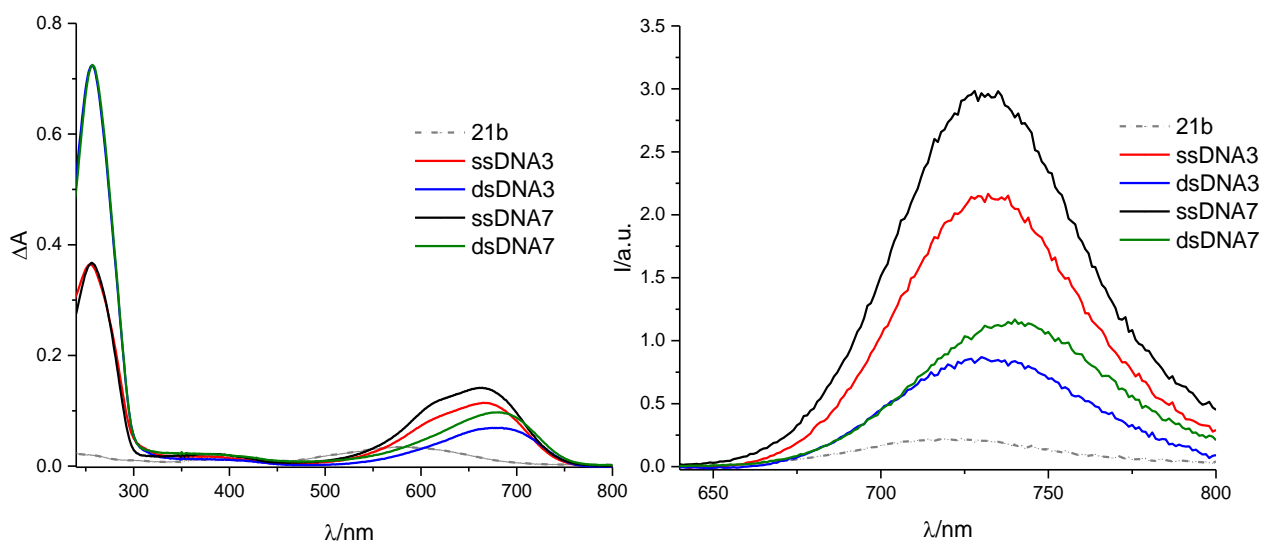


**Figure 13** UV/Vis absorption (left), fluorescence (right) of ssDNA3 (2.5  $\mu\text{M}$ ), ssDNA7 (2.5  $\mu\text{M}$ ), azide **21b** (2.5  $\mu\text{M}$ ), in comparison; 10 mM NaPi buffer, pH = 7, 250 mM NaCl,  $\lambda_{\text{exc}} = 615$  nm, maxima at  $\lambda_{\text{em}} = 715$  nm (**21b**),  $\lambda_{\text{em}} = 732$  nm (ssDNA3),  $\lambda_{\text{em}} = 732$  nm (dsDNA3),  $\lambda_{\text{em}} = 730$  nm (ssDNA7),  $\lambda_{\text{em}} = 742$  nm (dsDNA7).

Therefore the comparison of the fluorescence characteristics of DNA4 and DNA8 (surrounded by thymidine) were also evaluated. The results indicated that the propyl linker (DNA8), influences the interaction of the dye with DNA even more than the guanosine, as observed by the higher fluorescence intensity of DNA8 compared to DNA4 both in single and double stranded DNA (Figure 14). It could be explained that the flexible linker encourages the fluorophore to intercalate into double stranded DNA which prohibits the possibility of rotation of the fluorescent dye together with the  $\pi$ - $\pi$  interaction of nucleobases towards the aromatic ring of the dye due to the increase in the fluorescence intensity. In contrast, when the rigid linker was present, the possibility of interaction with the nucleobases in DNA via  $\pi$ - $\pi$  interaction was limited thus corresponding to the low fluorescence intensity observed.

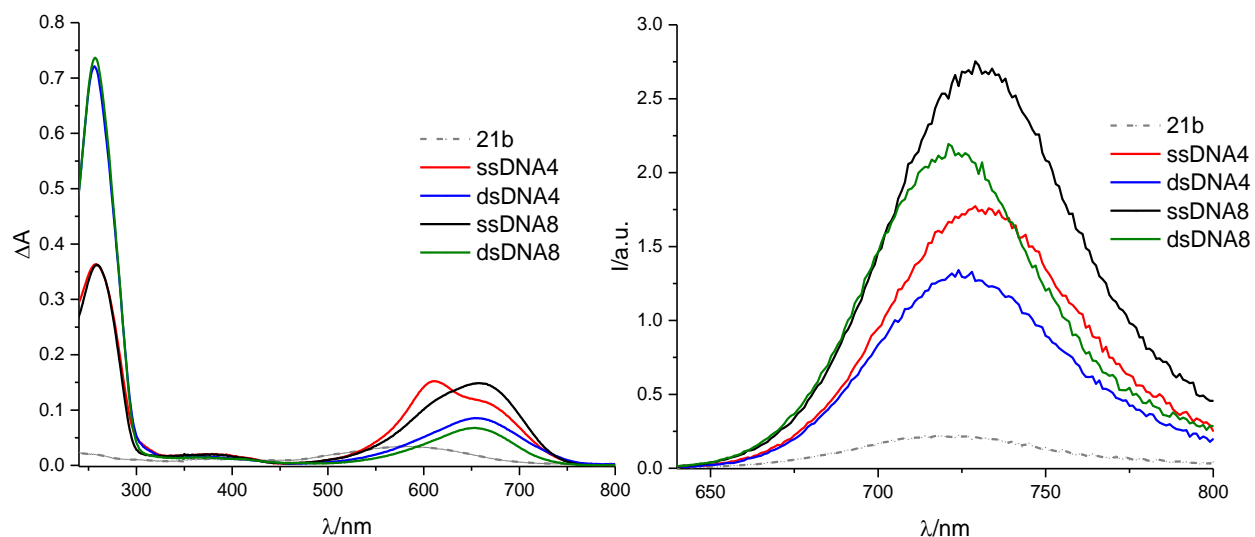


**Figure 14** UV/Vis Absorption (left), fluorescence (right) of ssDNA4 (2.5  $\mu\text{M}$ ), ssDNA8 (2.5  $\mu\text{M}$ ), azide **21b** (2.5  $\mu\text{M}$ ), in comparison; 10 mM NaPi buffer, pH = 7, 250 mM NaCl,  $\lambda_{\text{exc}} = 615$  nm, maxima at  $\lambda_{\text{em}} = 715$  nm (**21b**),  $\lambda_{\text{em}} = 732$  nm (ssDNA4),  $\lambda_{\text{em}} = 724$  nm (dsDNA4),  $\lambda_{\text{em}} = 730$  nm (ssDNA8),  $\lambda_{\text{em}} = 721$  nm (dsDNA8).

The quantum yields of the single stranded DNA3-DNA8 and their corresponding double strands as well as the melting temperatures were measured. Table 1 summarizes all optical properties. The results show that the quantum yields of the labeled DNA3-DNA8 showed a higher values than that the free dye **21b** and the double stranded DNA were found to be slightly higher than that of the single stranded DNA in all cases. Interestingly, in the case of DNA8, the fluorescence shows the highest value of 13.2% corresponding to the previous results from fluorescence spectroscopy. Additionally, the melting temperatures of duplex DNAs were evaluated. In the case of DNA3 and DNA7,  $T_m$  values were found to be an astonishing 5.5 °C lower than the unmodified duplex (66.5 °C). Likewise DNA4 and DNA8 were decreased by 2.5 °C and 1.5 °C respectively, compared to unmodified reference duplex (59.5 °C) <sup>[82]</sup>. It is evident, that the significant influence of the interaction of the fluorophore with the nucleic acids plays an important role to discriminate between hybridized strands.

**Table 1.** Optical properties of fluorescent labeled oligonucleotides.

DNA	$\lambda_{\text{max, abs}}$ [nm]	$\lambda_{\text{max, em}}$ [nm]	$\phi_F$ [%]	$T_m$ [°C]
<b>21b</b>	591	715	1.64	-
ssDNA3	670	732	9.2	-
<b>dsDNA3</b>	<b>682</b>	<b>732</b>	<b>9.4</b>	<b>61</b>
ssDNA7	664	732	9.8	-
<b>dsDNA7</b>	<b>680</b>	<b>742</b>	<b>10.0</b>	<b>61</b>
ssDNA4	612	730	8.7	-
<b>dsDNA4</b>	<b>657</b>	<b>729</b>	<b>9.4</b>	<b>54</b>
ssDNA8	658	730	8.6	-
<b>dsDNA8</b>	<b>654</b>	<b>721</b>	<b>13.2</b>	<b>53</b>

### 3.3 Fluorescent labeling in living cells

Fluorescently tagged biomolecules have revolutionized the way in which scientists observe and investigate biological processes [2, 83]. The major advantages of this method are its high sensitivity tracking with excellent temporal and spatial resolution. There are several methods to selectively tag the biological target; (I) Immunofluorescence labeling which offers high selectivity and sensitivity by reducing non-specific background signals [2]. However, due to the limitation of their size which can only be applied to certain targets together with frequently observed photo bleaching phenomenon [2] had led to limit applications. (II) Genetically encoded fluorescent proteins (FPs) [84] can be used to tag proteins of interest in various colors such as green [84b], blue and yellow for example. This method offers a high sensitivity therefore concluding its non-toxicity to cells. However, a major problem in applying FPs methods in living organisms is their size (27 kDa). Regarding to this limitation, an alternative method is to introduce organic dyes which are less than 1 kDa in size into biomolecules. The latter method is the most promising strategy due to the manipulation of the fluorophores properties via simple chemical reactions. A third method, which allows the fluorescent tagging of biomolecules are bioorthogonal reactions (Figure 15).

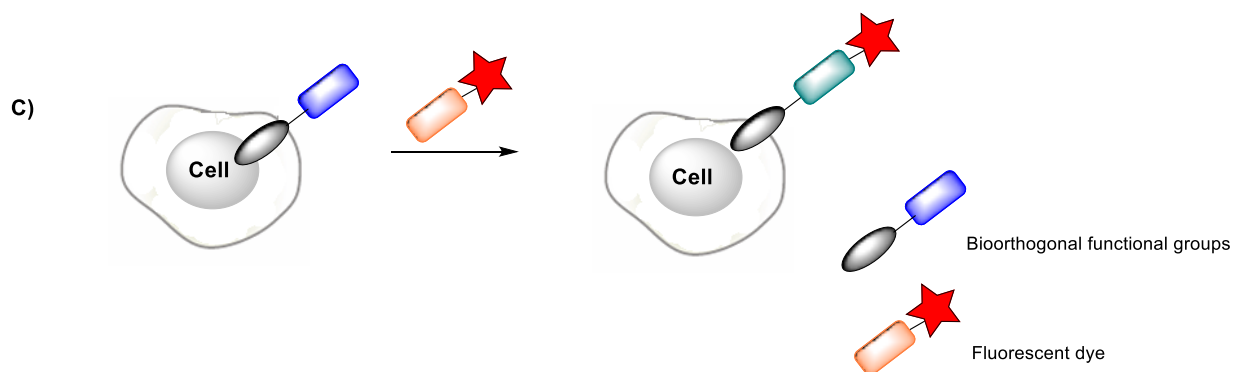
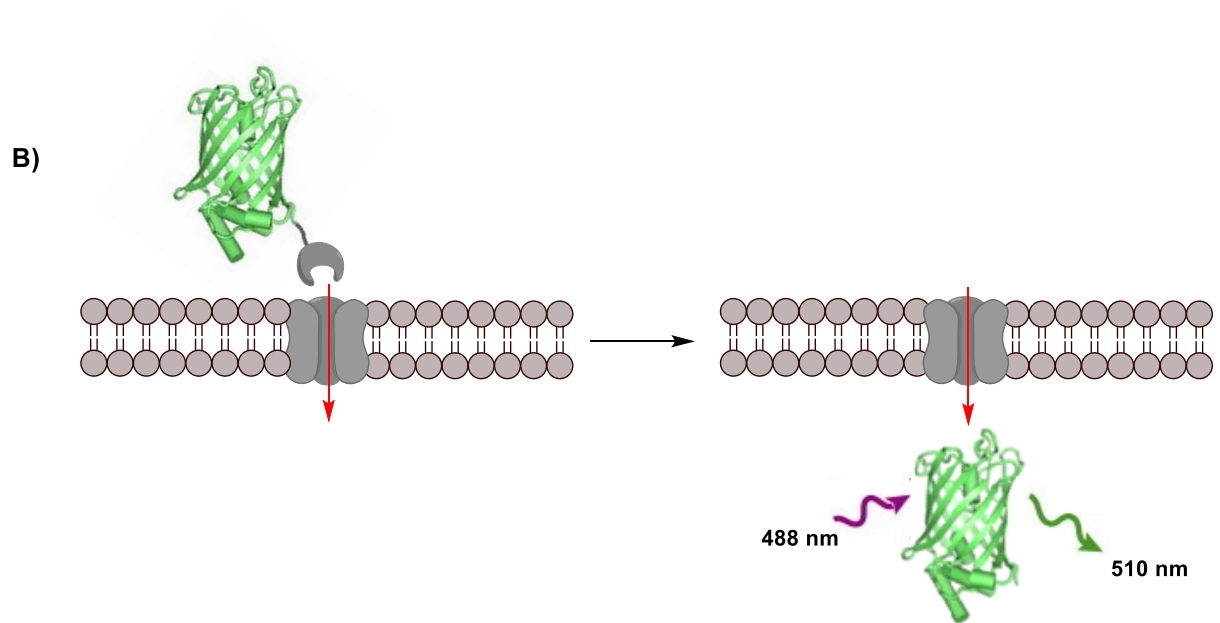
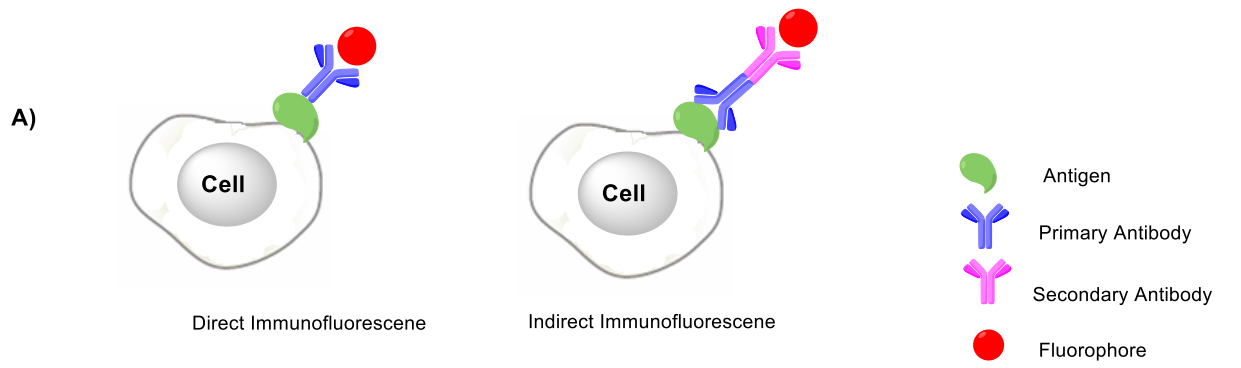


**Figure 15** Schematic living cell imaging methods: **A)** Immunofluorescent Technique, **B)** Genetically encoded fluorescent protein, **C)** Bioorthogonal conjugation.

### 3.3.1 Presynthetic fluorescent labeling in cells

DNA2 and DNA6 were conjugated with the azido-modified dye **21b** and purified by RP-HPLC. After identification by MALDI-TOF the oligonucleotides were hybridized with their unmodified complementary strands. These labeled double strands DNA were transfected into *HeLa* cells by using Screenfect®A as a medium solution and subsequently visualized by confocal fluorescent microscopy (Figure 16).

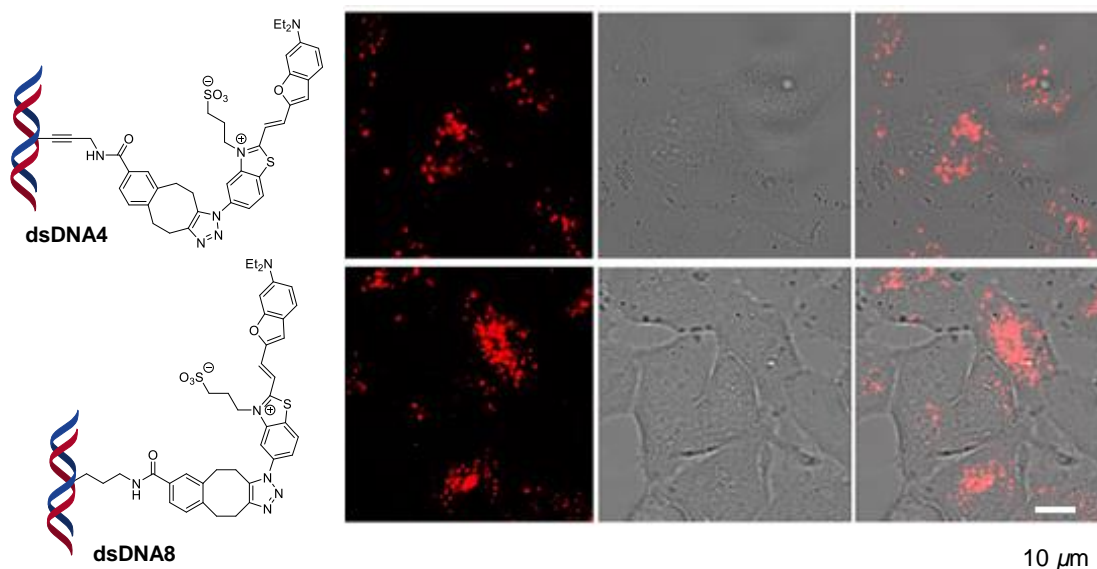
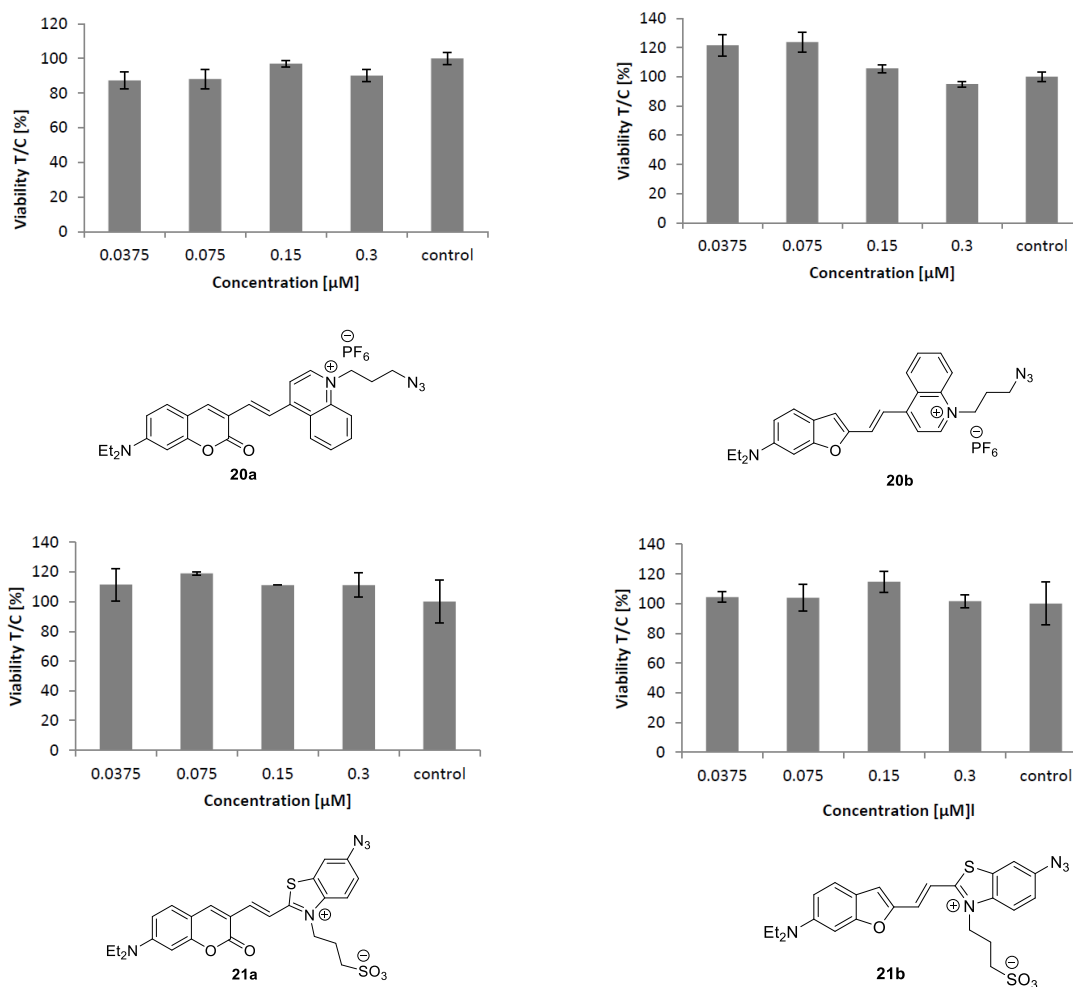


**Figure 16** Images of *HeLa* cells transfected with dsDNA4 and dsDNA8; left row fluorescence image, middle row: bright field image; right row: overlay of both images; bar indicate 10  $\mu\text{m}$ .

It is evident that the flexible linker of the covalently attached COMBO-triazole fluorophore on DNA plays an important role in enhancing the fluorescence intensity which was observed by the brightness of cell's image of dsDNA8 in comparison with dsDNA4 from confocal fluorescence microscopy. This result tracks well with the previous experiments of fluorescence spectroscopy and quantum yield values.

### 3.3.2 Postsynthetic fluorescent labeling in cells

Regarding prior results, it is indicated that fluorescent tag of COMBO-modified DNA could be transfected into *HeLa* cells without showing significant toxicity. Accordingly, the cells cytotoxicity was determined in order to investigate *in vivo* applicability of a set of azido-modified dyes **20a-22b**. The standard method so called, CellTiter 96® Non-Radioactive Cell Proliferation Assay (Promega) was employed. The set of azido-modified dyes **20a-22b** were transfected into cells at different concentrations and incubated for 72 h. The negative control for 100% dead cells and positive control was included. After 72 h, all cell lines were treated with the tetrazolium salt solution and absorbance was measured at a wavelength of 595 nm. The results revealed that none of these azide-modified dyes shown significant toxicity in comparison to the control experiments (Figure 17).



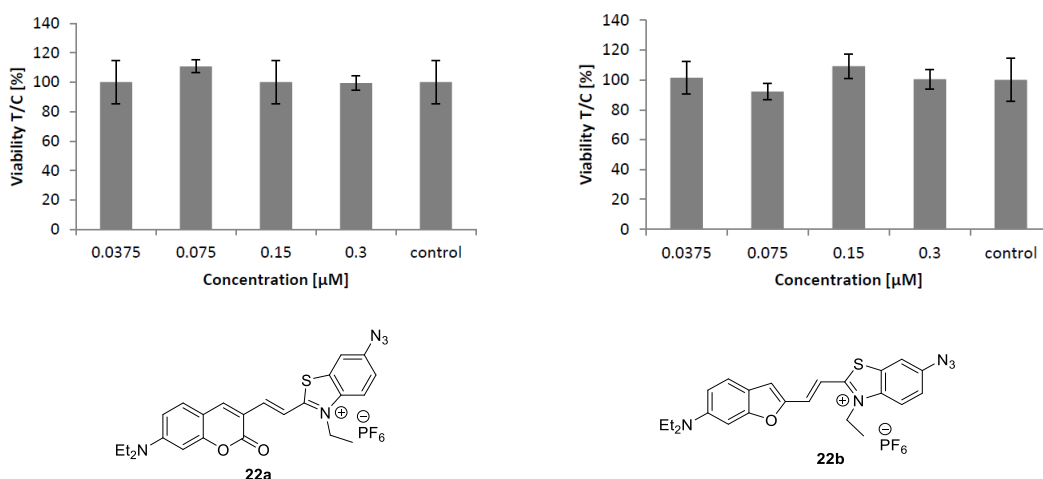


**Figure 17** Cell viability of *HeLa* cell after treatment with azido-modified dyes **20a-22b**.

Therefore the next approach is to perform the “copper-free click” reaction inside the living cells. It is noteworthy that, DNA $\mathbf{8}$  showed the most promising results by enhancing the fluorescence intensity. Therefore the single strand COMBO-modified DNA $\mathbf{6}$  was chosen and transfected into *HeLa* cells by using Screenfect $\text{\textcircled{R}}$ A as a medium solution prior to the ligation step. A set of azido-modified dyes **20a-22b** were employed in order to investigate the effect of the polarity of the dyes of membrane-permeability for future experiments. The results revealed that the transfected COMBO-modified DNA inside *HeLa* cells could specifically conjugate with all dyes compared with the non-transfected control experiments without nonspecific fluorescence back ground that could originate from adsorption to the hydrophobic or negatively charged surface on DNA. Remarkably, the coumarin derivatives (**21a**, **22a**) showed specific DNA-tagged in the nuclei, while the benzo-furan dyes (**21b**, **22b**) were preferably taken up in endosomal vesicles (Figure 18).

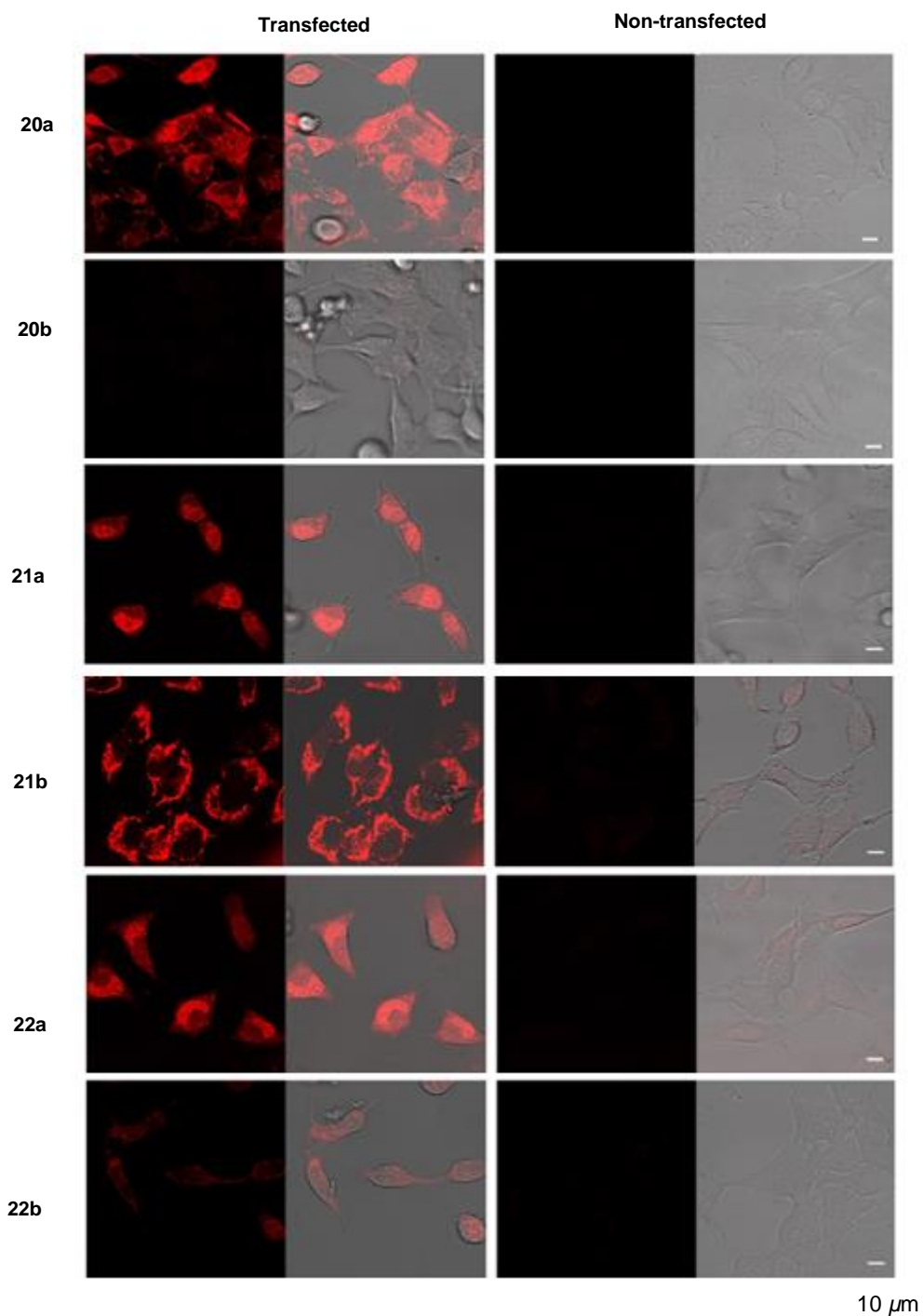


**Figure 18** *In vivo* click experiments of DNA6 and a set of azido fluorescence dyes **20a-22b**;  $1 \times 10^4$  *HeLa* cells are transfected with ssDNA6 and subsequently incubated with dyes **20a-22b**. Left columns: fluorescence confocal image; right columns: fluorescence image merged with bright field. Scale bar 10  $\mu$ m.

Remarkable results from the cell experiments showed that a set of fluorescent dyes **20a-22b** could be conjugated with COMBO-modified DNA<sup>6</sup> inside living cells under physiological conditions, to provide the brightness in fluorescence and high selectivity that was observed compared with a non-transfected DNA experiment. The major advantage of this method is, that the reaction can proceed without requirement of metal catalysts or high temperatures with regard to a bioorthogonal reactions requirement. Moreover, the various types of azido-modified fluorescent dyes could be conjugated with COMBO-modified DNA in low concentrations under aqueous media conditions. To extend the advantage of using monobenzocyclooctyne (COMBO) as a bioorthogonal component candidate with other ring strained cyclooctynes for investigation and elucidation of the biological processes with respect to toxicity, reactivity and selectivity in biological systems the next approach was to employ the advantages of the polymerases for primer extension experiments.

### 3.4 Enzymatic DNA synthesis

Since the 1950s, the modification of nucleosides bearing reactive moieties on nucleobases or their analogues have been tremendously investigated and applied in various fields such as chemical biology<sup>[85]</sup> and material science<sup>[86]</sup>. However, most of them are chemically synthesized via the advances of the phosphoramidite method on solid support<sup>[87]</sup>. Despite this method being facile, robust and scalable, the major drawbacks are (I) the difficulty of the synthesis of long nucleotides (>100 NT), (II) the limitation of some functional groups which can react with phosphoramidites (prone to be oxidized by the phosphorus (III) atoms such as azide) and (III) the modified-building blocks must be stable enough to survive the strong basic conditions of the cleavage step. An alternative method to incorporate modified-building blocks is to take (2'-deoxy)ribonucleotide triphosphates (dNTPs or NTPs) as substrates for enzymatic synthesis using the advantages of diverse polymerases to synthesize the DNA or RNA of interest from 5'→3' direction by the primer extension method (Figure 19).

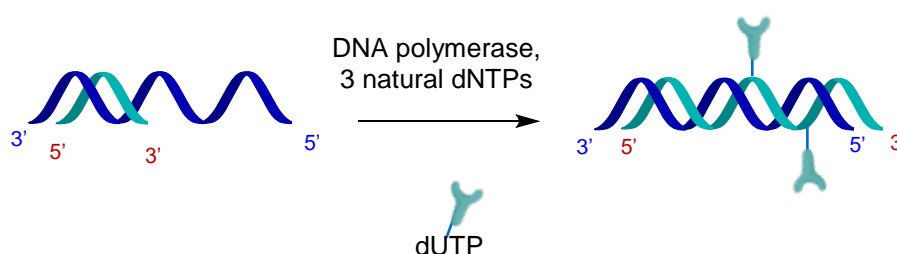


**Figure 19** Primer extension experiment (PEX) of modified-(2'-deoxy)ribonucleotide triphosphate building block in the presence of natural dNTPs catalyzed by a DNA polymerase.

The polymerase incorporates the upcoming nucleotide triphosphate at the 3'-end of the primer strand against the nascent base pair of the complementary template strand by the advances of Watson-Crick base pairing. If one or more of the natural dNTP(s) are replaced by modified building blocks, the polymerase incorporates the modified analogue in every position opposite to the complementary template strand. In this strategy, single or several modifications can be engineered by the change of the sequence of the template strand. This modified-nucleotide triphosphate building block can be incorporated either adjacent to each other or separated by a number of natural bases. Recently, the capability of DNA polymerases were revealed by Marx and co-workers<sup>[88]</sup>. The DNA polymerase accepts the base-modified nucleoside exclusively at C5 of pyrimidines and C7 of 7-deazapurines because those substituents are located in the major groove which does not affect the canonical base pairing. Moreover, the study showed that a more flexible linker could increase the efficiency of the incorporation due to the increase in hydrogen-bond capability. Additionally, the bulky modified building block, which could stabilize the growing primer of adjacent modification via  $\pi$ - $\pi$  interaction, showed more efficient transformation<sup>[88-89]</sup>. The most promising DNA polymerases for primer extension of base-modified nucleotide building blocks are *Thermus aquaticus* (*Taq*) namely, *Klen Taq* DNA polymerases classified as family A, *Deep Vent* and *Vent* are generally used when high temperatures are needed; those polymerases share the crucial activity of deficient 3'→5' exonuclease. Later studies indicated that the DNA polymerase family B which is thermo-stable, has a higher efficiency than the DNA polymerase family A; *Thermococcus kodakarensis* (*KOD*) and *Pyrococcus furiosus* (*Pfu*) for instance<sup>[88, 90]</sup>. The higher efficiency can be explained by the orientation of the reactive site of *KOD* polymerases where the extension proceeds above minor groove and therefore the upcoming modified-building block does not interact with the tip of the domain. In contrast, the corresponding area in family A is extended over the major groove where those substituents may clash the tip of domain (Figure 20).

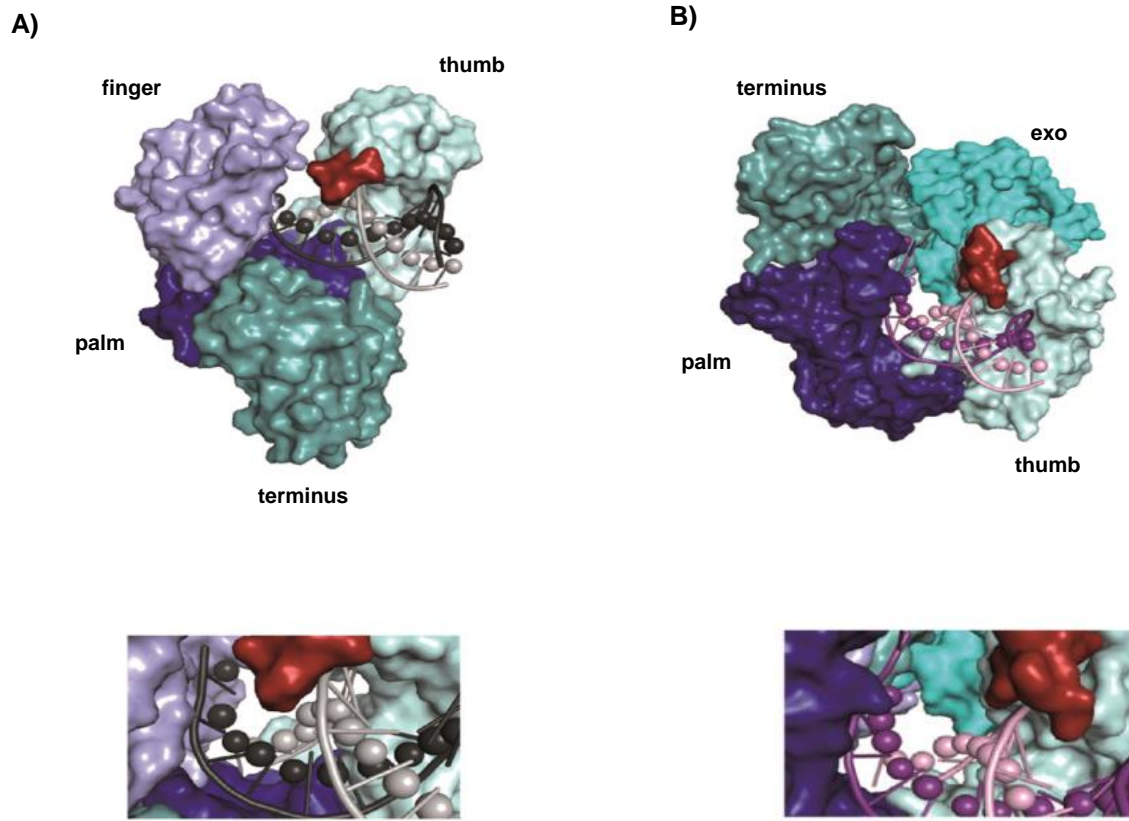
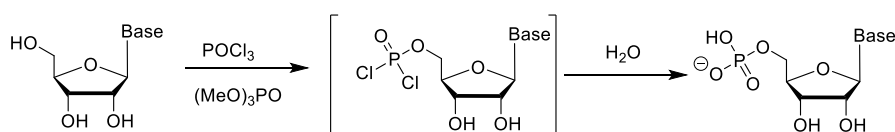


**Figure 20** The comparison of the DNA environments in family A and B DNA polymerases. **A)** *Klen Taq* DNA polymerase (PDB ID 3SZ2), **B)** *KOD* DNA polymerase (4K8Z) in binary complex <sup>[88]</sup>.

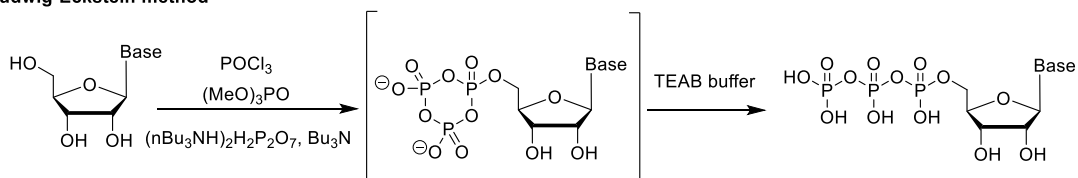
### 3.4.1 Preparation of the COMBO-modified 2'-deoxyuridine triphosphate building block 24

To extend the advantages of SPAAC as a bioorthogonal tool for a fluorescent labeling in living cells the nucleotide triphosphates were prepared and incorporated into DNA by the advantage of the polymerases and subsequently conjugated with their reaction partners. One of the first methods for preparation of nucleotide triphosphates is the *Yoshikawa* method <sup>[91]</sup>. This procedure was carried out by reaction of unprotected nucleosides with phosphorus oxychloride and subsequent hydrolysis to obtain the monophosphate product (Scheme 15A) which can be further reacted with pyrophosphate to provide the desired nucleotide triphosphate in the final step. However the major drawback of using the *Yoshikawa* procedure is the competition of reactive hydroxyl group of the ribose-sugar to obtain a mixture of the undesired products. To overcome this problem *Ludwig* and *Eckstein* <sup>[92]</sup> reported a one-pot, 3-steps reaction developed in late 1980s (Scheme 15B). The reaction was carried out by using the chlorophosphate intermediate which was directly treated with pyrophosphate before hydrolysis. The corresponding cyclic triphosphate intermediate was then hydrolyzed in the presence of TEAB buffer in the final step.

A) Yoshikawa method

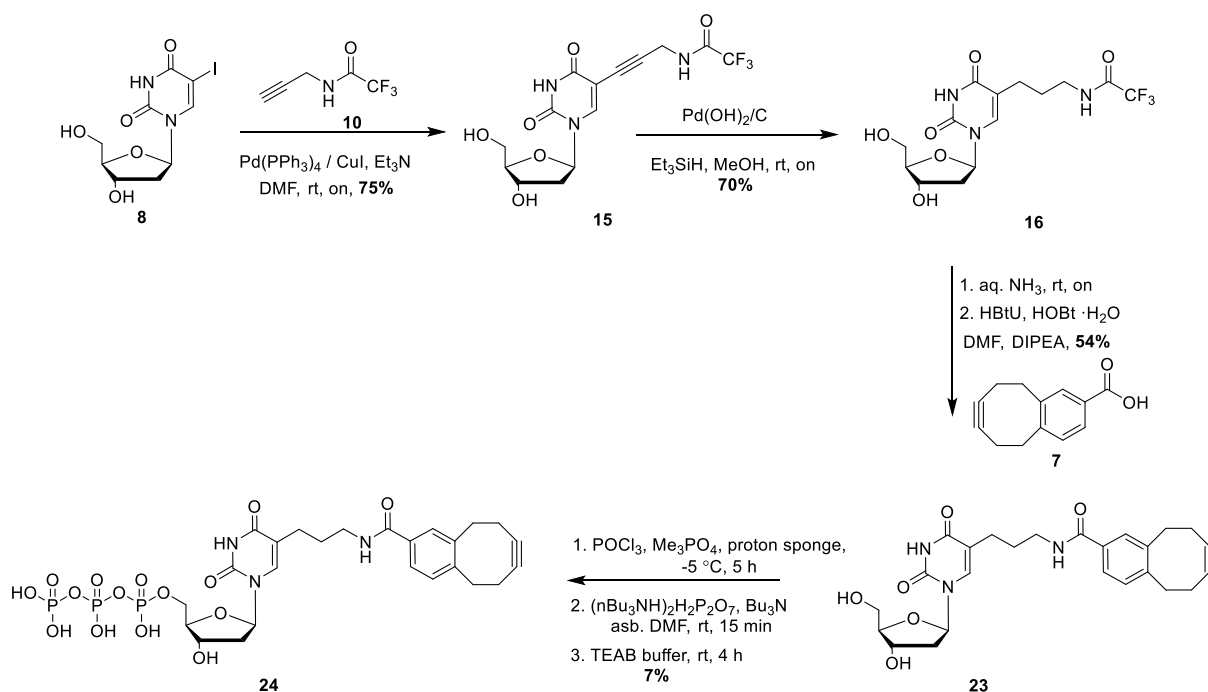


B) Ludwig-Eckstein method



**Scheme 15** Phosphorylation of base-modified nucleoside: **A)** Yoshikawa method, **B)** Ludwig-Eckstein method.

The COMBO-modified 2'-deoxyuridine triphosphate **24** can be synthesized in 4 steps (Scheme 16). Precursor **23** was achieved by the standard method as mentioned above (Scheme 14) with 54% yield. Hence, the key step to achieve precursor **24** was the phosphorylation of the unprotected nucleoside building block **23** using the methodology of *Ludwig et al.* [92]. The reaction was carried out by treating the building block **23** with phosphorus oxychloride (POCl<sub>3</sub>) in the presence of trimethylphosphate and proton sponge at -5 °C for 5 h yielding in a cyclic reactive triphosphate intermediate. This was rapidly treated with pyrophosphate and tributylamine at room temperature for 15 min. At this point the reaction mixture was slowly added to a TEAB buffer (pH = 7) at room temperature for 4 h and subsequently frozen and lyophilized. The crude product was then purified by RP-HPLC using a gradient of ACN-TEAB as eluent. The product-containing fractions were combined, freeze-dried and quantified by absorption spectroscopy at 260 nm which was obtained in 7% yield.



**Scheme 16** Preparation of COMBO-modified 2'-deoxyuridine triphosphate **24**.

### 3.4.2 Primer Extension Experiment (PEX)

Evaluation of the capability to accept base-modified 2'-deoxynucleotides by different polymerases; *Vent (exo-)*, *Deep Vent (exo-)*, *KOD XL* and *Homo Klen Taq* were first investigated. It has been reported that the modification of pyrimidine nucleobases are favored at C5 and C7 of 7-deazapurine in order to avoid the disturbance of the Watson-Crick base pairing <sup>[88]</sup>. *Vent (exo-)*, *Deep Vent (exo-)*, *Homo Klen Taq* and *KOD XL* DNA polymerase were chosen for this experiment because their advantages are (I) deficiency of 3'→5'-exonuclease activity which is suitable to employ base-modified nucleoside triphosphates, and (II) the elongation reaction can be performed at high temperature which can accelerate the reaction rate of artificial nucleotide building blocks to that of natural triphosphate units (dNTPs). Primer extension experiments were performed by using primer **P1** which contained fluorescein at the 5'-terminus in order to follow the elongated product, by excitation wavelength of 471±20 nm and emission wavelength of 535±20 nm on gels after electrophoresis. Template **T1** was chosen as standing start experiment which means that the modified-building block is directly elongated after the cytidine natural nucleoside at the 3'-end terminus of primer. In addition, **P2** and **P3** were used as reference for the thymidine elongated product 24 NT (**P2**) and full length elongated product 35 NT (**P3**) in the presence of only natural nucleoside triphosphates, both of them are marked with fluorescein at 5'-end (Figure 21).

**T1**            3'-CTG-GGT-GAG-GTA-GCT-CTA-AAG-AG A-GGC-GGC-TCG-CG-5'

**P1**            5'-Flu-GAC-CCA-CTC-CAT-CGA-GAT-TTC-TC-3'

**P2**            5'-Flu-GAC-CCA-CTC-CAT-CGA-GAT-TTC-TC T-3'

**P3**            5'-Flu-GAC-CCA-CTC-CAT-CGA-GAT-TTC-TC T-CCG-GCC-AGC-GC-3'

**Figure 21** Standing start experiment; template **T1**, primer **P1**, thymidine elongated product 24 NT reference (**P2**), full length elongated natural nucleoside triphosphate reference 35 NT (**P3**).

The primer extension of the COMBO-modified 2'-deoxyuridine triphosphate **24** was performed at 72 °C and catalyzed by the polymerases, *Vent* (*exo*-) and *Deep Vent* (*exo*-). In addition the negative experiment control was also performed in order to investigate their capability of accepting the artificial nucleotide triphosphate of the polymerase (Figure 22).

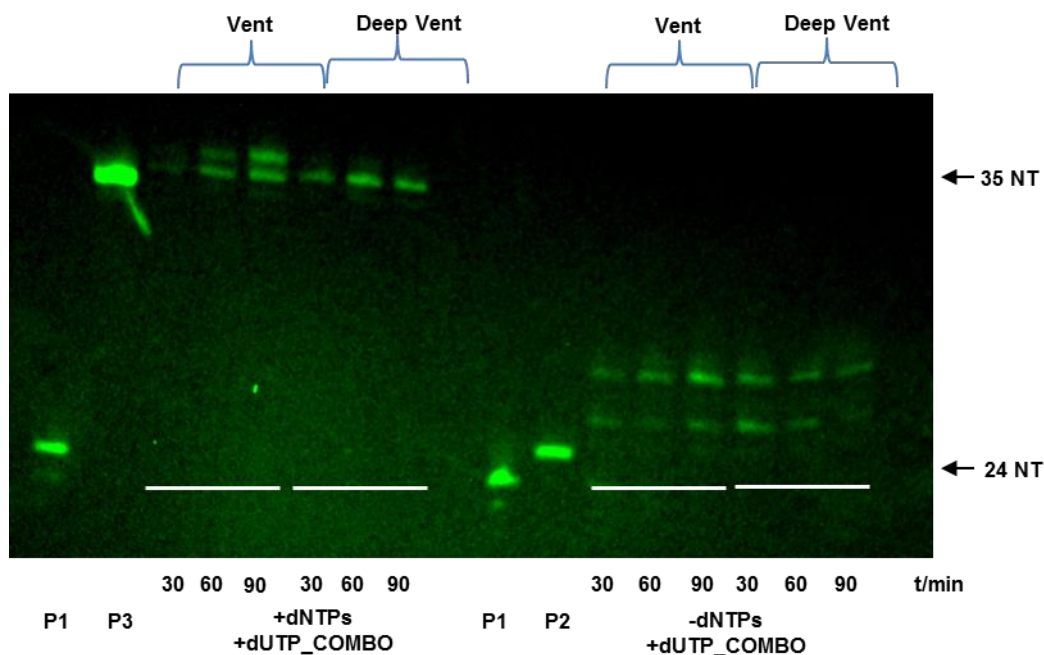


**Figure 22** PAGE analysis of standing start experiments of **P1/T1** with *Vent* (*exo*-), *Deep Vent* (*exo*-) at 72 °C.

The results from denaturing polyacrylamide gel electrophoresis (PAGE) indicated that the COMBO-modified nucleotide triphosphate **24** was accepted by the polymerases, which were evidenced by the fully elongated product after 30 min for *Deep Vent* (*exo*-) whereas *Vent* (*exo*-) was found to elongate incompletely even if the reaction time was extended to 90 min. In order to ensure the capability of the polymerase to accept the building block, a negative control experiment was conducted in parallel. It is evident that when only the COMBO-modified 2' -deoxyuridine triphosphate **24** was added into a reaction mixture, the slower-moving band of the full length elongated products was missing.

The standing start experiment of **P1/T1** catalyzed by *Hemo Klen Taq* DNA polymerase was performed at 64 °C. The results showed that the full length elongated product was observed after 30 min and the slower-moving band was missing when only the COMBO-modified triphosphate **24** was added into the reaction mixture. The difference of electrophoretic mobility on the gel in comparison to those of the reference primer **P1** and full length elongated DNA **P3** indicated that the COMBO-modified building block **24** was accepted by the polymerases with high efficient incorporation (Figure 23).

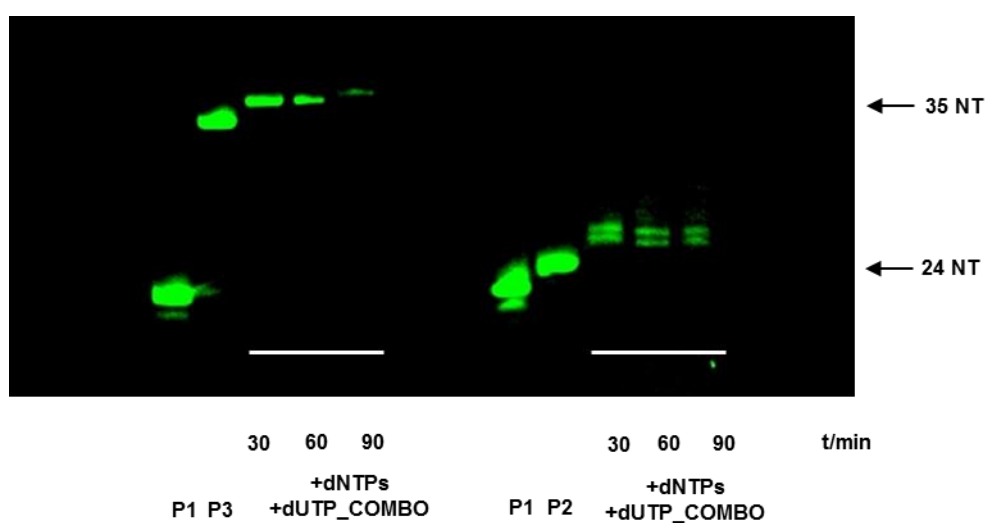


**Figure 23** PAGE analysis of standing start experiments of **P1/T1** with *Hemo Klen Taq* at 64 °C.

### 3.4.3 Postsynthetic fluorescent labeling of COMBO-modified DNA

To extend the advances of the application of COMBO moiety as a bioorthogonal component for fluorescent labeling of DNA, the “copper-free click” reaction with fluorescent dyes was investigated. The full length elongated product was treated with a tetrazine-modified rhodamine dye **25** under various reaction conditions in order to ensure the conjugation of bulky fluorophores with the lipophilic COMBO moiety. The conjugation was followed by PAGE analysis (Figure 24).

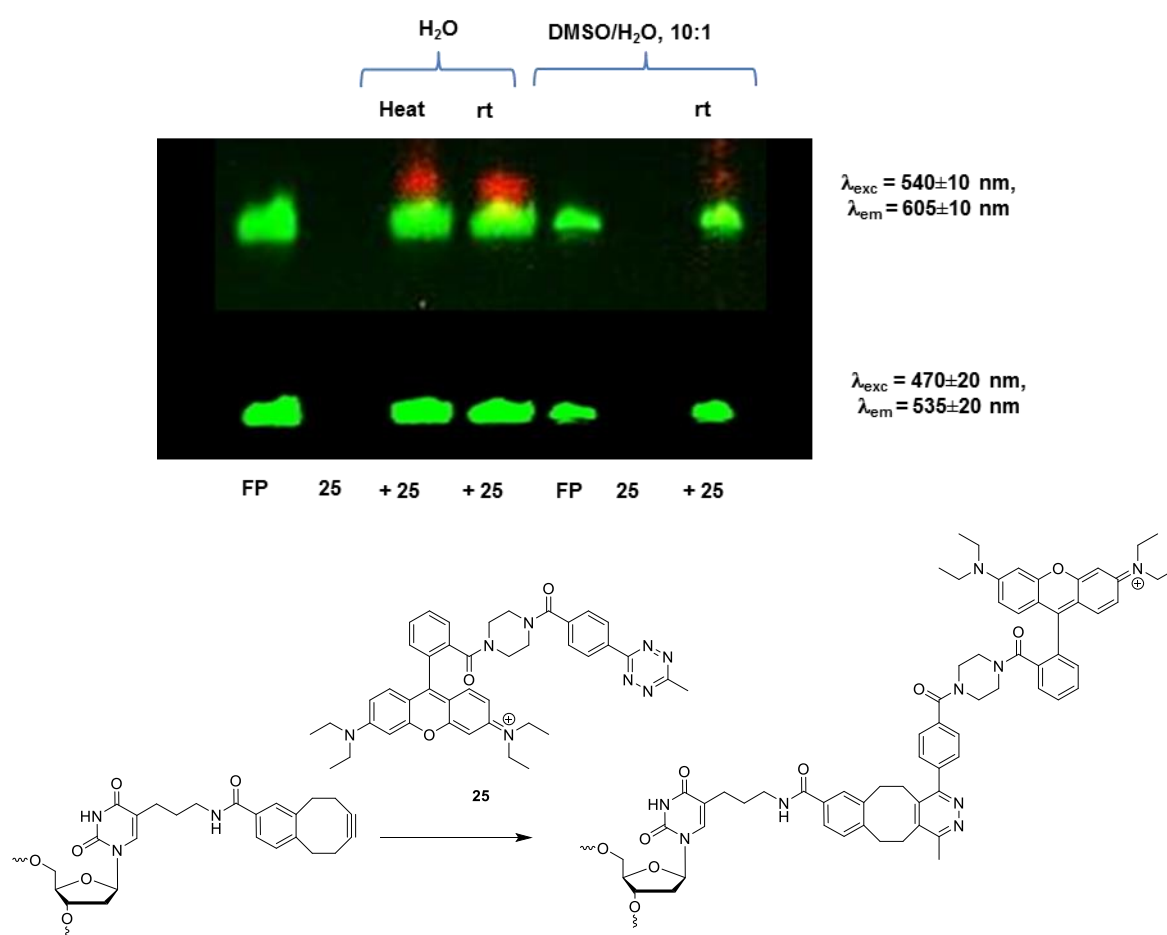


**Figure 24** PAGE analysis of the ligation of full length elongated DNA catalyzed by *Hemo Klen Taq* at 64 °C with tetrazine-modified rhodamine dye **25** in aqueous media and a mixture of DMSO-H<sub>2</sub>O (10:1). Green indicates the fluorescence of fluorescein ( $\lambda_{exc} = 470 \pm 20$  nm and  $\lambda_{em} = 535 \pm 20$  nm). Red indicates the fluorescence of rhodamine ( $\lambda_{exc} = 540 \pm 10$  nm and  $\lambda_{em} = 605 \pm 10$  nm).

It was hardly seen that the conjugated product was obtained regarding the result from PAGE analysis. As expected the slower-moving gel band on both channels (green and red) could be observed if the ligation step had occurred. It was hard to clarify that either the elongation was not successful or the “click” reaction was not accomplished. According to the result from “click” experiment, a significantly slower-moving band of the conjugated product was not observed due to only a slightly red band in the rhodamine channel in PAGE analysis being obtained. It might be explained that the COMBO-modified nucleotide triphosphate was successfully incorporated. Nevertheless, the cyclooctyne reactive site seems to be orientated inside of the double helix in a way that sterically hinders the reactive site. The results revealed that the steric hindrance of the cyclooctyne plays an important role in the ligation efficiency. According to the result from the *in vivo* experiments, it was demonstrated that the single stranded COMBO-modified DNA6 could selectively ligate with the set of azied-modifid dyes **20a-22b** under physiological conditions. To clarify this issue, the extension experiment was performed by elongating the building block into the 5'-terminal position. Primer **P8** and template **T3** were chosen for the terminal incorporation experiment at 5'-terminus where it was expected that the reactive moiety will orientate out of the double helix in order to be conjugated more efficiently by the fluorescent dye in aqueous media (Figure 25).

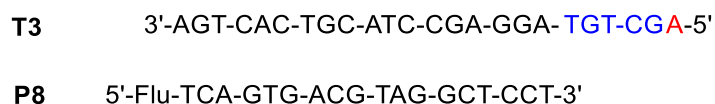


**Figure 25** 5'-terminus incorporation experiment; template **T3** obtained 24 NT, primer **P8** obtained 18 NT.

The incorporation of the COMBO-modified triphosphate **24** into DNA was first performed at 37 °C and catalyzed by *Hemo Klen Taq* and *KOD XL* DNA polymerase in order to avoid the decomposition of the building block. The click step was performed under the same reaction conditions as the **P1/T1** experiment. The elongation progress and ligated adduct were followed by PAGE analysis (Figure 26). The result from PAGE analysis showed that the incorporation of the COMBO-modified triphosphate **24** at the 5'-terminus was successful after 90 min for *Hemo Klen Taq*, and 30 min for *KOD XL* DNA polymerase compared with the primer **P8**.

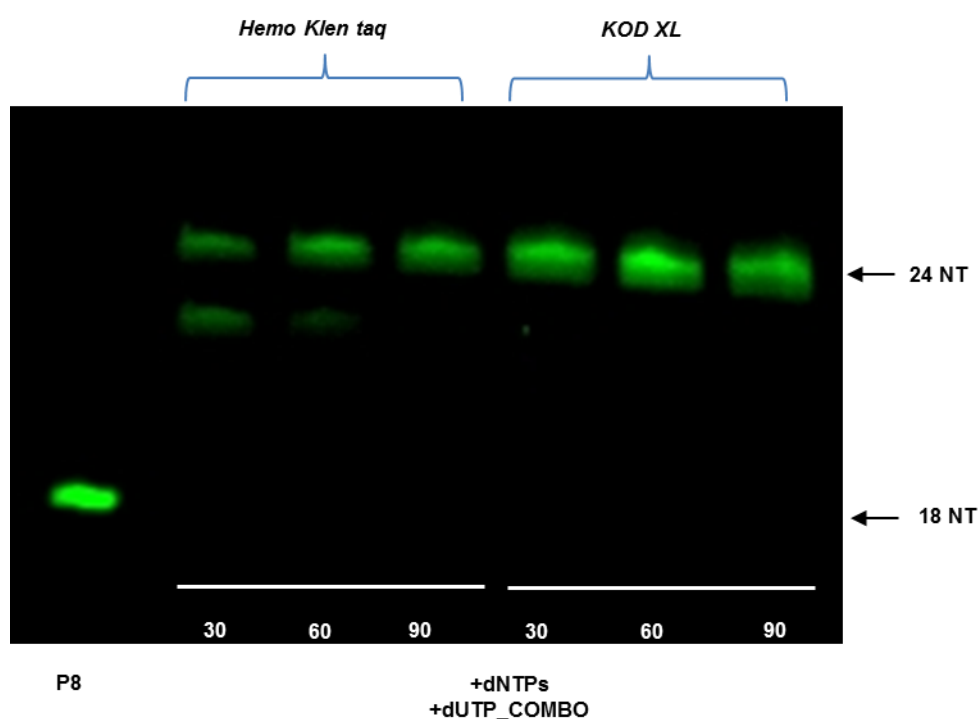
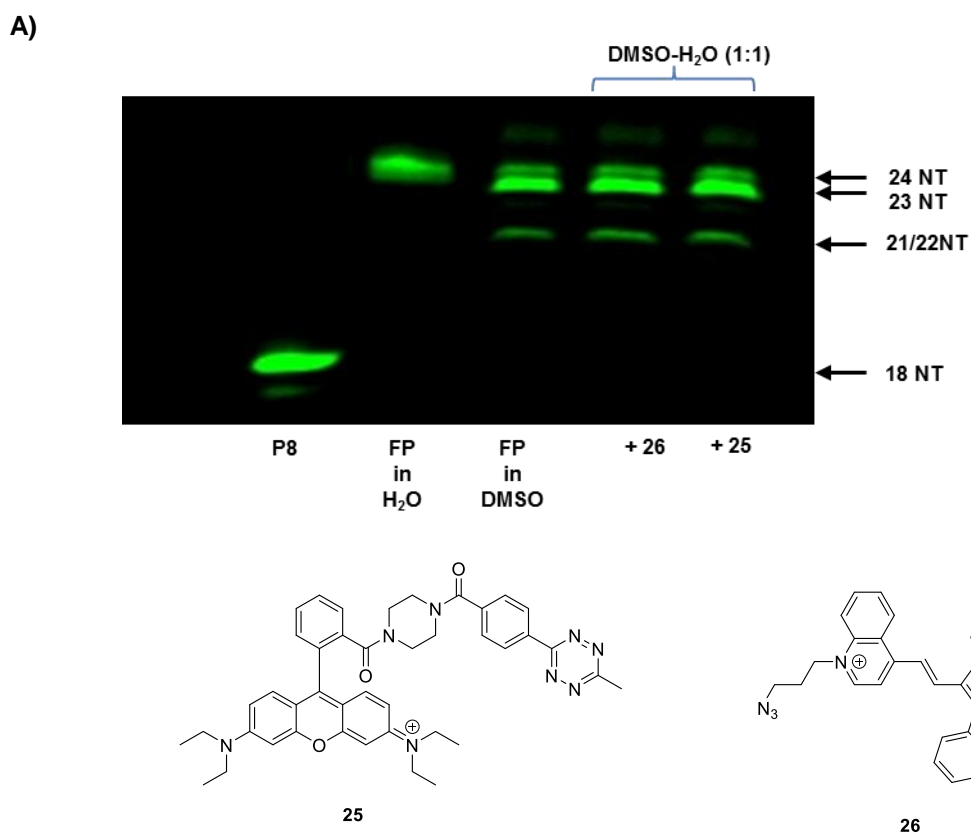


**Figure 26** PAGE analysis of 5'-terminus extension experiment; primer **P8** catalyzed by *Hemo Klen Taq* and *KOD XL* DNA polymerase at 37 °C. Green indicates the fluorescence of fluorescein ( $\lambda_{\text{exc}} = 470 \pm 20$  nm and  $\lambda_{\text{em}} = 535 \pm 20$  nm).

The full length oligonucleotide product was desalted, concentrated and dissolved in water to reach a final concentration of 750 nM. Subsequently, conjugation with either the tetrazine-modified rhodamine dye **25** or the azido-modified dye **26**. The reaction was carried out in a mixture solution of DMSO-H<sub>2</sub>O (1:1) at room temperature for 24 h. The reaction was directly applied to gel electrophoresis (Figure 27A). It can clearly be seen that no new slower-moving band was observed both in the green and the red channels. When having a closer look at the fluorescein channel, the elongated product, (which was dissolved in a mixture of DMSO-H<sub>2</sub>O (1:1)) showed the fragmentation of the extension product, which was not observed when only water was used as a solvent. It is noteworthy that DMSO could cause strand breaks in DNA. Regarding the results from PAGE analysis it is indicated that the elongated product of the COMBO-modified DNA was broken into 3 small DNA fragments which were 23 NT (breaking at elongated position of COMBO-modified building block), 21/22 NT (adenosine or guanosine) and the slightly remained full length product (24 NT) (Figure 27B). This result indicates that the DNA polymerases accepted the COMBO-modified 2'-deoxyuridine triphosphate as a new reactive building block but unfortunately the conjugation reaction conditions were not suitable to perform the “click” reaction in the presence of DMSO as a co-solvent.



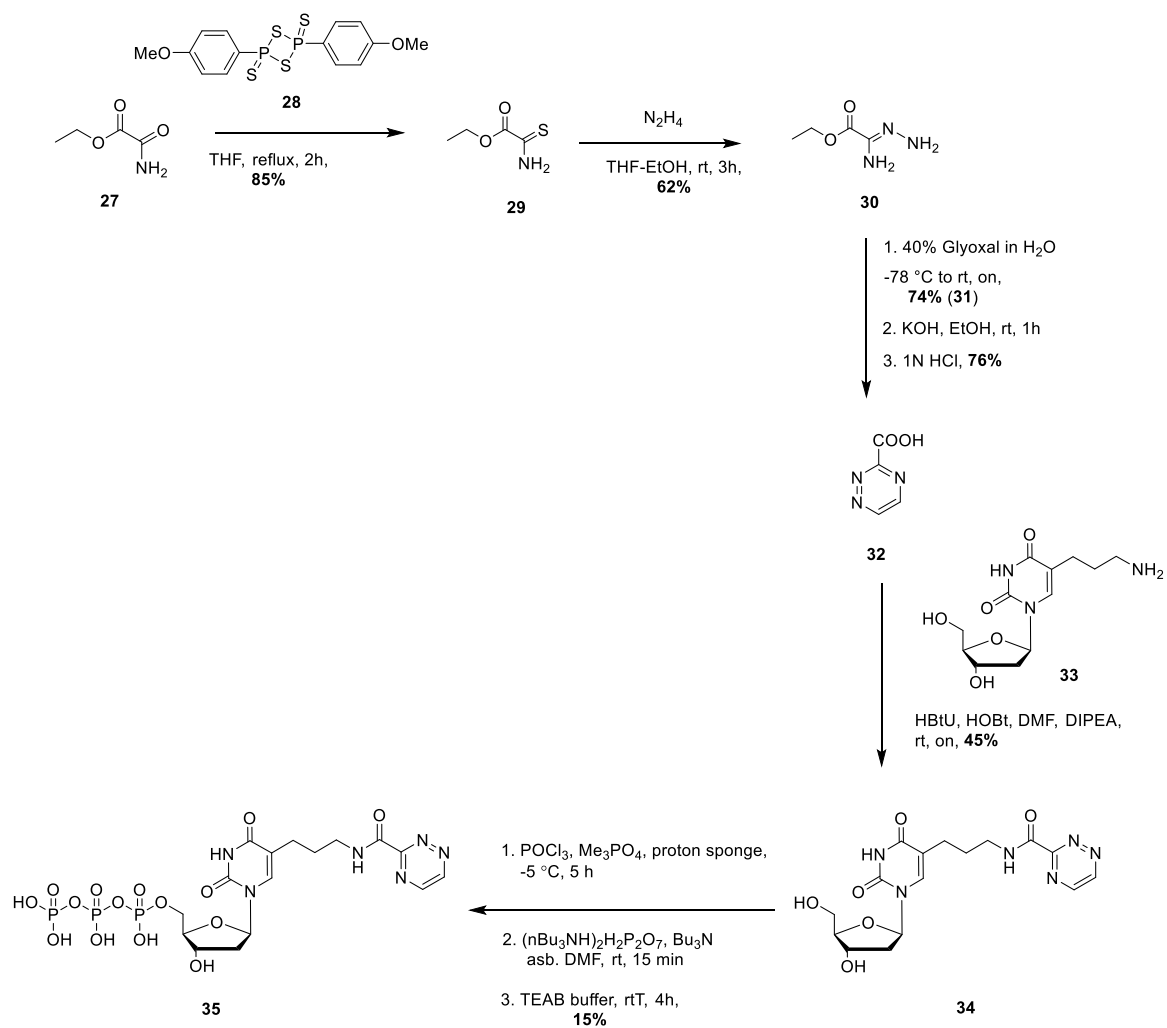
**B)**

<b>FP</b>	5'-Flu-TCA-GTG-ACG-TAG-GCT-CCT-ACAGCU-3'	<b>24 NT</b>
	5'-Flu-TCA-GTG-ACG-TAG-GCT-CCT-ACAGC-3'	<b>23 NT</b>
	5'-Flu-TCA-GTG-ACG-TAG-GCT-CCT-ACA(G)-3'	<b>21/22 NT</b>

**Figure 27** **A)** PAGE analysis of the “click” reaction of full length elongated product (**FP**) with azide-modified dye **26** and tetrazine-modified rhodamine dye **25** performed at room temperature in a mixture solution of DMSO-H<sub>2</sub>O (1:1), **P8** primer. **B)** Full length elongated DNA and their possible strand break of DNA.

### 3.5 Preparation of the 1,2,4-triazine-modified 2'-deoxyuridine triphosphate building block **35**

The 1,2,4-triazine-modified 2'-deoxyuridine triphosphate building block **35** was synthesized in 6 steps. The key intermediate 3-carboxy-1,2,4-triazine (**32**) was achieved by the reaction of commercially available ethyl oxamate (**27**) and Lawesson's reagent (**28**) to provide the reactive intermediate **29** which was subsequently treated with a 1 M solution of hydrazine in THF to obtain ethyl amino(hydrazo)acetate (**30**) in 62% yield. The ethyl-1,2,4-triazine-3-carboxylate (**31**) was obtained in 74% yield by the condensation reaction of **30** with 40% glyoxal in water solution, which was further treated with KOH followed by acidified with 1 N HCl to give the corresponding product **32** in 76% yield. The peptide coupling of aminopropyl-2'-deoxyuridine **33** with 3-carboxy-1,2,4-triazine (**32**) was then performed under standard reaction conditions, followed by phosphorylation of **34** using the methodology of *Ludwig et al.* The crude product **35** was then purified by RP-HPLC using a gradient of ACN-TEAB as eluent. The product-containing fractions were combined, freeze-dried and quantified by absorption spectroscopy at 260 nm which gave a yield of 15% (Scheme 17).



**Scheme 17** Preparation of 1,2,4-triazine-modified 2'-deoxyuridine triphosphate building block **35**

### 3.5.1 Primer extension experiment and fluorescent labeling of 1,2,4-triazine-modified DNA

The investigation of the capability of DNA polymerases to accept the 1,2,4-triazine-modified 2'-deoxyuridine triphosphate **35** was performed by using a variety of polymerases. *Vent (exo-)*, *Deep Vent (exo-)*, *Homo Klen Taq* and *KOD XL* DNA polymerase were chosen for this approach by their advances as mentioned above. The 1,2,4-triazine moiety was attached to the C5 position of 2'-deoxyuridine which was tolerated by all polymerases. Primer extension experiments were performed by using the primer **P1**; containing fluorescein at the 5'-terminus in order to follow the elongation product by following ( $\lambda_{exc} = 471 \pm 20$  nm and  $\lambda_{em} = 535 \pm 20$  nm) after gel electrophoresis. Template **T1** was chosen as standing start experiment which means that the 1,2,4-triazine-modified triphosphate **35** will directly be incorporated after the cytidine natural triphosphate monomer at the 3'-end terminus of the primer. Template **T4** was designed for double modification which means that the modified-building blocks are incorporated next to each other, template **T5** for double modification and the modified-building blocks are incorporated separate from each other by 3 nucleobases. Template **T6** is for triple incorporation of modified-building blocks next to each other. In addition, **P2** and **P3** were used as reference for the thymidine; elongated product (24 NT) and full length elongation product in the presence of only natural nucleoside triphosphate (dNTPs) obtained 35 NT, respectively (Figure 28).

<b>T1</b>	3'-CTG-GGT-GAG-GTA-GCT-CTA-AAG-AG A-GGC-GGC-TCG-CG-5'
<b>T4</b>	3'-CTG-GGT-GAG-GTA-GCT-CTA-AAG-AG G-GCA-ACG-TCG-CG-5'
<b>T5</b>	3'-CTG-GGT-GAG-GTA-GCT-CTA-AAG-AG G-GCA-CGG-ACG-CG-5'
<b>T6</b>	3'-CTG-GGT-GAG-GTA-GCT-CTA-AAG-AG G-GCA-AAC-TCG-CG-5'
<b>P1</b>	5'-Flu-GAC-CCA-CTC-CAT-CGA-GAT-TTC-TC-3'

**Figure 28** Primer extension experiment; template **T1**, template **T4** for double modification next to each other, template **T5** for double modification separated by 3 bases, template **T6** for triple modification next to each other, primer **P1**.

The incorporation of the 1,2,4-triazine-modified 2'-deoxyuridine was first investigated by using **P1/T1** for standing start experiments catalyzed by *KOD XL* and *Hemo Klen Taq* DNA polymerase at 37 °C. The results showed that the elongated product was observed. However, after 90 min the extension process was still not yet completed (Figure 29). It is noteworthy that at such a low temperature the DNA polymerase had a lower reactivity. Accordingly, the extension step was then investigated at a higher temperature, for instance at the maxima efficiency of the applied DNA polymerases.

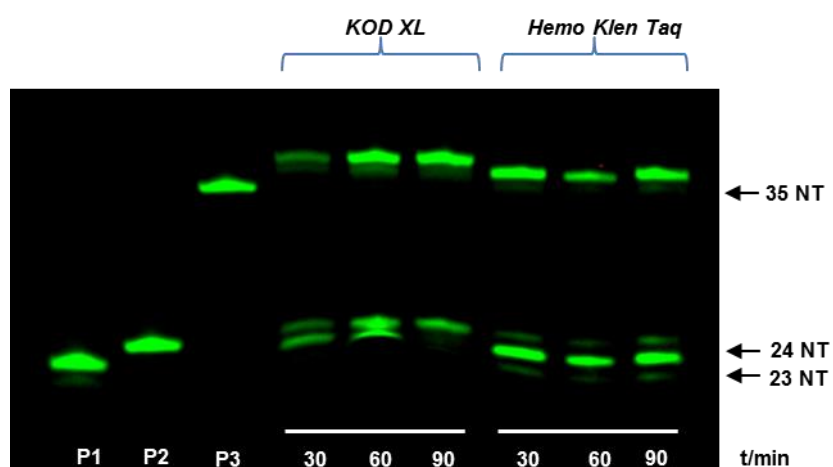


**Figure 29** Standing start experiment of **P1/T1** with *KOD XL* and *Hemo Klen Taq* DNA polymerase at 37 °C.

In this approach *KOD XL* DNA polymerase was chosen and the extension was performed at 64 °C. The remarkable result from PAGE analysis indicated that the triazine-modified building block **35** was accepted by *KOD XL* which gave the desired extension product after 30 min as evidenced by the presence of a slower-moving band in comparison to primer **P1** and the full length elongated primer **P3** as reference. In addition, the negative control experiment was also investigated under the same reaction conditions. It can clearly be seen that the difference in gel mobility shows the absence of the full length elongated product (35 NT) which was observed when only 1,2,4-triazine-modified 2'-deoxyuridine triphosphate **35** was present in the reaction mixture (Figure 30).

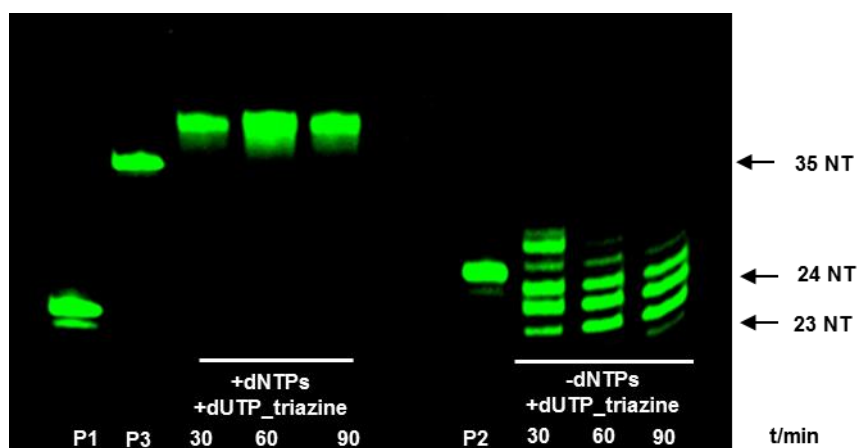


**Figure 30** Standing start experiment of **P1/T1** with *KOD XL* DNA polymerase at 64 °C.

Moreover, a set of primer extension experiments were performed using various DNA polymerases at 64 °C in order to further investigate the capability of DNA polymerases in accepting the 1,2,4-triazine-modified 2'-deoxyuridine triphosphate **35** (Figure 31).

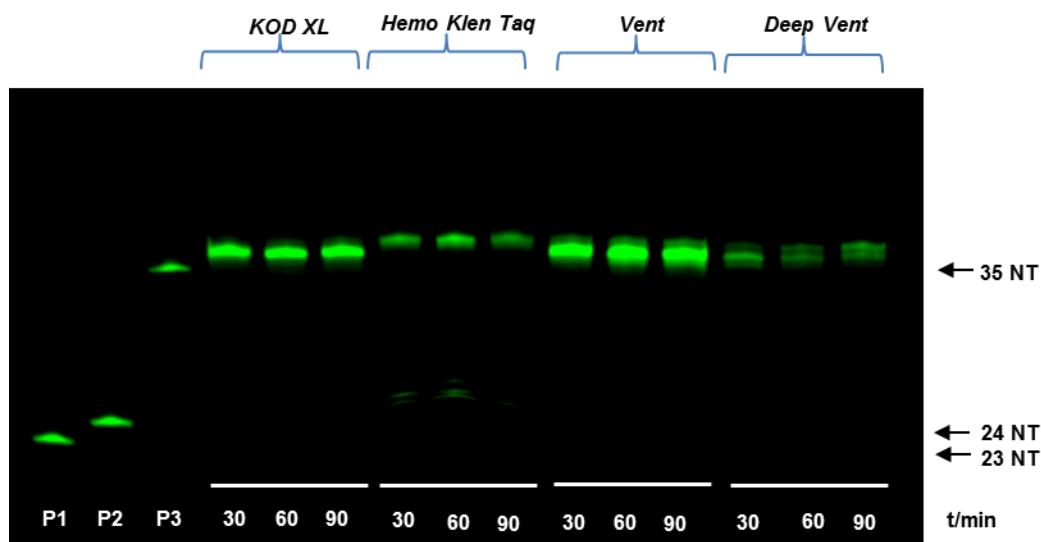


**Figure 31** Standing start experiment of **P1/T1** with *KOD XL*, *Hemo Klen Taq*, *Vent (exo-)* and *Deep Vent (exo-)* DNA polymerase at 64 °C.

The elongated product was observed after 30 min in all cases which can clearly be seen from the difference of the electronegative mobility on the gel compared to **P1**, **P2** and **P3**, respectively. The successful incorporation of the 1,2,4-triazine-modified building block **35** into DNA by using various DNA polymerases led to further investigation of the ability of this reactive probe for postfluorescent labeling of DNA. The reaction between 1,2,4-triazine-modified DNA with BCN-modified rhodamine **36** was first performed in a mixture of H<sub>2</sub>O-DMSO (100:1) at room temperature without a desalting step. The conjugated product was elucidated by PAGE analysis. The result from the PAGE indicated that the conjugated product was obtained in 74% yield after treatment with BCN-modified rhodamine dye **36** at room temperature for 1 h in the presence of a 1000 equivalent of the dye **36**. It was observed that when the dye **36** was added another 1000 equivalent to the reaction mixture, the DA product was

obtained in the same yield 74%. In addition when the coupled step was extended to 3 h in the presence of 1000 equivalent of BCN-modified rhodamine dye **36**, the ligated product was still obtained in the same yield which was 74%, respectively (Figure 32).

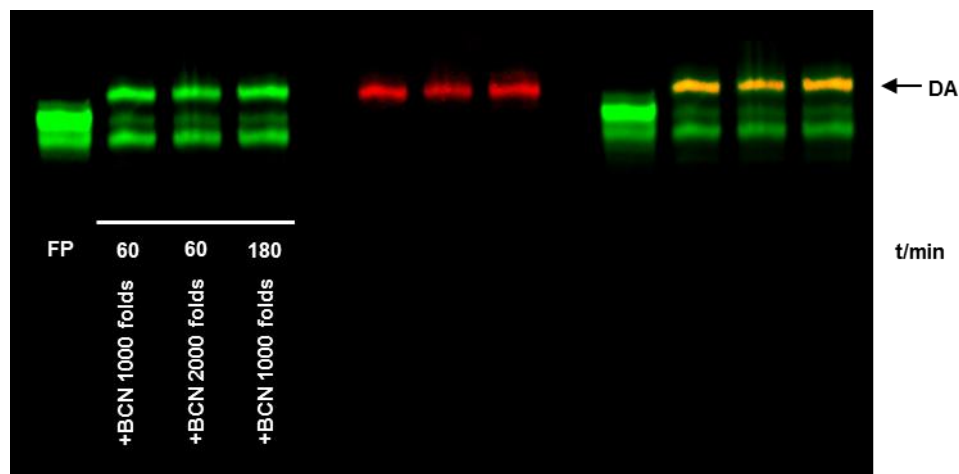


**Figure 32** Diels-Alder reaction of the extension product (**P1/T1**) with BCN-modified rhodamine dye **36** at room temperature in a mixture solution of H<sub>2</sub>O-DMSO (100:1) without desalted step. Green indicates the fluorescence of fluorescein, red indicates the fluorescence of rhodamine.

Therefore, 1000 equivalent of BCN-modified rhodamine dye **36** will be used as a standard condition for other experiments. Regarding the prior experiments, that used a lower equivalent than 1000, the ligation step required a longer reaction time and/or the excess equivalent of the dye might affect the stability of DNA with respect the dye was dissolved in DMSO. Moreover, the conjugation product yield could be enhanced by an additional desalting step prior to the conjugation step. The primer extension experiments were conducted under the same reaction conditions subsequently, desalted, freeze-dried and dissolved in water to reach the final concentration of 750 nM prior to the ligation steps. After treating with fluorescent dye **36** for 1 h the corresponding conjugated product was directly applied to PAGE. The results indicated that the efficiency of the Diels-Alder reaction had increased from 74% yield to 82% yield (Figure 33).

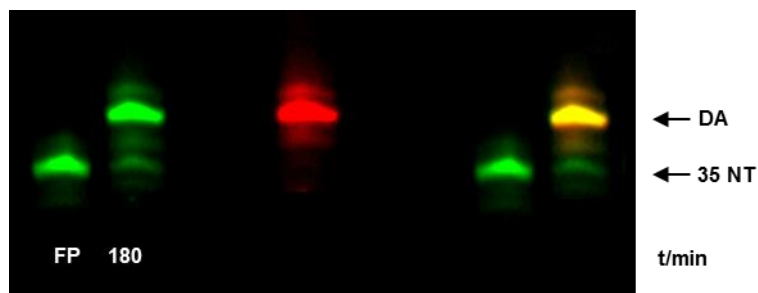


**Figure 33** Diels-Alder reaction of the extension product (**P1/T1**) with BCN rhodamine dye **36** at room temperature for 3 h in a mixture solution of H<sub>2</sub>O-DMSO (100:1) after desalting step.

The successful results from single labeling in DNA led to the investigation of the capability of multiple incorporations of the 1,2,4-triazine-modified building block **35** by using the advances of DNA polymerases. The primer extension experiment was conducted using the primer **P1** with the templates; **T4**, **T5** and **T6**, respectively. Regarding the elongation reaction from previous results, the modified building block **35** was accepted at higher than 50 °C. The extension reaction was first investigated at 55 °C catalyzed by *Deep Vent (exo-)* DNA polymerase. It was obvious that the extension was completed after 60 min for the incorporation at adjacent positions **P1/T4**. On the other hand, when the modified building blocks were incorporated separate from each other by 3 bases, the results indicated that the *Deep Vent (exo-)* DNA polymerase tolerated the first incorporation but lacked efficiency to incorporate the next modified building block. Nevertheless, the full length product was observed after 30 min. As expected, the triple incorporation of modified building blocks adjacent to another is even more challenging. The results showed that after 60 min the extension product was obtained together with several shorten incomplete elongated DNA strands (Figure 34). An explanation could be that at a lower temperature, the efficiency of the DNA polymerase to accept the bulky modified-building block was limited. As mentioned above, *Deep Vent (exo-)* DNA polymerase has its maximum activity at 72 °C.

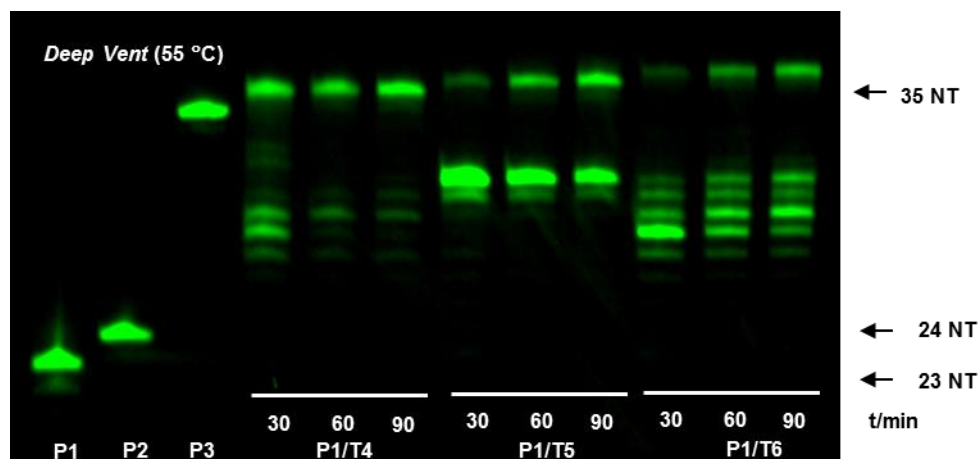


**Figure 34** Primer extension experiments of double incorporation of modified-building blocks next to each other (**P1/T4**), double incorporation of modified-building blocks separated from each other by 3 bases (**P1/T5**) and triple incorporation of modified-building blocks line next to each other (**P1/T6**) with *Deep Vent* (*exo*-) DNA polymerase at 55 °C.

In order to overcome this problem, the primer extension experiment was conducted at 72 °C. The results from gel electrophoresis indicate that the extension was successful in obtaining the full length extension product after 90 min via incorporation adjacent to another and separate by 3 bases (**P1/T4** and **P1/T5**) even though the truncated products were also observed. Surprisingly, the elongation of **P1/T6** was not proceeding under this condition (Figure 35). It is noteworthy that compared to previous experiments, the *Deep Vent* (*exo*-) DNA polymerase accepted the triple incorporation at 55 °C. It could be explained by the steric hindrance of 1,2,4-triazine-modified 2'-deoxyuridine building blocks **35** which decreased the capability of the polymerase at higher temperatures.

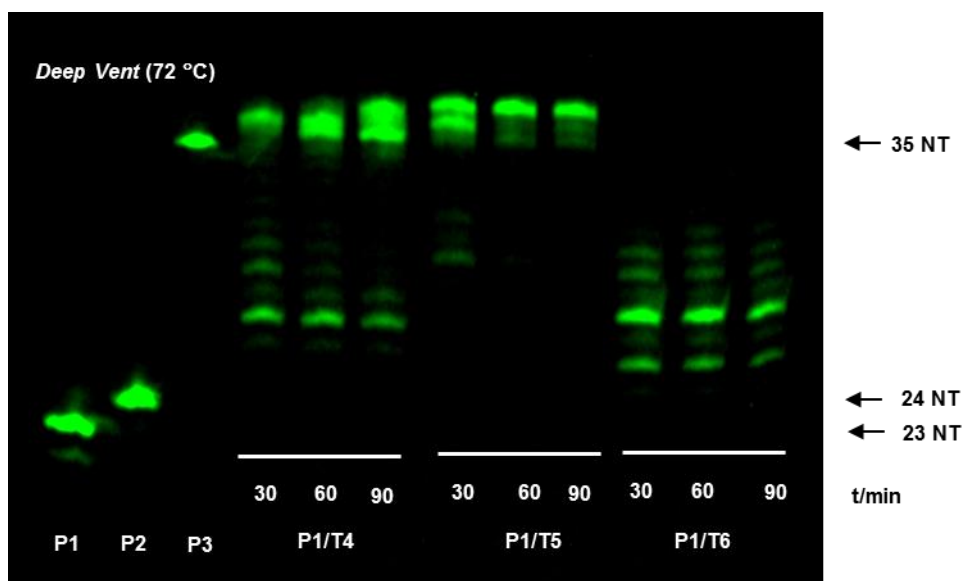


**Figure 35** Primer extension experiment of double incorporation of modified-building block adjacent to another (**P1/T4**), double incorporation of modified-building block separated from each other 3 bases (**P1/T5**) and triple incorporation of modified-building block adjacent next to another (**P1/T6**) with *Deep Vent* (*exo*-) DNA polymerase at 72 °C.

An alternative DNA polymerase for the extension experiments at moderate temperatures with high probability to accept the bulky modified-building block is *KOD XL*. The extension experiments with the modified building block, **P1/T4**, **P1/T5** and **P1/T6** were conducted at 64 °C. The full length elongated product **P1/T4** was observed after 90 min. Interestingly, the elongation by 1,2,4-triazine-modified building blocks **35** which were separated from each other by 3 bases **P1/T5**, remarkably showed the completed extension within 30 min. As mentioned above, the multiple incorporations of modified building blocks adjacent to each other are even more challenging. It could clearly be seen on the gel that the full length elongated product of **P1/T6** was also obtained after 90 min. However, several shorter DNA strands as incomplete products were also obtained (Figure 36).

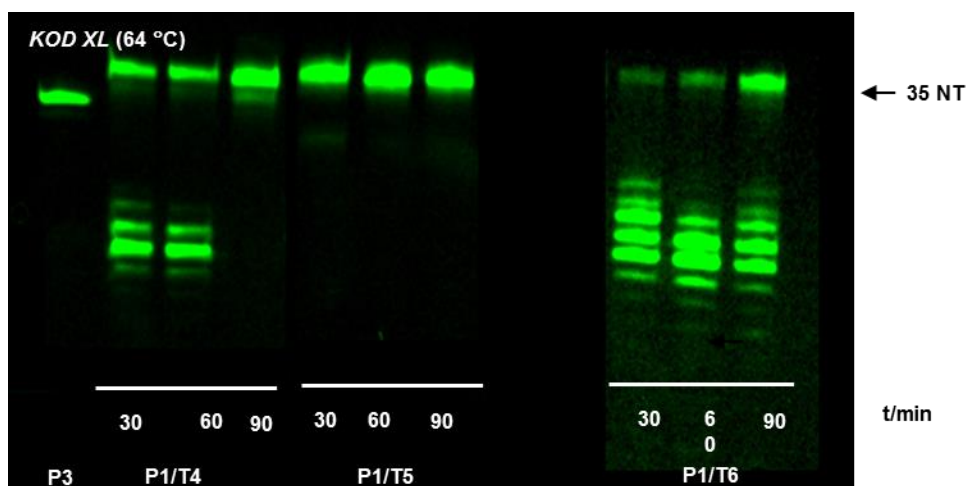


**Figure 36** Primer extension experiments of double incorporation of modified-building blocks adjacent to another (**P1/T4**), double incorporation of modified-building blocks separated from each other by 3 bases (**P1/T5**) and triple incorporation of modified-building blocks adjacent next to another (**P1/T6**) with *KOD XL* DNA polymerase at 64 °C.

After successful multiple incorporations of the 1,2,4-triazine-modified building block **35** into DNA, the next step was to perform the Diels-Alder reaction (DA) with BCN-modified rhodamine dye **36**. The full length elongated product of **P1/T4**, **P1/T5** and **P1/T6** was desalted and freeze-dried prior to the conjugation reaction step. The crude product was then dissolved in water to reach the final concentration of 750 nM and subsequently mixed with BCN-modified rhodamine dye **36** (1000 fold) in a mixture of H<sub>2</sub>O-DMSO (100:1) at room temperature for 1 h and 3 h respectively. The visualization of PAGE analysis was performed by using  $\lambda_{\text{exc}} = 470 \pm 20$  nm and  $\lambda_{\text{em}} = 535 \pm 20$  nm for fluorescein (green) and  $\lambda_{\text{exc}} = 540 \pm 10$  nm and  $\lambda_{\text{em}} = 605 \pm 10$  nm for rhodamine (red). It was clearly seen that the conjugation of 1,2,4-triazine-modified DNA, where the modified positions were adjacent to each other, **T4** could be labeled by the DA reaction within 1 h and provided mixtures of single and double ligation products. Interestingly, after a 3 h reaction time, both the conjugated products were observed in 100% yield (Figure 37).

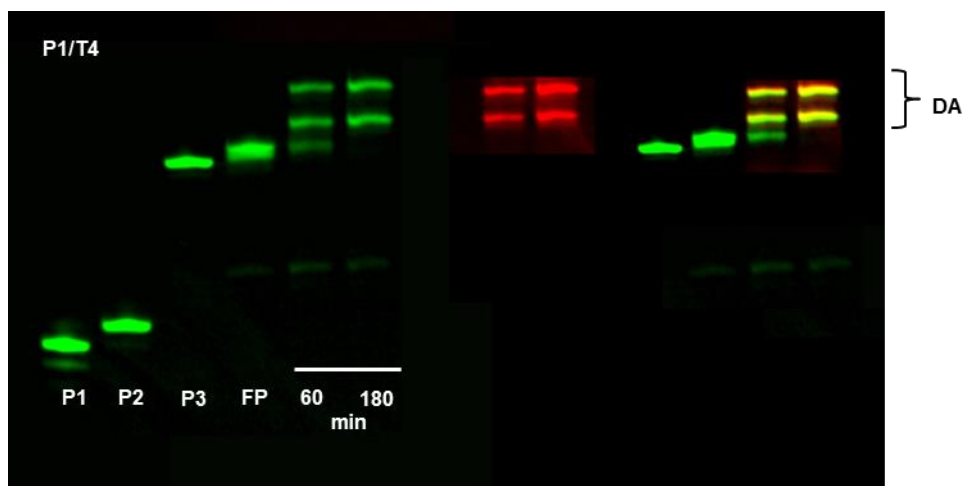


**Figure 37** PAGE analysis of conjugation reaction of extension product **P1/T4** in comparison with **P1**, **P2**, **P3** and full length elongated product (**FP**). Green indicates the fluorescence emission of fluorescein ( $\lambda_{\text{exc}} = 470 \pm 20$  nm and  $\lambda_{\text{em}} = 535 \pm 20$  nm). Red indicates the fluorescence emission of rhodamine dye ( $\lambda_{\text{exc}} = 540 \pm 10$  nm and  $\lambda_{\text{em}} = 605 \pm 10$  nm).

The conjugation of extension product **P1/T5** with BCN-rhodamine dye **36** was performed under the same reaction conditions. PAGE analysis showed that the conjugation reaction proceeded even faster than that for **P1/T4**. The DA products were obtained in 100% yield within 1 h (Figure 38). It could be explained by the steric hindrance of the 1,2,4-triazine-moieties on DNA, when the incorporation into two adjacent positions inhibits the efficiency of the DA reaction and longer ligation times are necessary. In contrast, when the modification positions were separated from each other by 3 bases for **P1/T5**, less steric hindrance occurs, and the reaction can proceed faster.

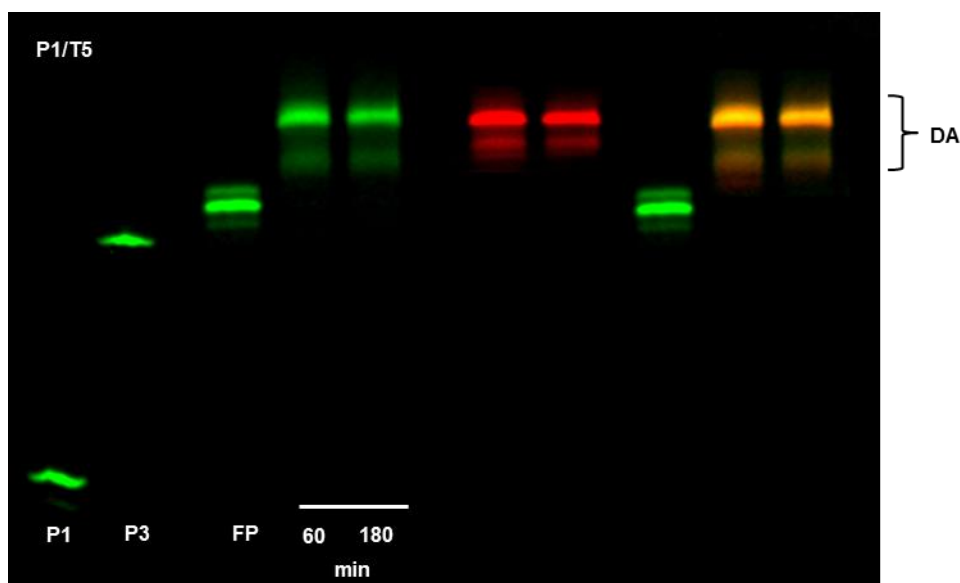


**Figure 38** PAGE analysis of conjugation reaction of extension product of **P1/T5** in comparison with **P1**, **P3** and full length elongated product (**FP**). Green indicates the fluorescence emission of fluorescein ( $\lambda_{\text{exc}} = 470 \pm 20$  nm and  $\lambda_{\text{em}} = 535 \pm 20$  nm). Red indicates the fluorescence emission of rhodamine dye ( $\lambda_{\text{exc}} = 540 \pm 10$  nm and  $\lambda_{\text{em}} = 605 \pm 10$  nm).

The reaction with the extension product of **P1/T6** was additionally performed. PAGE analysis showed that the conjugated product could be observed within 1 h to provide a mixture of single, double and triple labeled products in 65% total yield (Figure 39). The DA products and full length product (**FP**) were found to be destroyed if reaction times exceeded 3 h, which was indicated by the difference in gel electrophoretic mobility. The shortened fragment DNA strands were observed by the fluorescein channel (green) but not by the rhodamine channel (red), indicating that the breaking position is on the 5'-position of the full length product corresponding, the remained fluorescein tag-DNA stranded. It might be due to the presence of DMSO as a co-solvent, as this causes DNA damage according to prior results (COMBO-modified DNA) where long reaction times were applied.

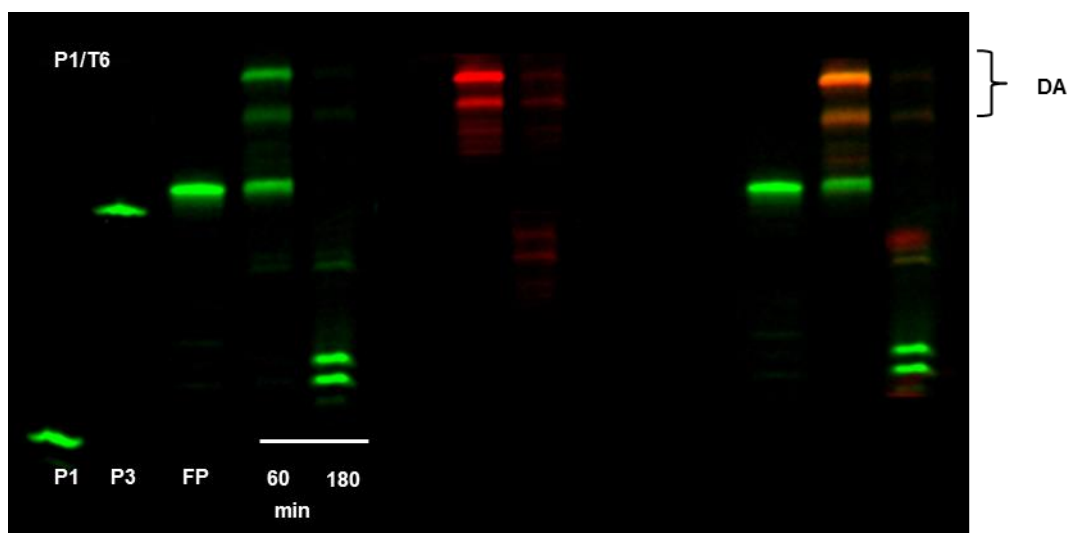


**Figure 39** PAGE analysis of conjugation reaction of extension product of **P1/T6** in comparison with **P1**, **P3** and full length elongated product (**FP**). Green indicates the fluorescence emission of fluorescein ( $\lambda_{exc} = 470 \pm 20$  nm and  $\lambda_{em} = 535 \pm 20$  nm). Red indicates the fluorescence emission of rhodamine dye ( $\lambda_{exc} = 540 \pm 10$  nm and  $\lambda_{em} = 605 \pm 10$  nm).

## 4 Conclusions

The postsynthetic labeling of base-modified oligonucleotides via strain-promoted reaction of reactive cyclooctyne- and triazine-modified nucleoside building blocks as a new class of bioorthogonal reactions were successful in both *in vitro* and *in vivo* experiments. The carboxymonobenzocyclooctyne (COMBO) moiety **7** was attached to 2'-deoxyuridine at C5-position via triple bond and single bond linkers with the purpose to investigate the influence of the rigid and flexible linkers on optical properties of modified-DNA. The incorporation of these bioorthogonally reactive moieties building blocks **14** and **19** into DNA was employed both by chemical DNA synthesis (phosphoramidite method) and enzymatic DNA synthesis (primer extension experiment with triphosphates). The copper-free click reaction of COMBO-modified DNAs with (E)-3-(6-azido-2-(2-(6-(diethylamino)benzofuran-2-yl)vinyl)benzo[d]thiazol-3-ium-3-yl)propane-1-sulfonate (**21b**) was successful within 3 h to provide the desired clicked-oligonucleotide product in moderate to high yield (58-87% yield). As expected the more flexible linker enhanced the brightness of fluorescence both in single and double strands DNA. With respect to their high fluorescence intensity, DNA**4** and DNA**8** were chosen for presynthetic fluorescent labeling for *in vivo* experiments (Figure 40).

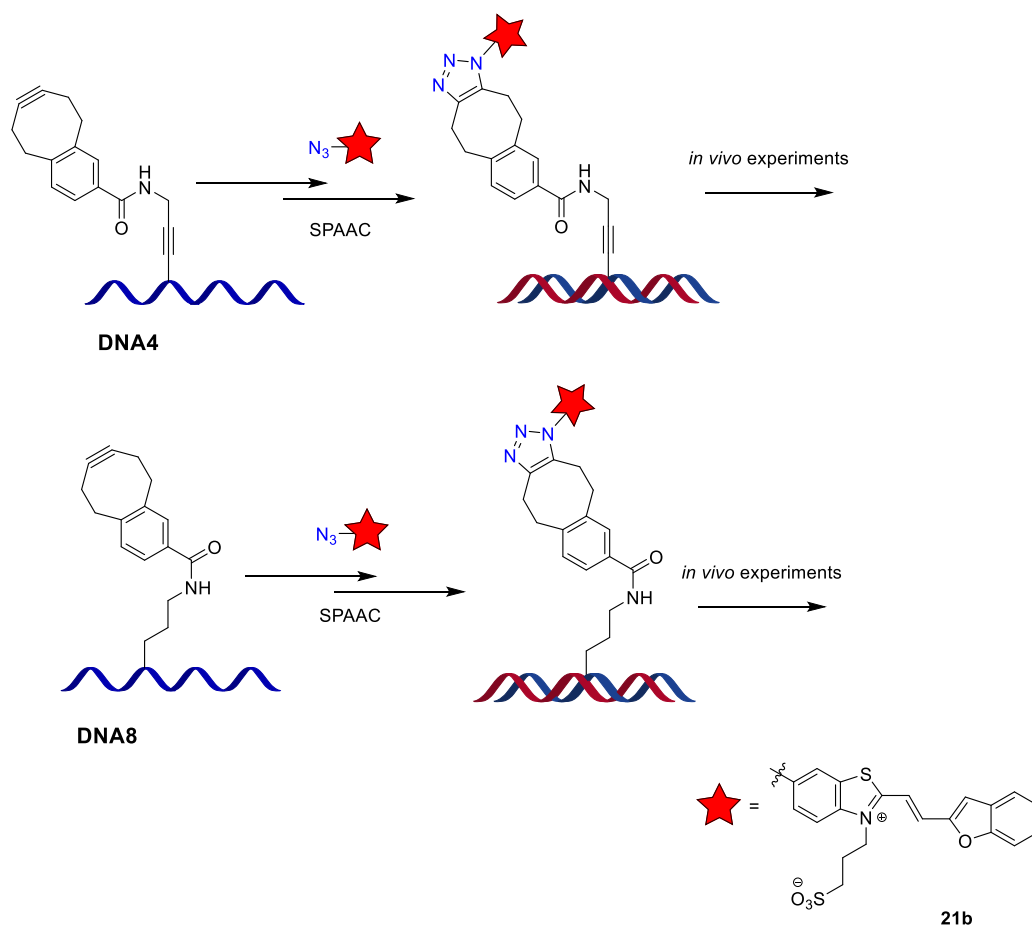


**Figure 40** “Copper-free click” reaction of chemical incorporated COMBO-modified DNA with azido dye **21b**.

The COMBO-modified DNA strands, DNA2 and DNA6 were conjugated with azide-modified dye **21b** at room temperature for 3 h. Subsequently the corresponding double strands dsDNA4 and dsDNA8 were transfected into *Hela* cells. Confocal fluorescence microscopy, visualized that the COMBO-modified DNA8 with the flexible linker provided higher fluorescence inside the cell compared to DNA4. According to its high fluorescence intensity inside cells, DNA6 was chosen for postfluorescent labeling in *in vivo* experiments. The COMBO-modified DNA6 was transfected prior to the ligation step. A set of azide-modified dyes **20a-22b**, were employed in order to investigate the polarity influence for membrane-permeability. The COMBO-modified DNA6 was successfully conjugated with these azide-modified dyes inside cells to provide bright fluorescence. Remarkably, the results showed that the coumarin derivatives dye **20a** and **21a** were found in nuclei whereas the benzo-furan components **20b** and **21b** are preferably in endosomal vesicles (Figure 41).

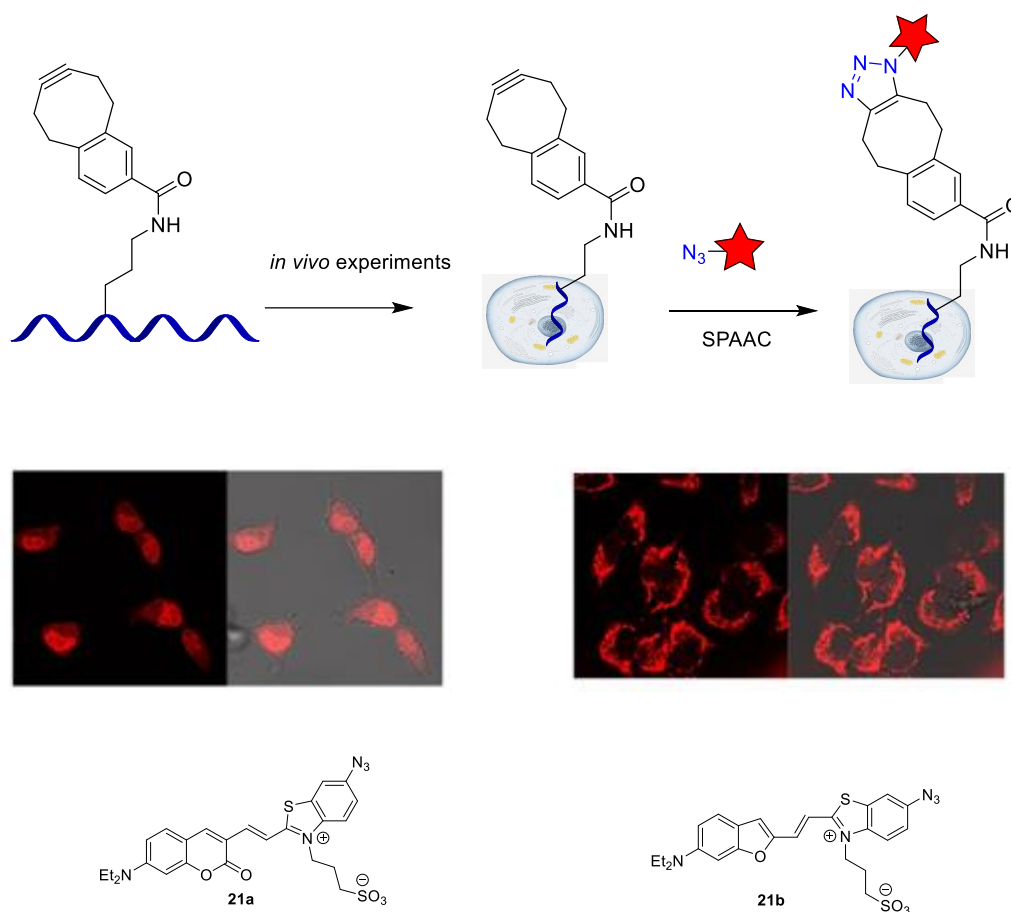


**Figure 41** Postsynthetic fluorescent labeling of COMBO-modified DNA in *HeLa* cells.

Unfortunately, the conjugation reactions of primer extension product (COMBO-modified DNA) with fluorescent dyes were not successful. It may be explained by the high lipophilicity of the COMBO moiety that hide it inside the double strand, therefore the click reactions did not occur. To overcome this problem an alternative compound which exhibits less lipophilicity is 3-carboxy-1,2,4-triazine (**32**). The 1,2,4-triazine-modified 2'-deoxyuridine triphosphate building block **35** was successfully prepared in high yield and subsequently incorporated into DNA via enzymatic DNA synthesis. The enzymatic incorporation of single and multiple positions was successful within 30 min after optimization of the elongation condition (Figure 42). The conjugation of extension products with the BCN-modified dye **36** was performed at room temperature for 1-3 h. The ligated products were obtained in 82% yield for single incorporation **P1/T1**, in quantitative yield for a mixture of single and double DA products of **P1/T4**, in quantitative yield for a mixture of single and double DA products

of **P1/T5** and 65% for the triple incorporation next to each other for **P1/T6**, respectively.

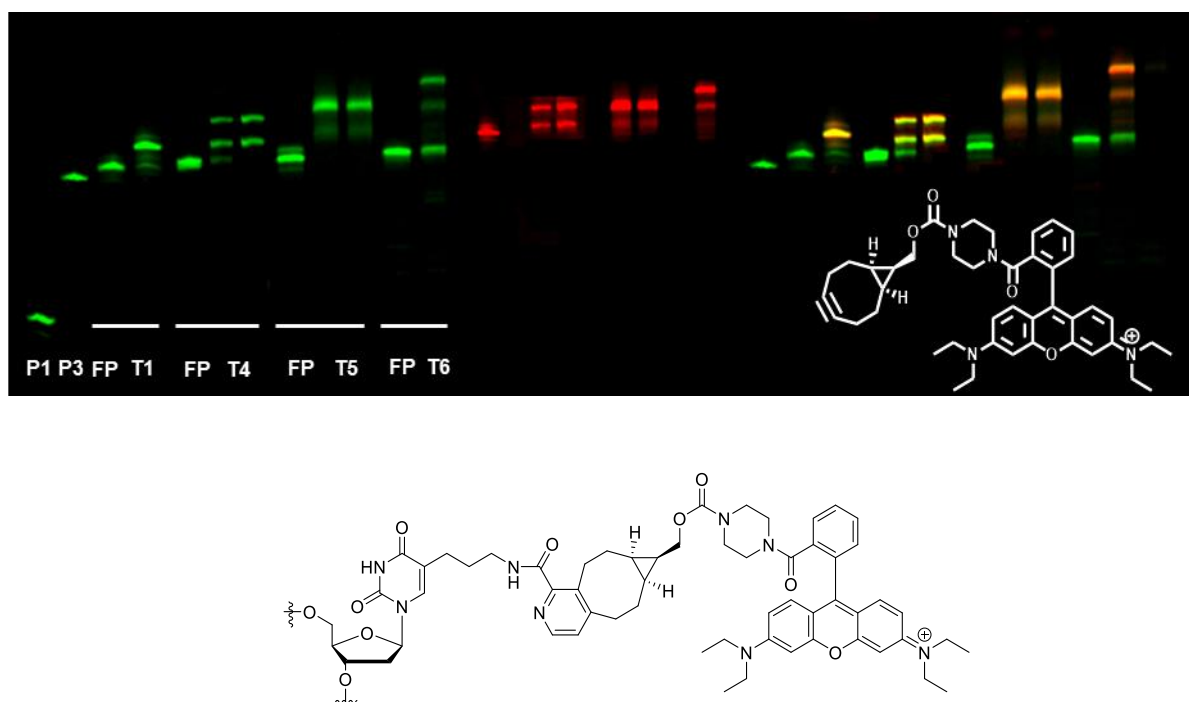


**Figure 42** Strain-promoted reactions of multiple incorporations of triazine-building blocks **35** with BCN-modified fluorescent dye **36**.

## 5 Experimental section

### 5.1 Materials and methods

#### Chemicals

Chemicals, required for synthesis were purchased and were used without further purification from *ABCR*, *Sigma Aldrich*, *Alfa Aesar*, *Acros*, *VWR* and *Fluka*. The storage and handling took place according to the manufacturer's instructions.

#### Solvent

The solvents which were used for the synthesis were purchased from *Acros*, stored under argon atmosphere in the presence of molecular sieves. For work-up and purification, solvent of technical grade were used unless otherwise mentioned. The deuterated solvents for NMR measurement were purchased from *euriso-top*.

#### Inert gas

The reactions were carried out under an argon atmosphere (argon 4.6). The required glass wares were evacuated, heated with a heat gun and refilled cycle to ensure an inert atmosphere before adding the reagents.

#### Ultrapure water

Ultrapure water was generated by a Milli-Q<sup>®</sup> Direct 8/16 plant from *Merck Millipore* from tap water.

### Thin layer chromatography (TLC)

Aluminum TLC plates, coated with silica gel 60 and fluorescent indicator F254 with a layer thickness of 0.25 mm from *Merck* were used. The optical detection was carried out with a UV handheld lamp via fluorescence quenching at  $\lambda = 254$  nm or at  $\lambda = 366$  nm. The analysis was carried out by staining either a solution of potassium permanganate (450 mg  $\text{KMnO}_4$ , 630 mg  $\text{K}_2\text{CO}_3$ , 45 mL  $\text{H}_2\text{O}$ , 750  $\mu\text{L}$  5%  $\text{NaOH}$ ) or 3% of  $\text{H}_2\text{SO}_4$  in  $\text{MeOH}$  followed by heating with a hot-air drier.

### Flash Chromatography (FC)

The silica gel technical grade (pore size of 60 Å and 230-400 mesh (40-63  $\mu\text{m}$ ) particle size) was purchased from *Sigma Aldrich*. The stationary phase was wet-packed and the substance was either applied as solution (dissolved with a suitable solvent) or dried (adsorbed onto silica gel). The required overpressure was generated with a hand pump. The required eluents were mixed volumetrically in measuring cylinders.

### High performance liquid chromatography (HPLC)

The purification of oligonucleotides and triphosphate building blocks were performed by using Reversed Phase Supelcosil™ LCC18 column (25 x 10 mm, 5  $\mu\text{m}$  for preparative separation) or a Supercosil™ LC-318 (25 cm x 4.6 mm, Supelcosil for analytical separation) on a Shimadzu HPLC system (autosampler SIL-10AD, pump LC-10AT, controller SCL-10A, diode array detector SPD-M10A) control by Class-VP software and degasser DGU-14A. The used flow rate was 1 ml/min (for analytical separation and 2.5 ml/min) or (for preparative separation). The elution; a gradient of acetonitrile (eluent B) and a 50 mM ammonium acetate buffer (pH = 6.5) in HPLC- $\text{H}_2\text{O}$  (eluent A) was used for oligonucleotide purification. Triethylammonium bicarbonate buffer (eluent A, 50 mM, pH = 7) was used for the purification of triphosphates. The detection wavelength was selected at the maxima absorption which refers to the characteristic of molecules.

**Table 2** Detection wavelength ( $\lambda$ ) of chromophore-modified DNA and fluorescent dye.

Chromophores	Detection wavelength ( $\lambda$ )
unmodified-DNA	260 nm
COMBO	290 nm
3-carboxy-1,2,4-triazine	320 nm
21b	610 nm

### Lyophilisation

For the sublimation drying, an Alpha 1-2 LD Plus lyophilization system from *Christ* was used. The samples were frozen in liquid nitrogen prior applied to lyophilization system.

### Solid-phase DNA synthesis

Solid-phase DNA synthesis was conducted on an Expedite Nucleic Acid Synthesizer System from *Applied Biosystems*. The device was operated under an argon atmosphere as a protective gas. CPG (Controlled Pore Glass) with a coverage of 1  $\mu\text{mol}$  (500  $\text{\AA}$ ) served as a solid phase. The chemicals and CPG columns for solid phase synthesis were obtained from Applied Biosystems (ABI), Glen Research, *Sigma Aldrich* and *Proligo Reagents*.

## Hybridization

The hybridisation of single stranded DNA with their complementary strands were performed in the presence of 10 mM sodium phosphate buffer (NaPi, pH = 7) and 250 mM NaCl at 90 °C for 10 min and allowed to slowly cool down to room temperature.

## Thermocycler

A thermal cycler used for primer extension experiments was used from *biometra/Analytik Jena*, model TGradient 96.

## Gel electrophoresis

The denaturing polyacrylamide gels were freshly prepared by mixing 12% acrylamide/bisacrylamide (19:1), 15.5 ml of acrylamide/bisacrylamide (19:1, 40% aqueous solution), 12.5 g of urea, 21 ml of 8.3 M of urea solution and 5 ml of 10 fold TBA buffer in the presence of 8.3 M urea solution (pH 8.0). The polymerization starts in the presence of 20  $\mu$ l of TEMED and 425  $\mu$ l of 10% APS solution. PAGE analysis was carried out under TBE buffer (2 mM EDTA, 89 mM TRIS base and 89 mM boric acid) as an electrolyte at 50 °C, 45 W for 60 min using *BioRad* sequencing chamber (38 cm x 50 cm) and Sequi-Gen GT Sequencing Cell (21 cm x 40 cm) with a PowerPac HV from *BioRad*.

## Fluorescence Imager

The visualization of the primer extension product was carried out with a Stella 8300 fluorescence imager from *Raytest*. The emission was recorded with a full-frame CCD camera with microlenses (cooled to -20 °C). The excitation wavelength and a suitable emission filter were selected for each chromophore ( $\lambda_{exc} = 470 \pm 20$  nm, and  $\lambda_{em} = 535 \pm 20$  nm; Cy2m,  $\lambda_{exc} = 540 \pm 10$  nm, and  $\lambda_{em} = 605 \pm 10$  nm; Cy3m and  $\lambda_{exc} = 630 \pm 10$  nm, and  $\lambda_{em} = 700 \pm 17.5$  nm; Cy5m).

The exposure time varied between 2-6 min with maximum distance (Stage 4). The Aida Image Analyzer v.450 from *Raytest* was used to evaluate the images.

### Nanodrop ND-1000 Spectrophotometer

The concentrations of synthesized oligonucleotides were determined by using the absorbance at 260 nm from *peQlab*.

### NMR measurements

Nuclear magnetic resonance spectra were measured either on *Bruker* Avance 300, Avance 400 or Avance DRX 500 at Karlsruhe Institute of Technology (KIT), Institute of Organic Chemistry, in 0.5 ml deuterated solvents. The chemical shifts of the signals were reported in ppm based on tetramethylsilane as the zero point. The calibration was carried out via the signal of the incompletely deuterated solvent. In the case of  $^1\text{H}$  spectra or the solvent itself for  $^{13}\text{C}$  measurements <sup>[93]</sup>.

$\text{CDCl}_3$ :	$^1\text{H}$ NMR: $\delta = 7.26$ ppm	$^{13}\text{C}$ NMR: $\delta = 77.16$ ppm
$\text{DMSO-d}_6$ :	$^1\text{H}$ NMR: $\delta = 2.50$ ppm	$^{13}\text{C}$ NMR: $\delta = 39.52$ ppm
$\text{CD}_3\text{OD}$ :	$^1\text{H}$ NMR: $\delta = 3.31$ ppm	$^{13}\text{C}$ NMR: $\delta = 49.00$ ppm

The coupling constants (J) were given in Hz. The multiplicity of  $^1\text{H}$  signals has been abbreviated as follow: s (singlet), d (doublet), t (triplet), q (quartet), p (pentett), dd (doublet of doublet) and m (multiplet).

### Mass spectrometry

The mass spectra were recorded by the analytical department of the Institute of Organic Chemistry using *Finnigan* model MAT 95. The electron impact ionization (EI) and fast atom bombardment (FAB) were used for ionization techniques. MALDI mass spectra were recorded on a Biflex IV from *Bruker Daltronics*. The synthesized oligonucleotides were mixed with a 3-hydroxypicolinic (HPA) acid matrix and triphosphates in a 2',4',6'-trihydroxyacetophenone matrix (THAP). The data are given in  $m/z$  with the intensity as a percentage of the basic peak.

### Optical spectroscopy

The optical measurements were carried out in quartz glass cuvettes from *Starna*. These were 1 cm in diameter and 1 ml in volume. The High Precision Cell Quartz Cells from *Hellma* were required when very small samples were measured (50  $\mu$ l with a light inlet of 3x3 mm).

### Absorption spectroscopy

The absorption spectra were measured on a Cary 100 Bio Spectrometer from *Varian* with a temperature unit (Cary 100 temperature controller) at 20 °C. The spectra were background-corrected against the absorption of the pure solvent. The recording parameters used were: SBW: 2.0 nm; Average Time 0.1 s; Data Interval 1.0 as well as Light Source Changeover 350 nm and 390 nm, respectively.

### Fluorescence spectroscopy

Fluorescence spectra were measured on a *Horiba Jobin-Yvon* Fluoromax-4-NIR fluorescence spectrometer. The samples were thermostated with a Peltier element LFI-3751 at 20 °C and the spectra were corrected based on the Raman dispersion of the solvent. The used settings were; increment 0.1 nm; increment time 0.2 s; excitation and emission bandpass of 5 nm.

## Quantum yield measurement

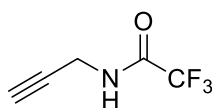
The quantum yields were determined on a Quantaaurus QY C11347 from *Hamamatsu* in single mode by using excitation wavelength at 615 nm.

## 5.2 Synthesis

Already literature known synthesis and spectroscopic data are not explicitly listed, but the corresponding literature references are given.

### 7.2.1 Synthesis of COMBO-modified nucleoside building block 14

#### 2,2,2-trifluoro-*N*-prop-2-ynylacetamide (**10**)



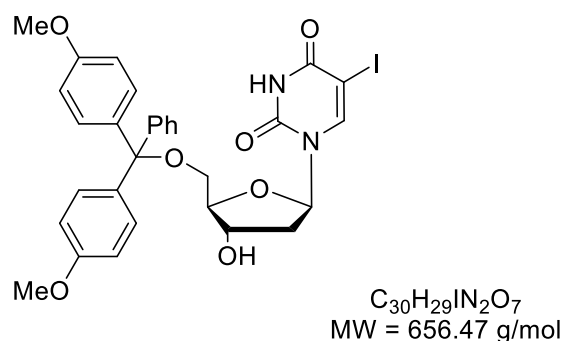
$C_5H_4F_3NO$   
MW = 151.09 g/mol

Ethyl trifluoroacetate (17.1 g, 120 mmol, 1.20 eq) was added dropwise into a cool solution of propargyl amine (5.51 g, 100 mmol, 1.00 eq) in MeOH at 0 °C. The reaction was allowed to stir at room temperature overnight. After completion of the reaction, the mixture was neutralized by saturated NaHCO<sub>3</sub> solution, extract with CH<sub>2</sub>Cl<sub>2</sub> and dried over Na<sub>2</sub>SO<sub>4</sub>. The solvent was then removed under reduced pressure and the crude product was purified by column chromatography, CH<sub>2</sub>Cl<sub>2</sub> (100%) to obtain colorless oil 14.2 g (94.06 mmol) in 94% yield.

TLC (CH<sub>2</sub>Cl<sub>2</sub>): R<sub>f</sub> = 0.62

The analytical data are consistent with the literature <sup>[94]</sup>.

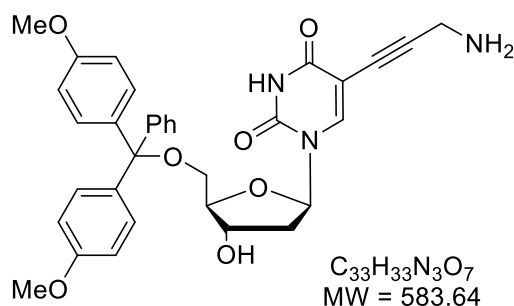
5'-O-4,4'-Dimethoxytrityl-5-iodo-2'-deoxyuridine (9)



In a dried flask, 5-iodo-2'-deoxyuridine (0.708 g, 2.00 mmol, 1.00 eq) and 4,4'-dimethoxytriphenylmethyl chloride (1.02 g, 3.00 mmol, 1.50 eq) were dissolved in anhydrous pyridine (5 ml). To the solution mixture was then added  $Et_3N$  (474  $\mu$ l, 3.40 mmol, 1.70 eq) and stirred at 40 °C for 18 h. After completion of the reaction, a solvent was removed under reduced pressure and the residue was purified by flash column chromatography (EtOAc-Hexane = 2:1+0.1%  $Et_3N$ ) to give a white solid 0.968 g (1.50 mmol) in 74% yield.

TLC (EtOAc-Hexane = 2:1+0.1%  $Et_3N$ ):  $R_f$  = 0.33

The analytical data are consistent with the literature <sup>[95]</sup>.

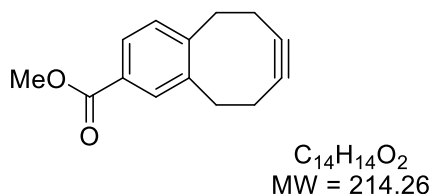
5-(3''-aminopropynyl)-5'-O-dimethoxytrityl-2'-deoxyuridine (**12**)

5'-DMT protected 5-Iodo-2'-deoxyuridine (0.180 g, 0.27 mmol, 1.00 eq), propargyltrifluoroacetamide (**10**) (0.123 g, 0.81 mmol, 3.00 eq), CuI (11.24 mg, 0.059 mmol, 0.220 eq) and tetrakis-(triphenylphosphine) palladium (0) (31.2 mg, 0.030 mmol, 0.01 eq) were dissolved in anhydrous DMF (5 ml). The mixture was degassed and anhydrous Et<sub>3</sub>N (76  $\mu$ l, 0.54 mmol, 2.0 eq) was added. The reaction mixture was allowed to stir at room temperature for 24 h. After completion of the reaction, the solution mixture was then filtered through celite, washed with EtOAc (10 ml). The solvent was removed under reduced pressure and the residue was then purified by flash column chromatography (CH<sub>2</sub>Cl<sub>2</sub>-Acetone = 5:1+0.1% Et<sub>3</sub>N) to give a light brown solid 0.079 g (0.120 mmol) in 72% yield. The corresponding adduct was then treated with 37% NH<sub>3</sub> in aqueous solution at room temperature for 24 h. The desired light brown solid was obtained quantitative yield without further purification.

TLC (CH<sub>2</sub>Cl<sub>2</sub>-MeOH = 10:1+0.1% Et<sub>3</sub>N): R<sub>f</sub> = 0.13

The analytical data are consistent with the literature <sup>[96]</sup>.

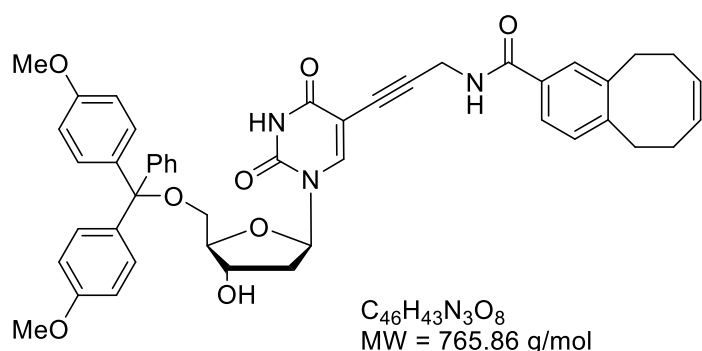
2-methoxycarbonyl-5,6,9,10-tetrahydro-7,8-dehydro-benzocyclooctene (**6**)



In a dried flask, K<sub>2</sub>OtBu (210 mg, 1.87 mmol, 2.50 eq) and 18-crown-6-ether (50.0 mg, 0.190 mmol, 0.250 eq) were placed. Then a mixture solution of hexane:1,4-dioxane (10:1, 100 ml) was added, the reaction mixture was heated up to 58 °C at this point a solution of carboxymethylbromobenzocyclooctene (**5**) (220 mg, 75.0 mmol, 1.00 eq) in hexane:1,4-dioxane (10:1, 10 ml) was added dropwise and allow to stir at this temperature for 90 min. After completion of the reaction, the solid was then filtered off, washed with EtOAc (20 ml), a solvent was then removed under reduced pressure. The desired product was obtained after purification by column chromatography (Hexane-EtOAc = 10:1) to obtain a light yellow solid 60 mg (0.028 mmol) in 38% yield.

TLC (hexane-EtOAc = 10:1): R<sub>f</sub> = 0.42

The analytical data are consistent with the literature <sup>[70]</sup>.

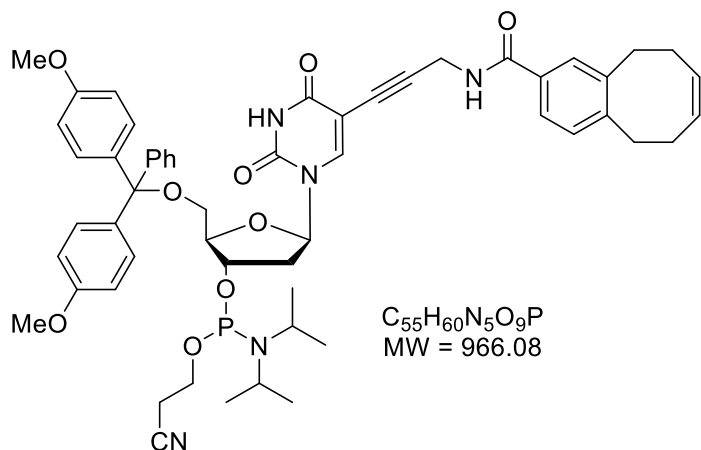
5-[(3''-COMBO-amino)prop-1-ynyl]-5'-O-dimethoxytrityl-2'-deoxyuridine (**13**)

In dried flask, COMBO acid **7** (20 mg 0.09 mmol, 1.0 eq), 5-(3''-aminopropynyl)-5'-O-dimethoxytrityl-2'-deoxyuridine (**12**) (58 mg, 0.09 mmol, 1.0 eq), HBtU (32 mg, 0.09 mmol, 0.094 eq) and HOBt (14.4 mg, 0.09 mmol, 1.0 eq) were placed. Anhydrous DMF (4 ml) was added into a reaction flask and allowed to stir under an argon atmosphere for 15 min. At this point, DIPEA (33  $\mu$ l) was added and resulting mixture was allowed to stir at room temperature for another 2 h. After completion of the reaction, then a solvent was removed under reduced pressure and the residue was purified by gradient flash column chromatography (100% EtOAc, EtOAc-MeOH 10:1+0.1 % Et<sub>3</sub>N) to give a light brown solid 36 mg (0.05 mmol) in 52% yield.

TLC (EtOAc-MeOH = 10:1): R<sub>f</sub> = 0.62

The analytical data are consistent with the literature <sup>[63d]</sup>.

5-(3''-COMBO-amino] prop-1-ynyl)-5'-O-dimethoxytrityl-2'-deoxyuridine-3-propyl diisopropylphosphoramidite (**14**)



COMBO-modified 5-(3''-aminopropynyl)-5'-O-dimethoxytrityl-2'-deoxyuridine (**13**) (36.0 mg, 0.05 mmol, 1.00 eq) was dissolved in anhydrous DCM (1.5 ml) at room temperature. To the resulting mixture was then added DIPEA (37.6  $\mu$ l, 0.220 mmol, 4.70 eq) and allowed to stir at room temperature under an argon atmosphere for 15 min. At this point,  $\beta$ -cyanoethyl-*N,N*-diisopropylchlorophosphoramidite (25.2  $\mu$ l, 0.11 mmol, 2.40 eq) was added and the reaction mixture was allowed to continue for another 2 h. After completion of the reaction, a crude product was directly applied to flash column chromatography (DCM-Acetone = 10:3 +0.1%+  $Et_3N$ ) to give a light yellow solid 25 mg (0.026 mmol) in 54% yield.

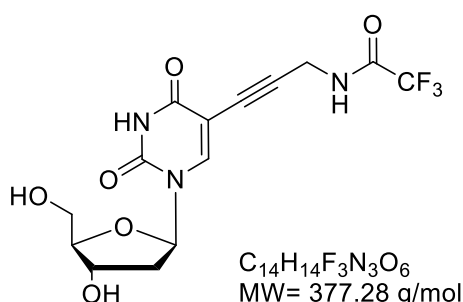
TLC (EtOAc-MeOH = 10:1):  $R_f$  = 0.62

HRMS (EI):  $m/z$  calcd for  $C_{55}H_{61}N_5O_9P_1$ : 966.4201 [M+H]; found: 966.4200.

$^{31}P$ -NMR (101 MHz, DMSO):  $\delta$  (ppm) = 150.07.

## 5.2.2 Synthesis of monobenzocyclooctyne nucleoside building block 19

5-(3''-aminopropynyl)-2'-deoxyuridine (**15**).



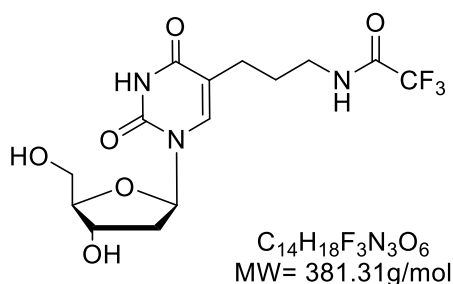
In a dried flask, 5-Iodo-2'-deoxyuridine (**8**) (0.708 g, 2.00 mmol, 1.00 eq), propargyltrifluoroacetamide (**10**) (0.907 g, 6.0 mmol, 3.0 eq), CuI (83.8 mg, 0.440 mmol, 0.220 eq) and tetrakis-(triphenylphosphine)-palladium(0) (231 mg, 0.200 mmol, 0.01 eq) were placed and dissolved in anhydrous DMF (10 ml). The solution mixture was degassed followed by the addition of anhydrous Et<sub>3</sub>N (1.20 ml, 8.00 mmol, 2.00 eq). The reaction mixture was allowed to stir at room temperature for 24 h under an argon atmosphere. After completion of the reaction, a crude product was filtered through celite and washed with MeOH (20 ml). The solvent was then removed under reduced pressure, the light brown solid 0.562 g (1.50 mmol) in 75% yield was obtained after purified by flash column chromatography (CH<sub>2</sub>Cl<sub>2</sub>-MeOH, 8:1).

TLC (MeOH-CH<sub>2</sub>Cl<sub>2</sub> = 8:1): R<sub>f</sub> = 0.40

<sup>1</sup>H-NMR (400 MHz, DMSO) : δ (ppm) = 10.11 (t, J = 5.6 Hz, 1H), 8.79 (s, 1H), 6.65 (s, 1H), 6.14 (t, J = 6.1 Hz, 1H), 5.29 (d, J = 4.3 Hz, 1H), 5.11 (t, J = 5.3 Hz, 1H), 4.45 (d, J = 4.6 Hz, 2H), 4.22 (dd, J = 5.9, 3.9 Hz, 1H), 3.92 (q, J = 3.8 Hz, 1H), 3.64 (qdd, J = 12.0, 5.3, 3.9 Hz, 2H), 2.40 (ddd, J = 13.4, 6.2, 4.1 Hz, 1H), 2.07 – 2.00 (m, 1H).

**<sup>13</sup>C-NMR** (101 MHz, DMSO) :  $\delta$  (ppm) = 171.8, 158.4, 154.4, 152.6, 139.3, 121.3, 106.2, 103.4, 88.9, 88.4, 70.3, 61.5, 41.9, 36.9.

**HRMS (EI)**: m/z calcd for C<sub>14</sub>H<sub>15</sub>N<sub>3</sub>O<sub>6</sub>F<sub>3</sub>: 378.0907 [M<sup>+</sup>]; found: 378.0908.

5-3''-[(trifluoroacetyl)amino] propyl-2'-deoxyuridine (**16**)

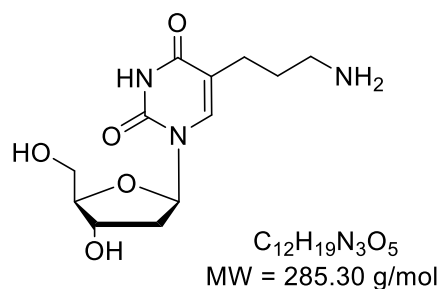
To a dried flask, 5-(3''-aminopropynyl)-2'-deoxyuridine (**15**) (200 mg 0.50 mmol, 1.00 eq) was placed and dissolved in anhydrous MeOH (10 ml) under an argon atmosphere. Then Pd(OH)<sub>2</sub> on carbon matrix (20% Wt, 10 mg) and triethylsilane (800  $\mu$ l, 5.0 mmol, 10.0 eq) were added and the reaction mixture was allowed to stir at room temperature for 24 h. After completion of the reaction, the resulting mixture was filtered through celite and the filtrate was concentrated under reduced pressure. The residue was purified by flash column chromatography (CH<sub>2</sub>Cl<sub>2</sub>-MeOH = 10:1) to provide pale yellow solid 134 mg (0.35 mmol) in 70% yield.

TLC (MeOH-CH<sub>2</sub>Cl<sub>2</sub> = 10:1): R<sub>f</sub> = 0.22

<sup>1</sup>H-NMR (400 MHz, DMSO) :  $\delta$  (ppm) = 11.28 (s, 1H), 9.39 (t, J = 5.8 Hz, 1H), 7.66 (s, 1H), 6.14 (t, J = 6.8 Hz, 1H), 5.21 (d, J = 4.2 Hz, 1H), 4.99 (t, J = 5.2 Hz, 1H), 4.26 – 4.17 (m, 1H), 3.74 (q, J = 3.6 Hz, 1H), 3.60 – 3.48 (m, 2H), 3.15 (q, J = 7.0 Hz, 2H), 2.18 (h, J = 8.1, 7.7 Hz, 2H), 2.12 – 2.00 (m, 2H), 1.69 – 1.56 (m, 2H).

<sup>13</sup>C-NMR (101 MHz, DMSO) :  $\delta$  (ppm) = 162.8, 155.6, 149.8, 135.9, 115.4, 112.1, 86.8, 83.4, 69.9, 60.8, 39.1, 38.4, 26.6, 23.3.

**HRMS (EI):** m/z calcd for C<sub>14</sub>H<sub>18</sub>F<sub>3</sub>N<sub>3</sub>O<sub>6</sub>: 382.1220 [M+H]; found: 382.1219.

5-(3''-amino propyl)-2'-deoxyuridine (**33**)

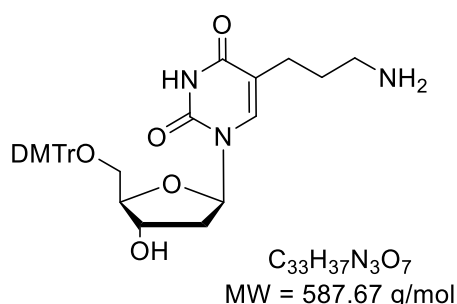
To a flask, 5-3''-(trifluoroacetyl) amino propyl-2'-deoxyuridine (**16**) (200 mg, 0.520 mmol, 1.00 eq) was placed and 10 ml of concentrated  $NH_3$  was then added and allowed to stir at room temperature for 24 h. After completion of the reaction, the solvent was removed under reduced pressure to obtain the quantitative yield of the desired light brown solid as a product without a further purification step.

**$^1H$ -NMR** (400 MHz, DMSO) :  $\delta$  (ppm) = 11.34 (s, 1H), 7.75 (s, 1H), 7.66 (s, 2H), 6.19 (t,  $J = 6.8$  Hz, 1H), 5.29 (d,  $J = 4.2$  Hz, 1H), 5.08 (s, 1H), 4.34 – 4.22 (m, 1H), 3.81 (q,  $J = 3.6$  Hz, 1H), 3.60 (dd,  $J = 7.9, 3.8$  Hz, 2H), 2.82 – 2.74 (m, 2H), 2.29 (t,  $J = 7.4$  Hz, 2H), 2.12 (dd,  $J = 6.8, 4.5$  Hz, 2H), 1.81 – 1.67 (m, 2H).

**$^{13}C$ -NMR** (101 MHz, DMSO) :  $\delta$  (ppm) = 163.2, 150.1, 136.6, 112.0, 87.1, 83.8, 70.2, 61.1, 39.3, 38.1, 25.9, 23.2.

**HRMS (EI)**:  $m/z$  calcd for  $C_{12}H_{20}N_3O_5$ : 286.1397 [M+H]; found: 286.1396.

5-(3''-aminopropyl)-5'-O-dimethoxytrityl-2'-deoxyuridine (**17**)



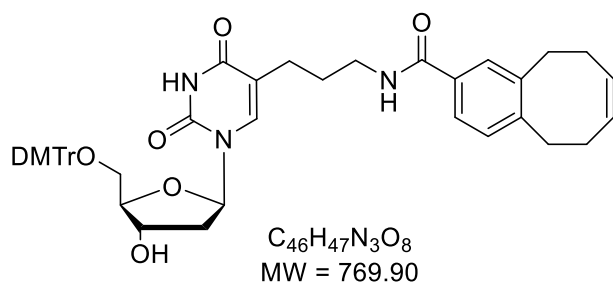
To the dried flask, 5-[3''-(trifluoroacetyl) amino] propyl-2'-deoxyuridine (**16**) (230 mg, 0.60 mmol, 1.00 eq) and dimethoxytrityl chloride (305 mg, 0.90 mmol, 1.50 eq) were placed, subsequently dissolved in anhydrous pyridine (2 ml) under an argon atmosphere. At this point, anhydrous  $Et_3N$  was added and the reaction mixture was warmed up to 40 °C and stirred at this temperature for 18 h. After completion of the reaction, the solvent was removed under reduced pressure, the crude product was then purified by column chromatography ( $CH_2Cl_2$ -MeOH = 100:3 + 0.1%  $Et_3N$ ) to provide yellow solid 403 mg (0.58 mmol) in 98% yield. The corresponding adduct was then treated with a concentrated  $NH_3$  overnight. The solvent was removed and the residue was lyophilized to obtain the desired product in quantitative yield without further purification.

**$^1H$ -NMR** (500 MHz, DMSO) :  $\delta$  (ppm) = 11.35 (s, 1H), 9.32 (t, J = 5.8 Hz, 1H), 7.39 (s, 1H), 7.36 (d, J = 7.6 Hz, 2H), 7.28 (t, J = 7.6 Hz, 2H), 7.25 – 7.18 (m, 5H), 6.86 (dd, J = 9.0, 2.3 Hz, 4H), 6.17 (t, J = 6.8 Hz, 1H), 5.30 (d, J = 4.6 Hz, 1H), 4.27 (dq, J = 8.3, 4.3 Hz, 1H), 3.88 – 3.81 (m, 1H), 3.71 (s, 6H), 3.22 – 3.10 (m, 2H), 2.95 (q, J = 6.9 Hz, 2H), 2.24 (dt, J = 13.7, 6.8 Hz, 1H), 2.17 – 2.05 (m, 1H), 1.88 (hept, J = 7.3, 6.7 Hz, 2H), 1.45 (dh, J = 13.0, 6.4 Hz, 2H).

**<sup>13</sup>C-NMR** (126 MHz, DMSO) :  $\delta$  (ppm) = 163.0, 157.9, 156.0, 155.7, 150.1, 144.5, 136.1, 135.2 (2C), 135.0 (2C), 129.5 (4C), 127.6 (2C), 127.5 (2C), 126.5, 116.9, 114.6, 113.0, 112.7, 85.5, 85.2, 83.7, 70.3, 63.7, 54.8, 38.4, 27.2, 23.6.

**HRMS (EI)** : m/z calcd for C<sub>33</sub>H<sub>37</sub>N<sub>3</sub>O<sub>7</sub> : 588.2704 [M+H]; found : 588.2702.

5-[(3''-COMBO-amino) prop-yl]-5'-O-dimethoxytrityl-2'-deoxyuridine (**18**)



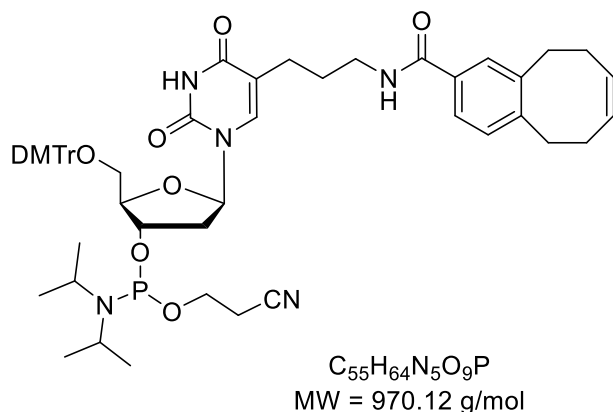
To a dried flask, 5-(3''-aminopropynyl)-5'-O-dimethoxytrityl-2'-deoxyuridine (**17**) (58.0 mg, 0.09 mmol, 1.00 eq), COMBO acid (**7**) (20.0 mg, 0.09 mmol, 1.00 eq), HBTU (32.0 mg, 0.084 mmol, 0.94 eq), HOBt (14.4 mg, 0.09 mmol, 1.00 eq) were placed and dissolved with anhydrous DMF (4 ml). The reaction mixture was stirred under an argon atmosphere for 5 min, and then DIPEA (33  $\mu$ l) was added, the resulting mixture was allowed to stir at room temperature for 2 hours. After completion of the reaction, the solvent was removed under reduced pressure. The residue was subsequently purified by column chromatography (EtOAc-MeOH = 9.5:0.5 + 0.1 % Et<sub>3</sub>N) to give a light yellow solid 52% yield.

TLC (EtOAc-MeOH = 9.5:0.5 + 0.1 % Et<sub>3</sub>N): R<sub>f</sub> = 0.50

<sup>1</sup>H-NMR (400 MHz, DMSO)  $\delta$  11.38 (s, 1H), 8.30 (q, J = 5.8 Hz, 1H), 7.55 (s, 1H), 7.47 (s, 1H), 7.38 (s, 1H), 7.36, (s, 2H), 7.34 – 7.23 (m, 7H), 6.87 (d, J = 8.3 Hz, 4H), 6.21 (t, J = 6.8 Hz, 1H), 5.33 (d, J = 4.6 Hz, 1H), 4.31 (t, J = 5.6 Hz, 1H), 3.89 – 3.85 (m, 1H), 3.70 (s, 6H), 3.28 – 3.13 (m, 2H), 3.15 – 3.02 (m, 5H), 2.58 – 2.55 (m, 2H), 2.38 – 2.32 (m, 2H), 2.30 – 2.25 (m, 1H), 2.17– 2.13 (m, 1H), 2.04 – 1.89 (m, 2H), 1.69 (s, 2H), 1.53 – 1.45 (m, 2H).

**<sup>13</sup>C-NMR** (100 MHz, DMSO)  $\delta$  (ppm) = 166.1, 163.6, 158.3, 150.5, 145.0, 142.9, 139.9, 139.7, 136.4, 135.7 (2C), 135.5 (2C), 133.4, 129.9, 129.4, 129.1, 128.6, 128.1, 127.9, 126.9, 125.7, 113.6, 113.5, 85.9, 85.7, 84.1, 70.7, 64.4, 55.2, 49.1, 45.9, 40.5, 38.5, 33.2, 32.9, 28.5, 27.7, 27.4, 24.2.

5-(3''-COMBO-amino] prop-yl)-5'-O-dimethoxytrityl-2'-deoxyuridine-3-propyl  
diisopropylphosphoramidite (**19**)



The COMBO-modified 5-(3''-aminopropyl)-5'-O-dimethoxytrityl-2'-deoxyuridine (**18**) (60 mg, 0.08 mmol, 1.00 eq) was dissolved in anhydrous DCM (3 ml) at room temperature. To the resulting mixture was then added DIPEA (64.0  $\mu$ l, 0.370 mmol, 4.70 eq) and allowed to stir at room temperature under an argon atmosphere for 15 min. At this point,  $\beta$ -cyanoethyl-*N,N*-diisopropylchlorophosphoramidite (42.0  $\mu$ l, 0.180 mmol, 2.40 eq) was added and the reaction mixture was allowed to continue for another 2 h. After completion of the reaction, a crude product was directly applied to flash column chromatography (DCM-Acetone = 5:2 + 0.1%+  $Et_3N$ ) to give a light yellow solid 68 mg (0.07 mmol) in 90% yield.

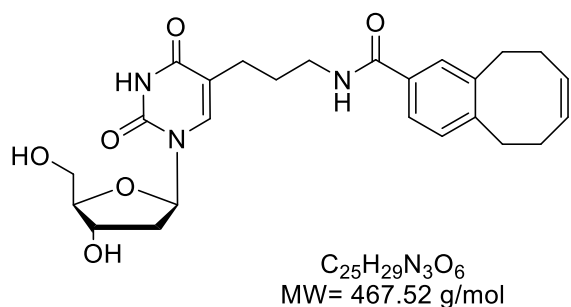
**TLC** (DCM-Acetone = 5:2 + 0.1%+  $Et_3N$ ):  $R_f$  = 0.06

**FAB**  $m/z$  (%) : 992.4 (50) (M+Na)

**$^{31}P$ -NMR** (101 MHz, DMSO):  $\delta$  (ppm) = 120.1.

### 5.2.3 Synthesis of monobenzocyclooctyne nucleotide triphosphate **24**

#### 5-[(3'-COMBO-amino)prop-yl]-2'-deoxyuridine (**23**)



In a dried flask, aminopropyl-2'-deoxyuridine (**33**) (54.2 mg, 0.190 mmol, 1.10 eq), COMBO acid (**7**) (35 mg 0.17 mmol, 1.0 eq), HBTU (57 mg, 0.16 mmol, 0.94 eq) and HOBt (25.6 mg, 0.17 mmol, 1.0) were dried under reduced pressure then anhydrous DMF (2 ml) was added and the reaction mixture was stirred at room temperature for 15 min. At this point, dried DIPEA (59  $\mu$ l) was added. The resulting mixture was allowed to stir under an argon atmosphere for another 2 hours. After completion of the reaction, a solvent was then removed and the crude product was purified by flash column chromatography (CH<sub>2</sub>Cl<sub>2</sub>-MeOH, 9:1) to give a light brown solid 43 mg (0.09 mmol) in 54% Yield.

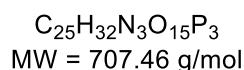
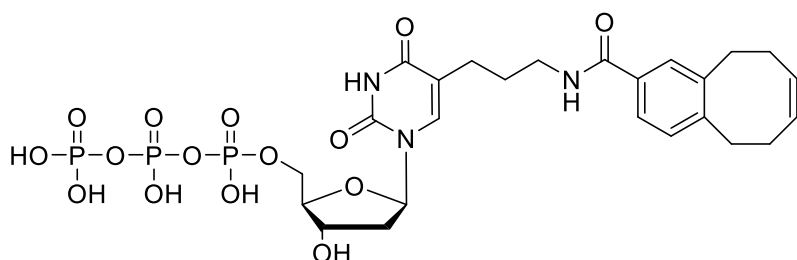
**TLC** (MeOH-CH<sub>2</sub>Cl<sub>2</sub> =9:1): R<sub>f</sub> = 0.53

**<sup>1</sup>H-NMR** (400 MHz, DMSO) :  $\delta$  (ppm) = 11.31 (s, 1H), 8.40 (t, J = 5.8 Hz, 1H), 7.73 (s, 1H), 7.67 (s, 1H), 7.63 (dd, J = 7.8, 1.9 Hz, 1H), 7.27 (d, J = 8.0 Hz, 1H), 6.18 (t, J = 6.8 Hz, 1H), 5.24 (d, J = 4.2 Hz, 1H), 5.05 (t, J = 5.2 Hz, 1H), 4.25 (dq, J = 6.3, 3.2 Hz, 1H), 3.77 (q, J = 3.7 Hz, 1H), 3.69 – 3.47 (m, 4H), 3.30 – 3.19 (m, 2H), 3.18 – 3.06 (m, 2H), 2.29 – 2.01 (m, 8H), 1.68 (p, J = 6.9 Hz, 2H).

**<sup>13</sup>C-NMR** (101 MHz, DMSO) :  $\delta$  (ppm) = 166.1, 163.4, 150.3, 144.3, 141.0, 136.4, 132.8, 130.6, 129.6, 125.1, 113.0, 99.4, 99.3, 87.3, 83.9, 70.4, 61.3, 53.5, 41.8, 38.4, 36.9, 36.6, 28.0, 23.9, 22.1.

**EI-MS** m/z (%) = 468.1 (90) (M+H<sup>+</sup>)

**HRMS (EI)**: m/z calcd for C<sub>25</sub>H<sub>30</sub>N<sub>3</sub>O<sub>6</sub>: 468.2129 [M+H]; found: 468.2131.

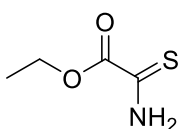
5-[(3''-COMBO-amino)prop-yl]-2'-deoxyuridine triphosphate (**24**)

The COMBO-modified oligonucleoside **23** (20.0 mg, 0.042 mmol, 1.00 eq), proton sponge (grinded, 13.5 mg, 0.063 mmol, 1.50 eq) and a magnetic stirring bar were placed into the reaction flask and subsequently dried under vacuum overnight. Then TMP (29  $\mu\text{l}$ ) was added and the reaction mixture was then cooled down to  $-5\text{ }^\circ\text{C}$ . At this point,  $\text{POCl}_3$  (4.1  $\mu\text{l}$ , 0.044 mmol, 1.05 eq) was then added to a solution via micropipette (one portion directly into the reaction mixture). The reaction was allowed to stir at  $-5\text{ }^\circ\text{C}$  for 4 h, another 0.4 eq (1.56  $\mu\text{l}$ ) of  $\text{POCl}_3$  was then added into a reaction mixture and allowed to stir for another 1 h. At this point, the solution of tributylammoniumpyrophosphate (139 mg, 0.252 mmol, 6.00 eq) and tributylamine (40  $\mu\text{l}$ ) in dried DMF was added. After 15 min at  $-5\text{ }^\circ\text{C}$  the reaction mixture was transferred dropwise into a solution of 0.1 M TEAB over 45 min (1.0 ml per 0.016 mmol of starting material; 4.0 ml). After stirring for 4 h at room temperature, the crude product was transferred into a falcon tube and freeze-dried under reduced pressure. The crude product was purified by RP-HPLC using gradient ACN-TEAB as eluent. The product-containing fractions were combined, freeze-dried and quantified by absorption spectrometry at 260 nm which was obtained in 7% yield.

**MALDI-MS** :  $m/z$  (%) = 703.6 [ $\text{MH}^+$ ]

## 5.2.4 Synthesis of 5-[(3''-1,2,4-triazine-amino)prop-yl]-2'-deoxyuridine (34)

### Ethyl amino(thio)acetate (29)



$C_4H_7NO_2S$   
MW = 133.17 g/mol

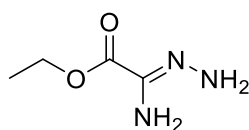
Ethyl oxamate **27** (2.90 g, 50.0 mmol, 2.0 eq) and Lawesson's reagent **28** (10.1 g, 25.0 mmol, 1.00 eq) were placed into a reaction flask which was dried under vacuum under an argon atmosphere then dissolved in THF (100 ml). The mixture solution was refluxed for 2 h. After completion of the reaction, the resulting mixture was cooled to room temperature and 20 g of silica gel were added. The solvent was removed under reduced pressure. The residue was then purified by flash column chromatography (Hexane-EtOAc, 7:3) to give a light yellow solid 5.43 g (40.8 mmol) in 85% yield.

**TLC** (Hexane-EtOAc = 7:3):  $R_f$  = 0.40

**$^1H$ -NMR** (300 MHz, DMSO):  $\delta$  (ppm) = 10.35 (s, 1H), 9.97 (s, 1H), 4.20 (qd,  $J$  = 7.1, 0.8 Hz, 2H), 1.25 (td,  $J$  = 7.1, 0.8 Hz, 3H).

**$^{13}C$ -NMR** (75 MHz, DMSO):  $\delta$  (ppm) = 190.3 (s), 162.1 (s), 61.8 (s), 13.5 (s).

**EI-MS**  $m/z$  (%) = 133.0 (100) ( $M^+$ )

Ethyl amino(hydrazono)acetate (**30**)

$C_4H_9N_3O_2$   
MW = 131.14 g/mol

To a dried reaction flask, ethyl amino(thioxo)acetate (**29**) (1.33 g, 10.0 mmol, 1.00 eq) was placed and dissolved in degassed EtOH (20 ml). The red solution was stirred at room temperature for 10 min then a solution of 1 M solution of hydrazine in THF (10 ml, 10.0 mmol, 1.00 eq) was added dropwise over 30 min during which hydrogen sulfide was liberated. The reaction mixture was allowed to stir at room temperature for further 2.5 h. After completion of the reaction, the solvent was then removed under reduced pressure to obtain the yellow-red residue which was further recrystallized from  $Et_2O-CH_2Cl_2$  [50 ml, 4:1 (v/v)] to give a yellow solid 2.15 g (16.4 mmol) in 82% yield.

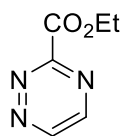
TLC (7:3 Hexane-EtOAc):  $R_f = 0.40$

$^1H-NMR$  (300 MHz, DMSO):  $\delta$  (ppm) = 5.69 (s, 2H), 5.35 (s, 2H), 4.13 (dt,  $J = 7.6, 6.7$  Hz, 2H), 1.21 (td,  $J = 7.1, 0.7$  Hz, 3H).

$^{13}C-NMR$  (75 MHz, DMSO):  $\delta$  (ppm) = 162.7 (s), 135.6 (s), 60.7 (s), 14.3 (s).

**EI-MS**  $m/z$  (%) = 131.1 (73) ( $M^+$ )

Ethyl-1,2,4-triazine-3-carboxylate (**31**)



$C_6H_7N_3O_2$   
MW = 153.14 g/mol

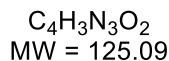
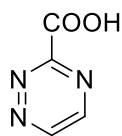
The cooled mixture solution (-78 °C) of ethyl amino(hydrazono)acetate (**30**) (2.62 g, 20.0 mmol, 1.00 eq) and acetic acid (3 mL, 0.4 mmol, 0.02 eq) in THF (50 ml) was added into a cooled (-78 °C) solution of 40% wt glyoxal in H<sub>2</sub>O (2.5 mL, 5.50 mmol, 1.10 eq) in THF (50 ml) in one portion. The reaction mixture was then stirred for another 15 min at -78 °C under an argon atmosphere. At this point, Et<sub>3</sub>N (4.2 mL, 30.0 mmol, 1.5.0 eq) was then added, the cooling bath was removed and the reaction mixture was allowed to warm up to room temperature overnight. After completion of the reaction, the solvent was removed and a residue was purified by flash column chromatography (EtOAc-Hexane, 7:3) to give a light yellow solid 2.27 g (14.8 mmol) in 74% yield.

TLC (7:3 EtOAc-Hexane): R<sub>f</sub> = 0.51

<sup>1</sup>H-NMR (400 MHz, DMSO): δ (ppm) = 9.62 (d, J = 2.5 Hz, 1H), 9.05 (d, J = 2.5 Hz, 1H), 4.45 (q, J = 7.1 Hz, 2H), 1.37 (t, J = 7.1 Hz, 3H).

<sup>13</sup>C-NMR (101 MHz, DMSO): δ (ppm) = 162.2 (s), 156.7 (s), 151.5 (s), 150.6 (s), 62.4 (s), 13.9 (s).

EI-MS m/z (%) = 153.1 (43) (M<sup>+</sup>)

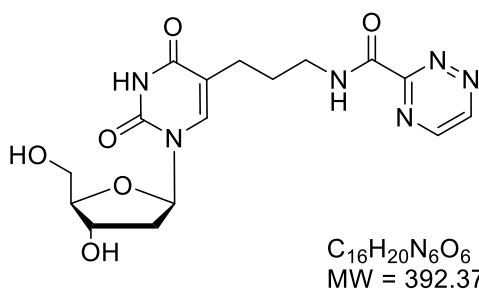
3-carboxy-1,2,4-triazine (**32**)

To a solution of Ethyl-1,2,4-triazine-3-carboxylate (**31**) (0.582 g, 3.80 mmol, 1.00 eq) in dry EtOH (5 ml) was added a solution of KOH (0.235 g, 4.18 mmol, 1.10 eq) in dry EtOH (5 ml) over 40 min at room temperature. The resulting light brown suspension was then allowed to stir at room temperature for another 15 min, then the precipitate was filtered off, wash with EtOH (20 ml) and dried under reduce pressure. The corresponding light brown solid was then dissolved in 1N HCl (4.18 mL) and freeze-dried overnight. The obtained mixture of potassium chloride and 1,2,4-triazine carboxylic acid was treated with water (10 ml) The resulting suspension was stirred for 40 min and filtered off, and washed with cold water. The desired light yellow solid was obtained 369.8 mg (2.90 mmol) in 76% yield.

**<sup>1</sup>H-NMR** (300 MHz, DMSO):  $\delta$  (ppm) = 9.58 (d, J = 2.5 Hz, 1H), 9.02 (d, J = 2.5 Hz, 1H).

**<sup>13</sup>C-NMR** (75 MHz, DMSO):  $\delta$  (ppm) = 163.8 (s), 157.9 (s), 151.3 (s), 150.6 (s).

5-(1,2,4-triazine-3-carboxylate-amino] propyl}-2'-deoxyuridine (**34**)



Aminopropyl-2'-deoxyuridine (**33**) (80 mg, 0.28 mmol, 1.0 eq), 3-carboxy-1,2,4-triazine (**32**) (38.8 g, 0.31 mmol, 1.10 eq), HBtU (98.6 mg, 0.26 mmol, 0.94 eq) and HOBt (37.8 mg, 0.28 mmol, 1.00 eq) were placed in dried flask under an argon atmosphere. Anhydrous DMF (3 mL) was added and the resulting mixture was stirred at room temperature for 15 minutes. At this point, DIPEA (103  $\mu$ l, 0.56 mmol, 2.20 eq) was added; the resulting mixture was stirred under argon atmosphere for 2 hours. After completion of the reaction, the residue was directly applied to flash column chromatography. The light yellow solid was obtained by using 9:1  $CH_2Cl_2$ -MeOH as an eluent 50.2 mg (0.13 mmol) in 45% yield.

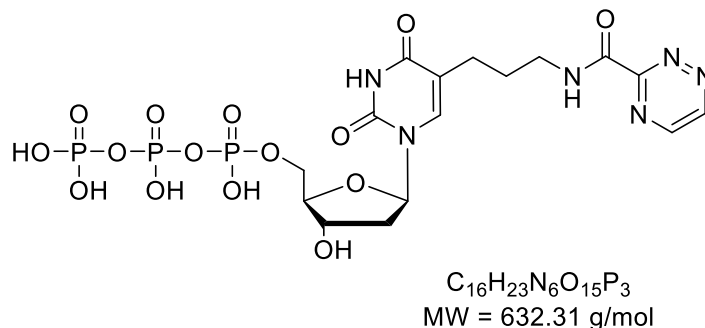
TLC (9:1  $CH_2Cl_2$ -MeOH):  $R_f$  = 0.2

$^1H$ -NMR (400 MHz, DMSO):  $\delta$  (ppm) = 11.30 (s, 1H), 9.57 (d,  $J$  = 2.5 Hz, 1H), 9.25 (t,  $J$  = 6.0 Hz, 1H), 9.02 (d,  $J$  = 2.5 Hz, 1H), 7.73 (s, 1H), 6.16 (dd,  $J$  = 7.6, 6.1 Hz, 1H), 5.29 – 5.04 (bs, 2H), 4.24 (dt,  $J$  = 5.9, 3.1 Hz, 1H), 3.76 (q,  $J$  = 3.5 Hz, 1H), 3.63 – 3.50 (m, 2H), 3.33 (q,  $J$  = 6.8 Hz, 2H), 2.33 – 2.19 (m, 2H), 2.18 – 2.01 (m, 2H), 1.72 (p,  $J$  = 7.2 Hz, 2H).

**<sup>13</sup>C-NMR** (101 MHz, DMSO):  $\delta$  (ppm) = 164.1 (s), 161.9 (s), 158.6 (s), 151.7 (s), 151.2 (s), 150.9 (s), 137.1 (s), 128.9 (s), 113.6 (s), 87.9 (s), 84.6 (s), 71.1 (s), 61.9 (s), 39.3 (s), 28.4 (s), 24.5 (s).

**HRMS (EI)**:  $m/z$  calcd for C<sub>16</sub>H<sub>20</sub>N<sub>6</sub>O<sub>6</sub>: 393.1517 [M+H]; found: 393.1571.

## 5.2.5 Synthesis of 5-(1,2,4-triazine-3-carboxylate-amino) propyl)-2'-deoxyuridine triphosphate (35)



The triazine-modified oligonucleoside **34** (20.0 mg, 0.05 mmol, 1.00 eq), proton sponge (grinded, 16.1 mg, 0.075 mmol, 1.50 eq) and magnetic stirring bar were dried under vacuum overnight prior the reaction. TMP (290  $\mu$ l) was added and the reaction mixture was cooled to -5  $^{\circ}$ C. At this point, POCl<sub>3</sub> (4.90  $\mu$ l, 0.053 mmol, 1.10 eq) was then added to a solution via micropipette (one portion directly into the reaction mixture). The reaction was allowed to stir at -5  $^{\circ}$ C for 4 h then another 0.4 eq (1.9  $\mu$ l) of POCl<sub>3</sub> was then added into a reaction mixture and allowed to stir at -5  $^{\circ}$ C for another 1 h. At this point, the solution of tributylammoniumpyrophosphate (165 mg, 0.3 mmol, 6.0 eq) and tributylamine (50  $\mu$ l) in dried DMF was added. After 15 min at -5  $^{\circ}$ C the reaction mixture was then added dropwise into a solution of 0.1 M TEAB over 45 min (1.0 ml per 0.016 mmol starting material; 4 ml). After 4 h stirring at room temperature the crude product was transferred into a falcon tube and freeze-dried under reduced pressure. The crude product was purified by RP-HPLC using a gradient ACN-TEAB as eluent. The product-containing fractions were combined, freeze-dried and quantified by absorption spectrometry at 260 nm which was obtained in 15% yield.

**MALDI-MS** : m/z (%) = 629.49 [MH<sup>+</sup>]

## 5.3 Solid-phase DNA synthesis

### 5.3.1 Synthesis

The automated solid-phase synthesis of the COMBO-modified DNA was carried out according to the phosphoramidite method on Expedite Nucleic Acid Synthesizer System from *Applied Biosystems*. The commercially available natural bases (A, C, T and G) were dissolved in acetonitrile (amidite diluent grade) and used as a 0.067 M solution for synthesis. The COMBO-modified phosphoramidites **14** and **19** were prepared as 0.1 M solution in abs. DCM prior the synthesis. For all oligonucleotides, the 5'-terminal DMTr protective group was removed (trityl-off synthesis) at the end of the synthesis. The following standard protocol was used for the incorporation of the building blocks of the natural bases A, G, C, T (Table 2). Other required reagent solutions are:

Dbk (Deblock): 3% dichloroacetic acid in dichloromethane

Wsh A (Wash A): acetonitrile

Wsh (Wash): acetonitrile

Act (Activator): 0.45 M tetrazole in acetonitrile

Cap A: acetic anhydride in THF / pyridine

Cap B: *N*-methylimidazole in THF / pyridine

Ox (Oxidizer): iodine in water / THF / pyridine

**Table 2:** Standard protocol for coupling of the phosphoramidites of natural bases using the example of natural base A. Dblk = 3% dichloroacetic acid in CH<sub>2</sub>Cl<sub>2</sub>, Wsh = MeCN, Act = 0.45 M tetrazole in MeCN, Caps = Ac<sub>2</sub>O in THF / pyridine (Cap A) and *N*-methylimidazole in THF / pyridine (Cap B), Ox = iodine in water / THF / pyridine.

Code	function	Mode	amount	time
<b>\$ Deblocking</b>				
144	Index Fract. Coll.	NA	1	0
0	Default	WAIT	0	1.5
141	Trityl Mon.	NA	1	1
16	Dblk	PULSE	10	0
16	Dblk	PULSE	50	49
38	Diverted Wsh A	PULSE	40	0
141	Trityl Mon.	NA	0	1
38	Diverted Wsh A	PULSE	40	0
144	Index Fract. Coll.	NA	2	0
<b>\$ Coupling</b>				
1	Wsh	PULSE	5	0
2	Act	PULSE	5	0
21	A + Act	PULSE	5	0
21	A + Act	PULSE	2	16
2	Act	PULSE	3	24
1	Wsh	PULSE	7	56
1	Wsh	PULSE	8	0
<b>\$Capping</b>				

12	Wsh A	PULSE	20	0
13	Caps	PULSE	8	0
12	Wsh A	PULSE	6	15
13	Wsh A	PULSE	14	0
<b>\$Oxidizing</b>				
15	Ox	PULSE	15	0
12	Wsh A	PULSE	15	0
<b>\$Capping</b>				
13	Caps	PULSE	7	0
12	Wsh A	PULSE	30	0

The COMBO-modified 2'-deoxyuridine building blocks were incorporated into DNA using 1200 s for coupling step and the number of pulses required was increased to 10.

**Table 3:** Protocol for coupling of COMBO-modified phosphoramidite building blocks **14** and **19**; **6** = artificial nucleoside building blocks.

Code	Function	Mode	amount	time
<b>\$ Coupling</b>				
1	Wsh	PULSE	5	0
2	Act	PULSE	5	0

23	6 + Act	PULSE	5	0
23	6 + Act	PULSE	5	600
2	Act	PULSE	5	400
1	Wsh	PULSE	7	200
1	Wsh	PULSE	8	0

After completion of the synthesis, the CPG-filled columns were dried under vacuum overnight then the glass particles were transferred into an Eppendorf tube. Subsequently, 700  $\mu$ l conc. ammonia solution were added (> 25%, trace select, *Fluka*) and after mixing, the suspension was incubated for 24 h at 36 °C. Ammonia was then removed from the resulting mixture by centrifuge at 35 °C, 100 mbar for 1 h. The supernatant was then separated from the residue by filtration. This was subsequently washed twice with in each case 300  $\mu$ l of HPLC water. The combined aqueous phases were lyophilized. The residue was then dissolved in 300  $\mu$ l of HPLC water and purified by RP-HPLC.

### 5.3.2 Purification, characterization and concentration determination

The purification of COMBO-modified DNA was carried out by RP-HPLC using a gradient of 50 mM ammonium acetate buffer (eluent A) and acetonitrile (eluent B). The detection wavelength at  $\lambda_{\text{abs}} = 260$  nm for COMBO-modified DNA and  $\lambda_{\text{abs}} = 290$  nm for the COMBO moiety were used for characterization. The following conditions for the analysis and preparative separation of the COMBO-modified oligonucleotides were given.

**Table 4** Gradient RP-HPLC and the detection wavelengths used for purification; A = 50 mM NH<sub>4</sub>OAc-buffer (pH = 6.5), B = MeCN.

COMBO-modified DNA	Column	Gradient	Detection
COMBO-DNA	<i>Supelcosil</i> LC-318	0 – 25% B (50 min)	$\lambda_{\text{abs}} = 260 \text{ nm}, 290 \text{ nm}$
COMBO-DNA + <b>21b</b>	<i>Supelcosil</i> LC-318	0 – 25% B (50 min)	$\lambda_{\text{abs}} = 260 \text{ nm}, 290 \text{ nm}, 610 \text{ nm}$

The combined DNA-fractions were then characterized by MALDI-TOF mass spectrometry and the concentration was determined by measuring the absorbance at 260 nm on ND 1000 spectrophotometer from *Nanodrop*. Nucleic Acids program was used to determine the absorbance at  $\lambda_{\text{abs}} = 260 \text{ nm}$ , Lambert-Beer's law was applied. The extinction coefficient of unmodified DNA strand can be calculated by the following formula at 260 nm.

$$\varepsilon_{260} = (A \varepsilon_A + G \varepsilon_G + T \varepsilon_T + C \varepsilon_C) \cdot 0.9$$

A = number of adenine bases  $\varepsilon_A = 15400 \text{ L}(\text{mol} \cdot \text{cm})^{-1}$

G = number of guanine bases  $\varepsilon_G = 11700 \text{ L}(\text{mol} \cdot \text{cm})^{-1}$

T = number of thymine bases  $\varepsilon_T = 8800 \text{ L}(\text{mol} \cdot \text{cm})^{-1}$

C = number of cytosine bases  $\varepsilon_C = 7300 \text{ L}(\text{mol} \cdot \text{cm})^{-1}$

0.9 = factor to account for hypochromicity

The extinction coefficients of the artificial building blocks were determined prior incorporation and are listed:

**Table 5** Molar extinction coefficients of base-modified nucleoside building blocks.

<b>Artificial nucleosides</b>	<b>Molar extinction coefficient [l/mol*cm<sup>-1</sup>]</b>
COMBO-building block <b>13</b>	7930
COMBO-building block <b>23</b>	8900
Triazine-building block <b>34</b>	8523

### 5.3.3 Strain-Promoted Azide-Alkyne Cycloaddition

**DNA1, 2, 5 and 6** (10 nmol) were dissolved in 100  $\mu$ l of HPLC water. To this solution was then added 21.4  $\mu$ l (11 nmol) of a 514  $\mu$ M azide-modified dye **21b**. The reaction mixture was shaken for 3 h at room temperature. After completion of the reaction, the residue was subsequently purified by RP-HPLC, characterized by MALDI-TOF mass spectrometry and quantified by absorption spectroscopy yielding the corresponding clicked product in 58% yield (**DNA3**), 63% yield (**DNA4**), 76% yield (**DNA5**) and 87% yield (**DNA8**), respectively.

**Table 6** SPAAC of COMBO-modified DNAs with azido fluorescent dye (**21b**)

DNA	Sequence 5'→3'
<b>DNA1</b>	5'-GCAGTCTG( <b>dU14</b> )GTCACTGA-3'
<b>DNA3</b>	5'-GCAGTCTG( <b>dU14 + 21b</b> )GTCACTGA-3'
<b>DNA2</b>	5'-GCAGTCTT( <b>dU14</b> )TTCACTGA-3'
<b>DNA4</b>	5'-GCAGTCTT( <b>dU14 + 21b</b> )TTCACTGA-3'
<b>DNA5</b>	5'-GCAGTCTG( <b>dU19</b> )GTTCACTGA-3'
<b>DNA7</b>	5'-GCAGTCTG( <b>dU19 + 21b</b> )GTCACTGA-3'
<b>DNA6</b>	5'-GCAGTCTT( <b>dU19</b> )TTCACTGA-3'
<b>DNA8</b>	5'-GCAGTCTT( <b>dU19 + 21b</b> )TTCACTGA-3'

## 5.4 Enzymatic DNA synthesis

### 5.4.1 Primer extension experiment (PEX)

The primer extension experiments were carried out by using the primer **P1** and a variation of template strands (**T1**, **T4**, **T5** and **T6**). The reference strands **P2** and **P3** were included for the better illustration of the observed bands.

<b>P1/T1</b>			
<b>T1</b>	3'	CTG-GGT-GAG-GTA-GCT-CTA-AAG-AG A-GGC-GGC-TCG-CG	5'
<b>P1</b>	5'	Flu-GAC-CCA-CTC-CAT-CGA-GAT-TTC-TC	3'
<b>P1/T4</b>			
<b>T4</b>	3'	CTG-GGT-GAG-GTA-GCT-CTA-AAG-AG G-GCA-ACG-TCG-CG	5'
<b>P1</b>	5'	Flu-GAC-CCA-CTC-CAT-CGA-GAT-TTC-TC	3'
<b>P1/T5</b>			
<b>T5</b>	3'	CTG-GGT-GAG-GTA-GCT-CTA-AAG-AG G-GCA-CGG-ACG-CG	5'
<b>P1</b>	5'	Flu-GAC-CCA-CTC-CAT-CGA-GAT-TTC-TC	3'
<b>P1/T6</b>			
<b>T6</b>	3'	CTG-GGT-GAG-GTA-GCT-CTA-AAG-AG G-GCA-AAC-TCG-CG	5'
<b>P1</b>	5'	Flu-GAC-CCA-CTC-CAT-CGA-GAT-TTC-TC	3'
<b>P2</b>	5'	Flu-GAC-CCA-CTC-CAT-CGA-GAT-TTC-TC T	3'
<b>P3</b>	5'	Flu-GAC-CCA-CTC-CAT-CGA-GAT-TTC-TC T-CCG-GCC-AGC-GC	3'

**Figure 39** Primer; **P1**, templates; **T1**, **T4**, **T5**, and **T6** and references; **P2** and **P3** for primer extension experiments. The primer and references are marked with fluorescein (Flu) at 5'-position.

The hybridization of primer and templates were carried out by using a thermocycler. First, primer and template were hybridized at 90 °C for 10 min and allowed to cool down to room temperature in 1 h. At this point, the mixture solution of natural triphosphate building blocks and artificial triphosphate building block were added. After adding the polymerase the reaction mixture was elongated under the given temperature (altered from DNA polymerase). In order to ensure that all the reaction tubes have the same concentration, the reaction solution of primer and templates were prepared as a stock solution and given in each reaction tubes the same volume. The concentration of primer and templates for extension experiment, DNA polymerases and reaction conditions were listed.

**Table 7** The polymerases and the reaction condition for extension experiment

Polymerases	Reaction conditions (1X)
<i>Vent (exo-)</i> <i>Deep Vent (exo-)</i>	ThermoPol® Reaction Buffer: 20 mM Tris-HCl, 10 mM (NH <sub>4</sub> ) <sub>2</sub> SO <sub>4</sub> , 10 mM KCl, 2 mM MgSO <sub>4</sub> , 0.1% Triton® X-100, pH 8.8
<i>Hemo Klen Taq</i>	Hemo Klen Taq reaction buffer: 60 mM Tricine, 5 mM (NH <sub>4</sub> ) <sub>2</sub> SO <sub>4</sub> , 3.5 mM MgCl <sub>2</sub> , 6% glycerol, pH 8.7
<i>KOD XL</i>	KOD DNA Polymerase: pH 8.0

**Table 8** The reaction condition for extension experiment

Substances	20 $\mu$ l reaction scale
Primer	750 nM (5 $\mu$ l)
Template	900 nM (6 $\mu$ l)
dATP, dCTP, dGTP, dU-triazineTP	100 nM (5 $\mu$ l)
Buffer	4.0 $\mu$ l for Hemo Klen Taq/ 2.0 $\mu$ l for others
DNA polymerase	0.25 $\mu$ l

After completion of reaction, to the reaction mixture was added 20  $\mu$ l of loading buffer solution (20 mM EDTA (disodium salt), 89 mM TRIS base, 89 mM boric acid, 4% Ficoll, 0.1% bromphenol blue, 0.02% xylene cyanol FF, 7 M urea) the resulting mixture was directly applied to PAGE or an additional desalt step was applied. The reaction solutions were freed from salts by gel filtration through an illustra NAP-5 column loaded with Sephadex G-25. The DNA was eluted according to the manufacturer's instructions, the DNA eluted with HPLC-H<sub>2</sub>O. The samples were then lyophilized, dissolved in HPLC-H<sub>2</sub>O to reach the final concentration of 750 nM were either directly mixed with loading buffer or used for ligation experiments.

### 5.4.2 Polyacrylamide gel electrophoresis (PAGE)

The preparation of the denaturing polyacrylamide gel electrophoresis (PAGE); 12% was carried out by a mixture of 15.5 ml of acrylamide / bisacrylamide (19: 1, 40% aqueous solution), 12.5 g of urea, 21 ml of 8.3 M aqueous urea solution and 5 ml of 10-fold concentrated TBE buffer (contained 8.3 M urea). The polymerization was performed by adding 20  $\mu$ l of TEMED and 425  $\mu$ l of a 10% APS solution to the mixture solution. After the casting, the gel was allowed to polymerize for 40 min. After completion, the gel was pre-heated by applying a voltage to the ideal separation temperature of 50 °C using 1-fold TBE buffer prior the application of the samples. The gel pockets of precipitated urea were purified by multiple washing with buffer solution subsequently 7  $\mu$ l of the sample was added into each gel pocket. The electrophoresis was carried out at 3000V and maximum 45 W for 1 h. The illustration was followed by fluorescence upon excitation at either  $470 \pm 20$  nm with corresponding fluorescein emission at  $535 \pm 20$  nm (Cy2 emission filter) or upon excitation of the dye fluorescence at  $540 \pm 10$  nm and an emission filter of  $605 \pm 20$  nm (Cy3 emission filter).

**Table 9** The concentration of TBE buffer used for PAGE

Substances	Concentrations
Tris	890 mM
Boric acid	890 mM
EDTA	20 mM

## 5.5 Click reaction of COMBO- and triazine-modified DNA with fluorescent dyes

The click reactions of COMBO- and triazine-modified DNA with fluorescent dyes were performed at room temperature. After desalt and dissolved in HPLC water to reach the final concentration of 750 nM the solution was mixed with 1000-fold of fluorescent dyes. The reaction mixture was then shaken for 1-3 h at room temperature. After completion of the reaction, 20  $\mu$ l of loading buffer was added and the resulting solution was directly applied to PAGE. The corresponding clicked product was then illustrated compared with the mobility of references **P1**, **P2** and **P3**, respectively. The yielding of clicked product was calculated by the integration of the fluorescence intensity of a slower-moving gel band compared with extension product band using the Aida Image Analyzer v.450 from *Raytest*.

## 5.6. Cells experiments

### 5.6.1 Pre-and postsynthetic fluorescent labeling in cells

The DNA2 and DNA6 were conjugated with the azide-modified dye **21b** in a mixture solution of H<sub>2</sub>O:DMSO (10:1) at room temperature for 3 h. After completion of the reaction, a solvent was removed and the crude product was dissolved in 300  $\mu$ l H<sub>2</sub>O subsequently purified by RP-HPLC. After identification by MALDI-TOF the corresponding DNA4 and DNA8 were hybridized with their unmodified complementary strands. These labeled DNA strands were transfected into *HeLa* cells by using Screenfect®A as a medium solution. In the case of postsynthetic fluorescent labeling, the single strand DNA6 was transfected into *HeLa* cells prior to the ligation step. The solution was rapidly mixed and incubated for 20 min at room temperature to allow the formation of the DNA-liposome complex. The transfection mixture was

transferred to cells in each well of 8-well chambers slide ( $\mu$  Slide 8 well ibiTreat, IBIDI, Maetinsried, Germany).

The cells were incubated at 37 °C, 5% CO<sub>2</sub> for 24 h which were washed with media and subsequently visualized by confocal fluorescence microscopy.

## 6 Literatures

- [1] S. Tolansky, *Biographical Memoirs of Fellows of the Royal Society* **1967**, *13*, 392-402.
- [2] H. Sahoo, *RSC Advances* **2012**, *2*, 7017-7029.
- [3] M. C. Osamu Shimomura, and Roger Tsien, *Nat cell Biol* **2003**, 1-7.
- [4] R. Wombacher and V. W. Cornish, *Journal of Biophotonics* **2011**, *4*, 391-402.
- [5] H. C. Hang, C. Yu, D. L. Kato and C. R. Bertozzi, *Proceedings of the National Academy of Sciences* **2003**, *100*, 14846-14851.
- [6] J. Dommerholt, F. P. J. T. Rutjes and F. L. van Delft, *Topics in Current Chemistry* **2016**, *374*, 16.
- [7] a) J. M. Baskin, J. A. Prescher, S. T. Laughlin, N. J. Agard, P. V. Chang, I. A. Miller, A. Lo, J. A. Codelli and C. R. Bertozzi, *Proceedings of the National Academy of Sciences* **2007**, *104*, 16793-16797; b) X. Ning, J. Guo, M. A. Wolfert and G.-J. Boons, *Angewandte Chemie International Edition* **2008**, *47*, 2253-2255; c) P. V. Chang, J. A. Prescher, E. M. Sletten, J. M. Baskin, I. A. Miller, N. J. Agard, A. Lo and C. R. Bertozzi, *Proceedings of the National Academy of Sciences* **2010**, *107*, 1821-1826; d) S. M. van den Bosch, R. Rossin, P. Renart Verkerk, W. ten Hoeve, H. M. Janssen, J. Lub and M. S. Robillard, *Nuclear Medicine and Biology* **2013**, *40*, 415-423; e) J. M. Baskin, K. W. Dehnert, S. T. Laughlin, S. L. Amacher and C. R. Bertozzi, *Proceedings of the National Academy of Sciences* **2010**, *107*, 10360-10365.
- [8] A. B. Luis Blanco, Jose M. Lharo, Gil Martins, Cristina Garmendia, and and M. Salasn, *The journal of biochemistry* **1989**, *264*, 8935-8940.
- [9] D. Rideout, T. Calogeropoulou, J. Jaworski and M. McCarthy, *Biopolymers* **1990**, *29*, 247-262.
- [10] B. A. Griffin, S. R. Adams and R. Y. Tsien, *Science* **1998**, *281*, 269-272.
- [11] K. Lang and J. W. Chin, *Chemical Reviews* **2014**, *114*, 4764-4806.
- [12] V. W. Cornish, K. M. Hahn and P. G. Schultz, *Journal of the American Chemical Society* **1996**, *118*, 8150-8151.
- [13] E. Saxon and C. R. Bertozzi, *Science* **2000**, *287*, 2007-2010.

- [14] a) A. J. Dirks, J. J. L. M. Cornelissen, F. L. van Delft, J. C. M. van Hest, R. J. M. Nolte, A. E. Rowan and F. P. J. T. Rutjes, *QSAR & Combinatorial Science* **2007**, *26*, 1200-1210; b) A. H. El-Sagheer and T. Brown, *Accounts of Chemical Research* **2012**, *45*, 1258-1267; c) V. Hong, N. F. Steinmetz, M. Manchester and M. G. Finn, *Bioconjugate Chemistry* **2010**, *21*, 1912-1916; d) D. Soriano del Amo, W. Wang, H. Jiang, C. Besanceney, A. C. Yan, M. Levy, Y. Liu, F. L. Marlow and P. Wu, *Journal of the American Chemical Society* **2010**, *132*, 16893-16899.
- [15] a) J. C. Jewett and C. R. Bertozzi, *Chemical Society Reviews* **2010**, *39*, 1272-1279; b) M. F. Debets, S. S. van Berkel, J. Dommerholt, A. J. Dirks, F. P. J. T. Rutjes and F. L. van Delft, *Accounts of Chemical Research* **2011**, *44*, 805-815.
- [16] F. Heaney, *European Journal of Organic Chemistry* **2012**, *2012*, 3043-3058.
- [17] a) B. C. Sanders, F. Friscourt, P. A. Ledin, N. E. Mbu, S. Arumugam, J. Guo, T. J. Boltje, V. V. Popik and G.-J. Boons, *Journal of the American Chemical Society* **2011**, *133*, 949-957; b) A. M. Jawalekar, E. Reubsæet, F. P. J. T. Rutjes and F. L. van Delft, *Chemical Communications* **2011**, *47*, 3198-3200.
- [18] N. A. McGrath and R. T. Raines, *Chemical Science* **2012**, *3*, 3237-3240.
- [19] a) Y. A. Lin, J. M. Chalker and B. G. Davis, *Journal of the American Chemical Society* **2010**, *132*, 16805-16811; b) Y. A. Lin, J. M. Chalker, N. Floyd, G. J. L. Bernardes and B. G. Davis, *Journal of the American Chemical Society* **2008**, *130*, 9642-9643.
- [20] a) N. K. Devaraj, R. Weissleder and S. A. Hilderbrand, *Bioconjugate Chemistry* **2008**, *19*, 2297-2299; b) N. K. Devaraj and R. Weissleder, *Accounts of Chemical Research* **2011**, *44*, 816-827; c) J. B. Haun, N. K. Devaraj, S. A. Hilderbrand, H. Lee and R. Weissleder, *Nature nanotechnology* **2010**, *5*, 660-665; d) R. Rossin, P. Renart Verkerk, S. M. van den Bosch, R. C. M. Volders, I. Verel, J. Lub and M. S. Robillard, *Angewandte Chemie International Edition* **2010**, *49*, 3375-3378; e) A. A. Neves, H. Stöckmann, Y. A. Wainman, J. C. H. Kuo, S. Fawcett, F. J. Leeper and K. M. Brindle, *Bioconjugate Chemistry* **2013**, *24*, 934-941.
- [21] R. K. V. Lim and Q. Lin, *Accounts of Chemical Research* **2011**, *44*, 828-839.
- [22] a) C.-X. Song, K. E. Szulwach, Y. Fu, Q. Dai, C. Yi, X. Li, Y. Li, C.-H. Chen, W. Zhang, X. Jian, J. Wang, L. Zhang, T. J. Looney, B. Zhang, L. A. Godley, L. M. Hicks, B. T. Lahn, P. Jin and C. He, *Nat Biotech* **2011**, *29*, 68-72; b) S. T. Laughlin, J. M. Baskin, S. L. Amacher and C. R. Bertozzi, *Science* **2008**, *320*, 664-667.

- [23] a) R. HUISGEN, *Proceedings of the Chemical Society* **1961**, 357-396; b) R. Huisgen, *Angewandte Chemie International Edition* **1963**, *2*, 565-598.
- [24] L. Liang and D. Astruc, *Coordination Chemistry Reviews* **2011**, *255*, 2933-2945.
- [25] R. HUISGEN, *Angew. Chem. internut. Edit.* **1963**, *2*, 633-696.
- [26] a) H. C. Kolb and K. B. Sharpless, *Drug Discovery Today* **2003**, *8*, 1128-1137; b) V. V. Rostovtsev, L. G. Green, V. V. Fokin and K. B. Sharpless, *Angewandte Chemie* **2002**, *114*, 2708-2711; c) D. M. Patterson, L. A. Nazarova and J. A. Prescher, *ACS Chemical Biology* **2014**, *9*, 592-605.
- [27] a) K. D. Hanni and D. A. Leigh, *Chemical Society Reviews* **2010**, *39*, 1240-1251; b) C. M. Nimmo and M. S. Shoichet, *Bioconjugate Chemistry* **2011**, *22*, 2199-2209.
- [28] G. C. Tron, T. Pirali, R. A. Billington, P. L. Canonico, G. Sorba and A. A. Genazzani, *Medicinal Research Reviews* **2008**, *28*, 278-308.
- [29] a) J.-F. Lutz and Z. Zarafshani, *Advanced Drug Delivery Reviews* **2008**, *60*, 958-970; b) C. Le Droumaguet, C. Wang and Q. Wang, *Chemical Society Reviews* **2010**, *39*, 1233-1239.
- [30] A. M. Jawalekar, N. Meeuwenoord, J. G. O. Cremers, H. S. Overkleeft, G. A. van der Marel, F. P. J. T. Rutjes and F. L. van Delft, *The Journal of Organic Chemistry* **2008**, *73*, 287-290.
- [31] E. M. Sletten and C. R. Bertozzi, *Angewandte Chemie International Edition* **2009**, *48*, 6974-6998.
- [32] a) T. R. Chan, R. Hilgraf, K. B. Sharpless and V. V. Fokin, *Organic Letters* **2004**, *6*, 2853-2855; b) C. Besanceney-Webler, H. Jiang, T. Zheng, L. Feng, D. Soriano del Amo, W. Wang, L. M. Klivansky, F. L. Marlow, Y. Liu and P. Wu, *Angewandte Chemie International Edition* **2011**, *50*, 8051-8056.
- [33] a) A. H. El-Sagheer and T. Brown, *Chemical Society Reviews* **2010**, *39*, 1388-1405; b) P. M. E. Gramlich, C. T. Wirges, A. Manetto and T. Carell, *Angewandte Chemie International Edition* **2008**, *47*, 8350-8358.
- [34] A. E. Speers and B. F. Cravatt, *Chemistry & Biology* **2004**, *11*, 535-546.
- [35] T. Liebert, C. Hänsch and T. Heinze, *Macromolecular Rapid Communications* **2006**, *27*, 208-213.
- [36] a) V. Aucagne and D. A. Leigh, *Organic Letters* **2006**, *8*, 4505-4507; b) H. T. Ten Brink, J. T. Meijer, R. V. Geel, M. Damen, D. W. P. M. Löwik and J. C. M. van Hest, *Journal of Peptide Science* **2006**, *12*, 686-692.

- [37] A. J. Link and D. A. Tirrell, *Journal of the American Chemical Society* **2003**, *125*, 11164-11165.
- [38] C. Beyer and H.-A. Wagenknecht, *Chemical Communications* **2010**, *46*, 2230-2231.
- [39] a) K. Fauster, M. Hartl, T. Santner, M. Aigner, C. Kreutz, K. Bister, E. Ennifar and R. Micura, *ACS Chemical Biology* **2012**, *7*, 581-589; b) M. Aigner, M. Hartl, K. Fauster, J. Steger, K. Bister and R. Micura, *ChemBioChem* **2011**, *12*, 47-51.
- [40] J. Gierlich, G. A. Burley, P. M. E. Gramlich, D. M. Hammond and T. Carell, *Organic Letters* **2006**, *8*, 3639-3642.
- [41] T. S. Seo, Z. Li, H. Ruparel and J. Ju, *The Journal of Organic Chemistry* **2003**, *68*, 609-612.
- [42] F. Seela, H. Xiong, P. Leonard and S. Budow, *Organic & Biomolecular Chemistry* **2009**, *7*, 1374-1387.
- [43] S. Berndl, N. Herzig, P. Kele, D. Lachmann, X. Li, O. S. Wolfbeis and H.-A. Wagenknecht, *Bioconjugate Chemistry* **2009**, *20*, 558-564.
- [44] B. O. Heidi-Kristin Walter<sup>1</sup>, Ute Schepers<sup>2</sup> and Hans-Achim Wagenknecht, *Beilstein J. Org. Chem.* **2017**, *13*, 127-137.
- [45] a) M. C. Kloetzel in *The Diels-Alder Reaction with Maleic Anhydride*, Vol. John Wiley & Sons, Inc., **2004**; b) O. Diels and K. Alder, *Justus Liebigs Annalen der Chemie* **1928**, *460*, 98-122.
- [46] A. D. de Araújo, J. M. Palomo, J. Cramer, M. Köhn, H. Schröder, R. Wacker, C. Niemeyer, K. Alexandrov and H. Waldmann, *Angewandte Chemie International Edition* **2006**, *45*, 296-301.
- [47] V. B. a. S. Howorka, *Nucleic Acids Research* **2009**, *37*, 1477-1485.
- [48] M. L. Blackman, M. Royzen and J. M. Fox, *Journal of the American Chemical Society* **2008**, *130*, 13518-13519.
- [49] A.-C. Knall and C. Slugovc, *Chemical Society Reviews* **2013**, *42*, 5131-5142.
- [50] a) J. Šečkutė and N. K. Devaraj, *Current Opinion in Chemical Biology* **2013**, *17*, 761-767; b) J. Šečkutė, J. Yang and N. K. Devaraj, *Nucleic Acids Research* **2013**, *41*, e148-e148.
- [51] R. A. A. Foster and M. C. Willis, *Chemical Society Reviews* **2013**, *42*, 63-76.

- [52] a) W. Chen, D. Wang, C. Dai, D. Hamelberg and B. Wang, *Chemical Communications* **2012**, 48, 1736-1738; b) A.-C. Knall, M. Hollauf and C. Slugovc, *Tetrahedron Letters* **2014**, 55, 4763-4766.
- [53] E. B. G. Cserép, O. Demeter, M. Kállay, H.-A. Wagenknecht, P. Kele *Synthesis* **2015**, 47, 2738-2744.
- [54] a) M. T. Taylor, M. L. Blackman, O. Dmitrenko and J. M. Fox, *Journal of the American Chemical Society* **2011**, 133, 9646-9649; b) M. R. Karver, R. Weissleder and S. A. Hilderbrand, *Bioconjugate Chemistry* **2011**, 22, 2263-2270.
- [55] J. Y. a. N. K. D. Jolita Š ec̃ kute\_ *Nucleic Acids Research* **2013**, 41, 1-9.
- [56] a) J. Schoch, M. Staudt, A. Samanta, M. Wiessler and A. Jäschke, *Bioconjugate Chemistry* **2012**, 23, 1382-1386; b) J. Schoch, M. Wiessler and A. Jäschke, *Journal of the American Chemical Society* **2010**, 132, 8846-8847; c) J. Schoch, S. Ameta and A. Jaschke, *Chemical Communications* **2011**, 47, 12536-12537.
- [57] a) P. N. Asare-Okai, E. Agustin, D. Fabris and M. Royzen, *Chemical Communications* **2014**, 50, 7844-7847; b) A. M. Pyka, C. Domnick, F. Braun and S. Kath-Schorr, *Bioconjugate Chemistry* **2014**, 25, 1438-1443.
- [58] A. T. Blomquist and L. H. Liu, *Journal of the American Chemical Society* **1953**, 75, 2153-2154.
- [59] G. Wittig and A. Krebs, *Chemische Berichte* **1961**, 94, 3260-3275.
- [60] N. J. Agard, J. A. Prescher and C. R. Bertozzi, *Journal of the American Chemical Society* **2004**, 126, 15046-15047.
- [61] G. H. Hur, J. L. Meier, J. Baskin, J. A. Codelli, C. R. Bertozzi, M. A. Marahiel and M. D. Burkart, *Chemistry & biology* **2009**, 16, 372-381.
- [62] C.-X. Song, K. E. Szulwach, Y. Fu, Q. Dai, C. Yi, X. Li, Y. Li, C.-H. Chen, W. Zhang, X. Jian, J. Wang, L. Zhang, T. J. Looney, B. Zhang, L. A. Godley, L. M. Hicks, B. T. Lahn, P. Jin and C. He, *Nature biotechnology* **2011**, 29, 68-72.
- [63] a) J. Dommerholt, S. Schmidt, R. Temming, L. J. A. Hendriks, F. P. J. T. Rutjes, J. C. M. van Hest, D. J. Lefeber, P. Friedl and F. L. van Delft, *Angewandte Chemie* **2010**, 122, 9612-9615; b) M. Shelbourne, T. Brown and A. H. El-Sagheer, *Chemical Communications* **2012**, 48, 11184-11186; c) P. van Delft, N. J. Meeuwenoord, S. Hoogendoorn, J. Dinkelaar, H. S. Overkleef, G. A. van der Marel and D. V. Filippov, *Organic Letters* **2010**, 12, 5486-5489; d) C. Stubinitzky, G. B. Cserep, E. Batzner, P. Kele and H.-A. Wagenknecht, *Chemical Communications* **2014**, 50, 11218-11221.

- [64] C. G. Gordon, J. L. Mackey, J. C. Jewett, E. M. Sletten, K. N. Houk and C. R. Bertozzi, *Journal of the American Chemical Society* **2012**, *134*, 9199-9208.
- [65] B. Gold, N. E. Shevchenko, N. Bonus, G. B. Dudley and I. V. Alabugin, *The Journal of Organic Chemistry* **2012**, *77*, 75-89.
- [66] M. F. Debets, C. W. J. van der Doelen, F. P. J. T. Rutjes and F. L. van Delft, *ChemBioChem* **2010**, *11*, 1168-1184.
- [67] E. M. Sletten, H. Nakamura, J. C. Jewett and C. R. Bertozzi, *Journal of the American Chemical Society* **2010**, *132*, 11799-11805.
- [68] J. A. Codelli, J. M. Baskin, N. J. Agard and C. R. Bertozzi, *Journal of the American Chemical Society* **2008**, *130*, 11486-11493.
- [69] G. de Almeida, E. M. Sletten, H. Nakamura, K. K. Palaniappan and C. R. Bertozzi, *Angewandte Chemie International Edition* **2012**, *51*, 2443-2447.
- [70] B. R. Varga, M. Kállay, K. Hegyi, S. Béni and P. Kele, *Chemistry – A European Journal* **2012**, *18*, 822-828.
- [71] a) I. Singh, C. Freeman and F. Heaney, *European Journal of Organic Chemistry* **2011**, *2011*, 6739-6746; b) I. Singh, C. Freeman, A. Madder, J. S. Vyle and F. Heaney, *Organic & Biomolecular Chemistry* **2012**, *10*, 6633-6639.
- [72] E. v. S. ieter van Delft, Nico J. Meeuwenoord, Herman S. Overkleeft, Gijsbert A. van der Marel\*, Dmitri V. Filippov\*, *Synthesis* **2011**, *17*, 2724-2732.
- [73] M. Shelbourne, X. Chen, T. Brown and A. H. El-Sagheer, *Chemical Communications* **2011**, *47*, 6257-6259.
- [74] K. N. Jayaprakash, C. G. Peng, D. Butler, J. P. Varghese, M. A. Maier, K. G. Rajeev and M. Manoharan, *Organic Letters* **2010**, *12*, 5410-5413.
- [75] C. Dai, L. Wang, J. Sheng, H. Peng, A. B. Draganov, Z. Huang and B. Wang, *Chemical Communications* **2011**, *47*, 3598-3600.
- [76] X. Ren, M. Gerowska, A. H. El-Sagheer and T. Brown, *Bioorganic & Medicinal Chemistry* **2014**, *22*, 4384-4390.
- [77] a) K. Lang, L. Davis, J. Torres-Kolbus, C. Chou, A. Deiters and J. W. Chin, *Nat Chem* **2012**, *4*, 298-304; b) K. Lang, L. Davis, S. Wallace, M. Mahesh, D. J. Cox, M. L. Blackman, J. M. Fox and J. W. Chin, *Journal of the American Chemical Society* **2012**, *134*, 10317-10320.
- [78] D. S. Liu, A. Tangpeerachaikul, R. Selvaraj, M. T. Taylor, J. M. Fox and A. Y. Ting, *Journal of the American Chemical Society* **2012**, *134*, 792-795.

- [79] a) D. N. Kamber, Y. Liang, R. J. Blizzard, F. Liu, R. A. Mehl, K. N. Houk and J. A. Prescher, *Journal of the American Chemical Society* **2015**, *137*, 8388-8391; b) J. Balcar, G. Chrisam, F. X. Huber and J. Sauer, *Tetrahedron Letters* **1983**, *24*, 1481-1484; c) B. R. Lahue, S.-M. Lo, Z.-K. Wan, G. H. C. Woo and J. K. Snyder, *The Journal of Organic Chemistry* **2004**, *69*, 7171-7182; d) E. C. Taylor and L. G. French, *The Journal of Organic Chemistry* **1989**, *54*, 1245-1249.
- [80] K. A. Horner, N. M. Valette and M. E. Webb, *Chemistry – A European Journal* **2015**, *21*, 14376-14381.
- [81] Á. Eördögh, J. Steinmeyer, K. Peewasan, U. Schepers, H.-A. Wagenknecht and P. Kele, *Bioconjugate Chemistry* **2016**, *27*, 457-464.
- [82] C. Wellner and H.-A. Wagenknecht, *Organic Letters* **2014**, *16*, 1692-1695.
- [83] M. Fernandez-Suarez and A. Y. Ting, *Nat Rev Mol Cell Biol* **2008**, *9*, 929-943.
- [84] a) H. Kimura, Y. Hayashi-Takanaka, T. J. Stasevich and Y. Sato, *Histochemistry and Cell Biology* **2015**, *144*, 101-109; b) B. Hochreiter, A. Pardo-Garcia and J. Schmid, *Sensors* **2015**, *15*, 26281.
- [85] a) M. Famulok, J. S. Hartig and G. Mayer, *Chemical Reviews* **2007**, *107*, 3715-3743; b) G. Mayer, *Angewandte Chemie International Edition* **2009**, *48*, 2672-2689.
- [86] T. Topping, N. V. Voigt, J. Nangreave, H. Yan and K. V. Gothelf, *Chemical Society Reviews* **2011**, *40*, 5636-5646.
- [87] S. L. Beaucage and M. H. Caruthers, *Tetrahedron Letters* **1981**, *22*, 1859-1862.
- [88] A. Hottin and A. Marx, *Accounts of Chemical Research* **2016**, *49*, 418-427.
- [89] S. Obeid, A. Baccaro, W. Welte, K. Diederichs and A. Marx, *Proceedings of the National Academy of Sciences* **2010**, *107*, 21327-21331.
- [90] M. Hocek, *The Journal of Organic Chemistry* **2014**, *79*, 9914-9921.
- [91] M. Yoshikawa, T. Kato and T. Takenishi, *Tetrahedron Letters* **1967**, *8*, 5065-5068.
- [92] Ludwig, *Acta Biochim. et Biophys. Acad. Sci. Hung.* *16*, 131-133.
- [93] H. E. Gottlieb, V. Kotlyar and A. Nudelman, *The Journal of Organic Chemistry* **1997**, *62*, 7512-7515.
- [94] A. S. K. Hashmi, T. Häffner, W. Yang, S. Pankajakshan, S. Schäfer, L. Schultes, F. Rominger and W. Frey, *Chemistry – A European Journal* **2012**, *18*, 10480-10486.

[95] N. P. F. Barthes, K. Gavvala, D. Bonhomme, A. S. Dabert-Gay, D. Debayle, Y. Mély, B. Y. Michel and A. Burger, *The Journal of Organic Chemistry* **2016**, *81*, 10733-10741.

[96] T. R. Battersby, D. N. Ang, P. Burgstaller, S. C. Jurczyk, M. T. Bowser, D. D. Buchanan, R. T. Kennedy and S. A. Benner, *Journal of the American Chemical Society* **1999**, *121*, 9781-9789.

## 7. Appendix

### 7.1 Publications

M. Merkel, K. Peewasan, S. Arndt, D. Ploschik, and H.-Achim Wagenknecht, Copper-Free Postsynthetic Labeling of Nucleic Acids by Means of Bioorthogonal Reactions. *ChemBioChem* **2015**, 16, 1541-1553.

Á. Eördögh, J. Steinmeyer, K. Peewasan, U. Schepers, H.-A. Wagenknecht, and P. Kele, Polarity Sensitive Bioorthogonally Applicable Far-Red Emitting Labels for Postsynthetic Nucleic Acid Labeling by Copper-Catalyzed and Copper-Free Cycloaddition. *Bioconjugate Chem* **2016**, 27, 457-464.

K. Peewasan, H.-A. Wagenknecht, 1,2,4-triazine-modified 2'-deoxyuridine triphosphate for efficient bioorthogonal fluorescent labeling of DNA. *ChemBioChem* **2017**, accepted.

### 7.2 Conferences

**2014** II. Doctoral seminar of the German Nucleic Acid Association (DNG), Bad-Herrenalb, poster presentation.

**2014** Postsynthetic Modification of Copper-free Clickable Monobenzo cyclooctyne Oligonucleotides Building Blocks as a Fluorescent Labeling of DNA, Deutsche Forschungsgemeinschaft (DFG) conference, poster presentation.

**2015** VII Postsynthetic Copper-free Click “reaction of Monobenzocyclooctyne Modified-Oligonucleotides” as Bioorthogonal Fluorescent Labelling (Poster presentation), Nucleinsäurechemie-Treffen, Berlin, Germany, poster presentation.

## 8 Declaration of honor

I hereby declare that I have authored the present work myself and that I have not used any sources or tools other than the ones indicated, as well as those which have been taken literally or in substance, as such, the electronic version agrees with the written one and I have read the Articles of Association of the Karlsruhe Institute of Art (KIT) to ensure good scientific practice, as amended from time to time. In addition, I assure that the collection and archiving of the primary data in accordance with section A (6) of the Rules for the Safeguarding of Good Scientific Practice of the KIT is secured by the Institute.

Karlsruhe, den 4.05.2017

---

Krisana Peewasan